Electronic Supplementary Material (ESI) for ChemComm.

Supplementary Information

Optimal Hydrogen Bond Surrogate for α-Helices

Stephen T Joy and Paramjit Arora

Department of Chemistry, New York University, New York, NY 10003

Table of Contents

	Page number
General	S2
Synthesis	S3-S29
Circular Dichroism Spectroscopy	S30-S33
Computational modeling	S34-S37
Mdm2 binding studies	S38-S40
NMR spectra	S41-S74
Supplementary References	S75-S75

General

Commercial-grade reagents and solvents were used without further purification except as indicated. Dichloroethane was distilled before use in the metathesis reactions. All reactions were stirred magnetically or mechanically shaken; moisture-sensitive reactions were performed under nitrogen/argon. Reverse-phase HPLC experiments were conducted with 0.1% aqueous trifluoroacetic acid and 0.1% trifluoroacetic acid in acetonitrile buffers as eluents on C_{18} reverse phase columns using a Beckman Coulter HPLC equipped with a System Gold 168 Diode array detector. Electrospray ionization mass spectrometry (ESI-MS) data was recorded on an Agilent 1100 series LC/MSD (XCT) electrospray trap. High-resolution mass spectrometry (HRMS) data was obtained on an Agilent 6224 Accurate-Mass time-of-flight spectrometer using atmospheric pressure chemical ionization source (APCI). Infrared spectra (IR) were recorded with a Thermo Nicolet AVATAR Fourier Transform IR spectrometer. The microwave reactions were performed in a CEM Discover single-mode reactor with controlled power, temperature, and time settings. Proton NMR spectra were recorded on a Bruker AVANCE 400 or 600 MHz spectrometer.

Synthesis

Peptide Synthesis

Peptides were synthesized on a CEM Liberty microwave peptide synthesizer using Fmoc solid-phase chemistry on Rink amide resin, and purified by reversed-phase HPLC. The identity and the purity of the peptides were confirmed by ESI-MS.

HBS Synthesis: RCM approach.

HBS peptides were synthesized as previously described.[1] Peptide sequences up to the $i+5^{th}$ residue of the putative helix were synthesized on solid phase on a CEM Liberty Series microwave peptide synthesizer. A solution of nosyl-protected *N*-allylglycine (3 eq) was preactivated with DIC (3 eq) and HOAt (3 eq) in NMP for 15 min before addition to the resin-bound peptide and subsequent shaking at room temperature for 2 h. Resin was washed sequentially with DMF, DCM, MeOH, DMF, and DCM. The resin-bound peptide was suspended in DMF, DBU (5 eq) and 2-mercaptoethanol (10 eq) were added, and the resin shaken for 30 min. Solution was removed and DBU/mercaptoethanol repeated once more for 30 min and again for 1 h to complete nosyl deprotection. Resin was washed sequentially with DMF, DCM, MeOH, DMF, and DCM. Coupling to the unprotected secondary amine was accomplished using the subsequent Fmoc-protected amino acid (20 eq), DIC (20 eq), and HOAt (20 eq), preactivated in NMP for 15 min followed by resin addition and shaking in the activated solution overnight. The resin was again washed sequentially with DMF, DCM, MeOH, DMF, and DCM to afford resin-bound Fmoc-protected peptide. Sequential coupling using the final Fmoc-amino acid and 4-pentenoic acid or 2,2-dimethyl-4-pentenoic acid (5 eq) with DIC (5 eq) and HOBt (5 eq) for 2 h each produced the bis-olefin. Ring-closing metathesis on the bis-olefin was performed using

Hoveyda-Grubbs II catalyst in dry 1,2-dichloroethane under microwave irradiation for 15 min at 120° C. Peptides utilizing 2,2-dimethyl-4-pentenoic acid were subjected to 30 min of microwave irradiation at 120° C. Peptides were side-chain deprotected and cleaved from resin using 95% trifluoroacetic acid (TFA) with 2.5% water and 2.5% triisopropylsilane (TIPS), precipitated from cold ether, and purified by reverse-phase HPLC on a C_{18} column and then characterized using ESI-MS.

Synthesis of alanine-rich HBS helices: Lactam approach via Knorr Amide Resin

Alanine-rich peptide sequences consisting only of alanine, azidolysine, and tyrosine were synthesized up to the $i+5^{th}$ residue of the putative helix on solid phase Knorr amide resin on a CEM Liberty Series microwave peptide synthesizer (Figure S1). A solution of the desired nosyl-protected N-alkylated linker glycine residue (3 eq) was preactivated with DIC (3 eq) and HOAt (3 eq) in NMP for 15 min before addition to the resin-bound peptide and subsequent shaking at room temperature for 12 h. Resin was washed sequentially with DMF, DCM, MeOH, DMF, and DCM. The resin-bound peptide was suspended in DMF, DBU (5 eq) and 2-mercaptoethanol (10 eq) were added, and the resin shaken for 30 min. Solution was removed and DBU/mercaptoethanol repeated once more for 30 min and again for 1 h to complete nosyl deprotection. Resin was washed sequentially with DMF, DCM, MeOH, DMF, and DCM. Coupling to the unprotected secondary amine was accomplished using the subsequent Fmoc-protected amino acid (20 eq), DIC (20 eq), and HOAt (20 eq), preactivated in NMP for 15 min followed by resin addition and shaking in the activated solution overnight. The resin was again washed sequentially with DMF, DCM, MeOH, DMF, and DCM to afford resin-bound Fmoc-protected peptide. Sequential coupling using the final Fmoc-amino acid (5 eq) with DIC (5 eq)

and HOBt (5 eq) for 2 h was followed by Fmoc deprotection to yield the full-length peptide with a free terminal amine.

Peptides were cleaved from resin using 95% TFA with 2.5% water and 2.5% TIPS, simultaneously removing terminal amine Boc protection, linker phenylisopropyl ester protection, and tyrosine side chain protection. The Z^{N}-HBS^{DM} linker employs a methyl ester instead of the acid labile phenylisopropyl ester, and is therefore subjected to a hydrolysis step where the peptide is stirred in 1/1 methanol/water (pH = 12) for 12 h at 4°C. The cleaved peptides possessing a free terminal amine, a deprotected linker carboxylic acid, and intact azidolysine residues are subjected to reverse-phase HPLC purification on a C_8 column.

The purified HBS precursors were dissolved in DMF to a final concentration of 1 mM. The solution was chilled to 4 °C before adding HOAt (1.2 eq), PyBop (1.2 eq), and DIPEA (6 eq) and stirring for 3 h at 4 °C. The solution was warmed to 22 °C and stirred for 12 h. The solvent was filtered and then removed under vacuum. Cyclized peptides were suspended in a solution consisting of 33% acetonitrile, 33% DMF, and 33% 0.1 M Tris buffer (pH = 8.0). Azidolysine reduction to lysine was completed by addition of tris(2-carboxyethyl)phosphine hydrochloride (TCEP-HCl, 10 eq) and 12 h agitation.[2] The solvent was removed under vacuum before resuspension in acetonitrile and water. The crude mixture was filtered, purified by reverse-phase HPLC on a C_{18} column and then characterized using ESI-MS.

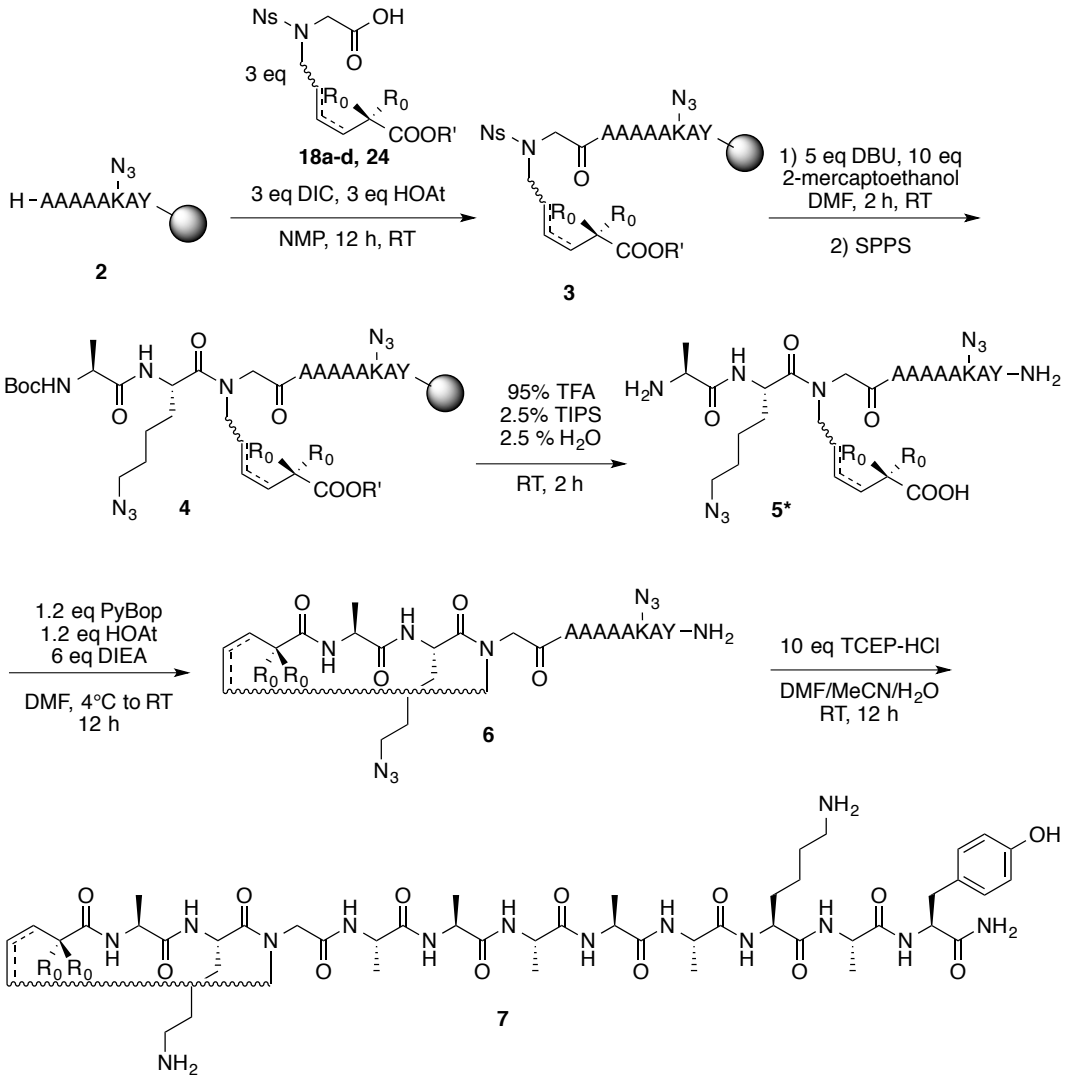

Figure S1. Synthesis of XAKG*AAAAAKAY-NH_2 HBS peptides using Knorr Amide resin and azidolysine for orthogonal side chain protection. *For Z^N-HBS^{DM}, synthesis of **6** required a methyl ester hydrolysis step in 50/50 methanol/water at pH = 12 for 12 h at 4°C.

HBS Synthesis: Lactam approach via Sieber Resin

Peptide sequences up to the $i+5^{th}$ residue of the putative helix were synthesized on solid phase Sieber resin on a CEM Liberty Series microwave peptide synthesizer (Figure S2). A solution of the desired nosyl-protected N-alkylated linker glycine residue (3 eq) was preactivated with DIC (3 eq) and HOAt (3 eq) in NMP for 15 min before addition to the resin-bound peptide and subsequent shaking at room temperature for 12 h. Resin was washed sequentially with DMF, DCM, MeOH, DMF, and DCM. The resin-bound peptide was suspended in DMF, DBU (5 eq) and 2-mercaptoethanol (10 eq) were added, and the resin shaken for 30 min. Solution was removed and DBU/mercaptoethanol repeated once more for 30 min and again for 1 h to complete nosyl deprotection. Resin was washed sequentially with DMF, DCM, MeOH, DMF, and DCM. Coupling to the unprotected secondary amine was accomplished using the subsequent Fmoc-protected amino acid (20 eq), DIC (20 eq), and HOAt (20 eq), preactivated in NMP for 15 min followed by resin addition and shaking in the activated solution overnight. The resin was again washed sequentially with DMF, DCM, MeOH, DMF, and DCM to afford resin-bound Fmoc-protected peptide. Sequential coupling using the final Fmoc-amino acid (5 eq) with DIC (5 eq) and HOBt (5 eq) for 2 h was followed by Fmoc deprotection to yield the full-length peptide with a free terminal amine. The resin was then washed with 1% TFA with 5% TIPS in DCM for 3 min (5x) to cleave the peptide from resin and deprotect the linker carboxylate.[3] The resin washes were combined and the solvent removed under vacuum to produce the crude peptide with side chain protection intact.

The crude peptide was dissolved in DMF to a final concentration of 1 mM. The solution was chilled to 4 °C before adding HOAt (1.2 eq), PyBop (1.2 eq), and DIPEA (6 eq) and stirring for 3 h at 4 °C. The solution was warmed to 22 °C and stirred for 12 h. The solvent was filtered

and then removed under vacuum. The crude HBS peptides were then side-chain deprotected in 95% TFA with 2.5% water and 2.5% TIPS, precipitated from cold ether, and purified by reverse-phase HPLC on a C_{18} column and then characterized using ESI-MS.

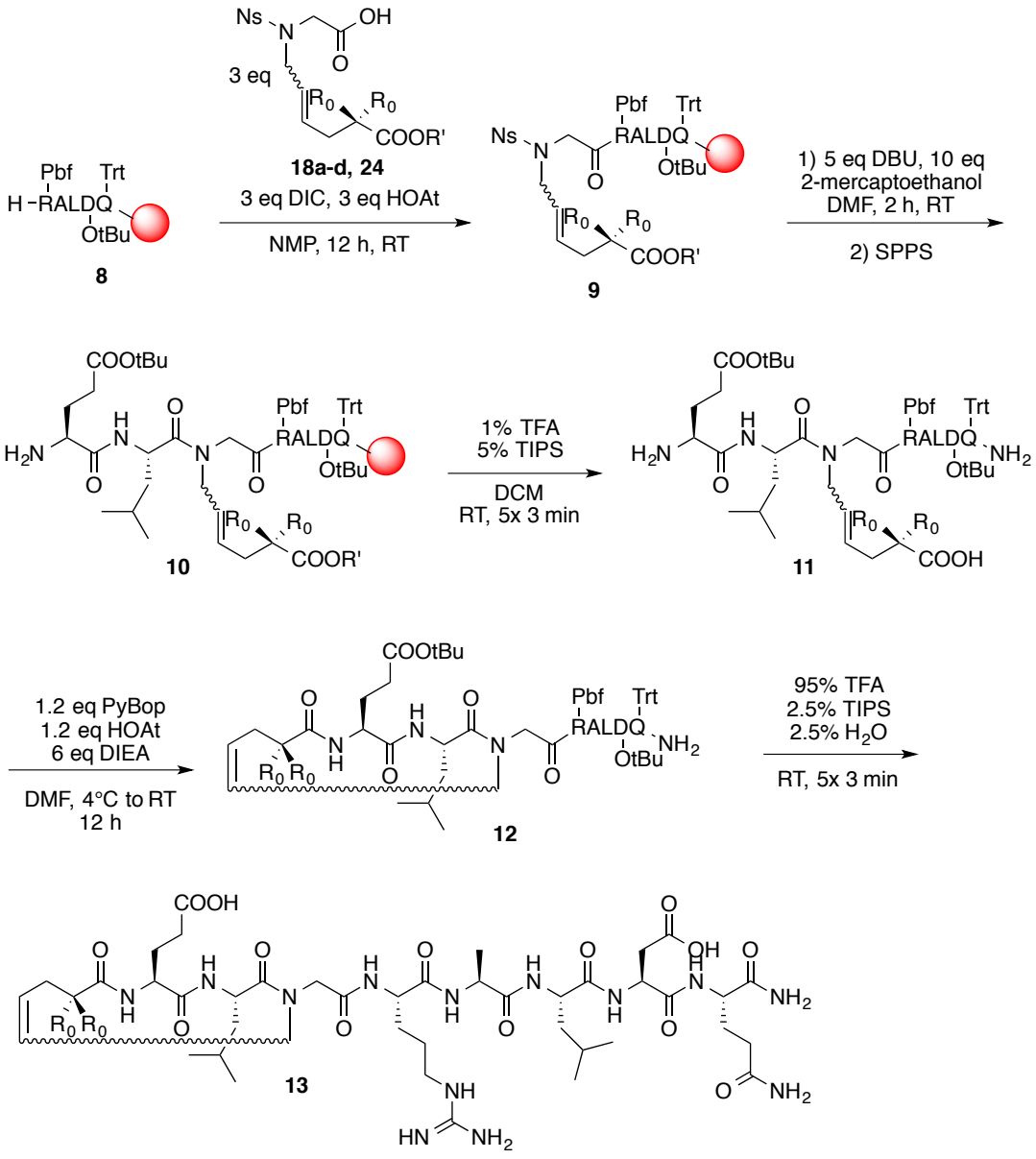

Figure S2. Synthesis of Hif HBS (XELG*RALDQ-NH_2) peptides using Sieber Amide resin and lactam closure. Sieber Amide resin methodology was also used to cyclize p53 HBS peptides (XQEG*FSDLWKLLS-NH_2).

Table S1. Calculated and observed molecular weights for peptides. *Denotes the observed $[M+2]^{2+}$ instead of $[M+H]^{+}$.

Sequence	HBS Type	MS (calculated)	MS (observed) $[M+H]^{+}$
Ac-AKGAAAAAKAY-NH_2	NA	1032.6	1033.5
XAKG*AAAAAKAY-NH_2	E^O-HBS	1084.6	1085.9
XAKG*AAAAAKAY-NH_2	E^O-HBS^{DM}	1112.6	1113.9
XAKG*AAAAAKAY-NH_2	Z^O-HBS	1084.6	1085.8
XAKG*AAAAAKAY-NH_2	Z^O-HBS^{DM}	1112.6	1113.8
XAKG*AAAAAKAY-NH_2	Z^N-HBS^{DM}	1112.6	1113.9
Ac-ELGRALDQ-NH_2	NA	941.5	942.8
XELG*RALDQ-NH_2	E^O-HBS	993.5	994.8
XELG*RALDQ-NH_2	E^O-HBS^{DM}	1021.6	1022.8
XELG*RALDQ-NH_2	Z^O-HBS	993.5	994.8
Ac-QEGFSDLWKLLS-NH_2	NA	1462.7	1463.9
XQEG*FSDLWKLLS-NH_2	E^O-HBS	1514.8	758.9*
XQEG*FSDLWKLLS-NH_2	E^O-HBS^{DM}	1542.8	772.9*
XQEG*FSDLWKLLS-NH_2	Z^O-HBS	1514.8	758.9*

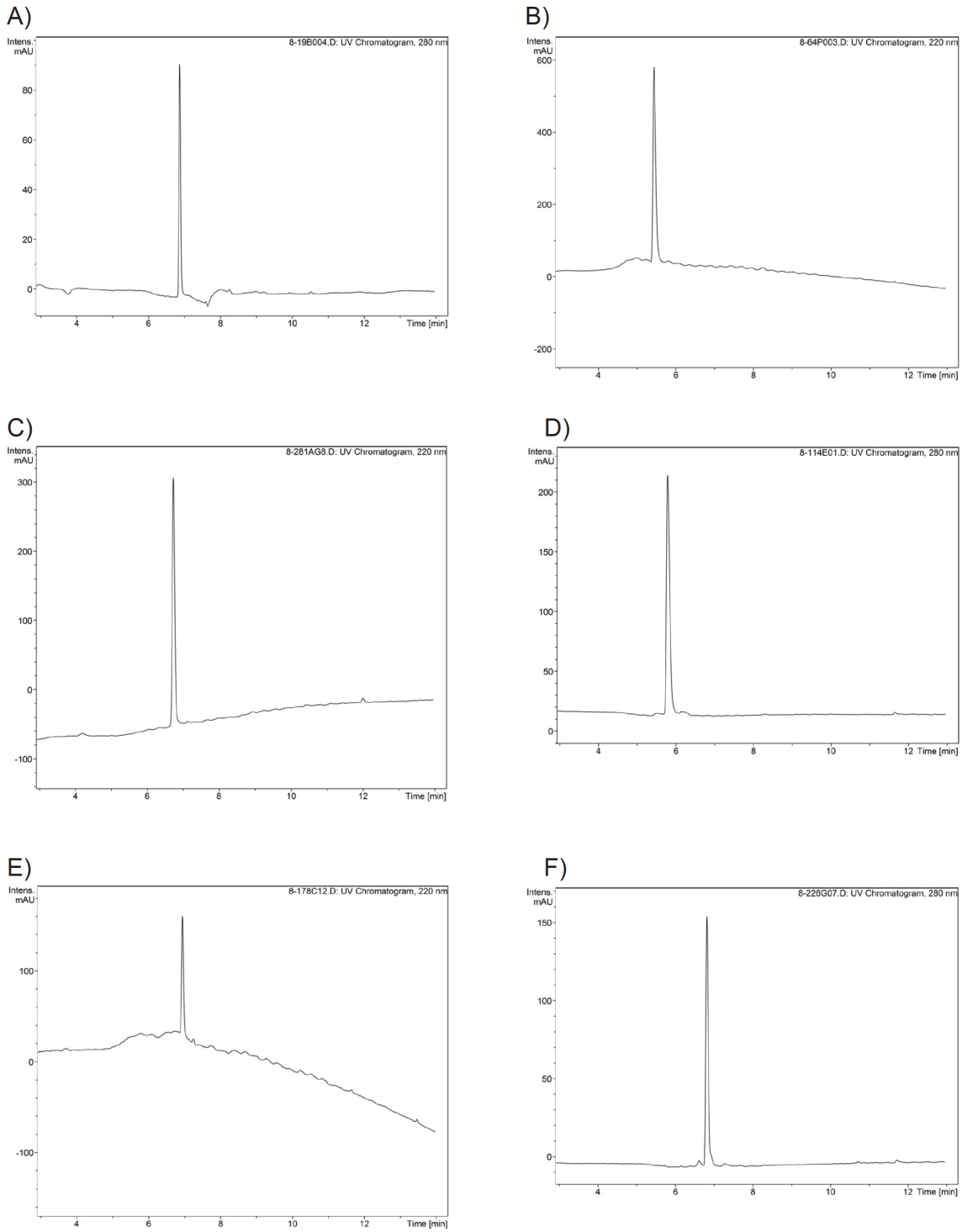

Figure S3. LC traces of alanine rich peptides. Traces for A) Ac-AKGAAAAAKAY-NH_2, B) E^O-HBS XAKG*AAAAAKAY-NH_2, C) Z^O-HBS XAKG*AAAAAKAY-NH_2, D) E^O-HBS^{DM} XAKG*AAAAAKAY-NH_2, E) Z^N-HBS^{DM} XAKG*AAAAAKAY-NH_2, and F) Z^O-HBS^{DM} XAKG*AAAAAKAY-NH_2.

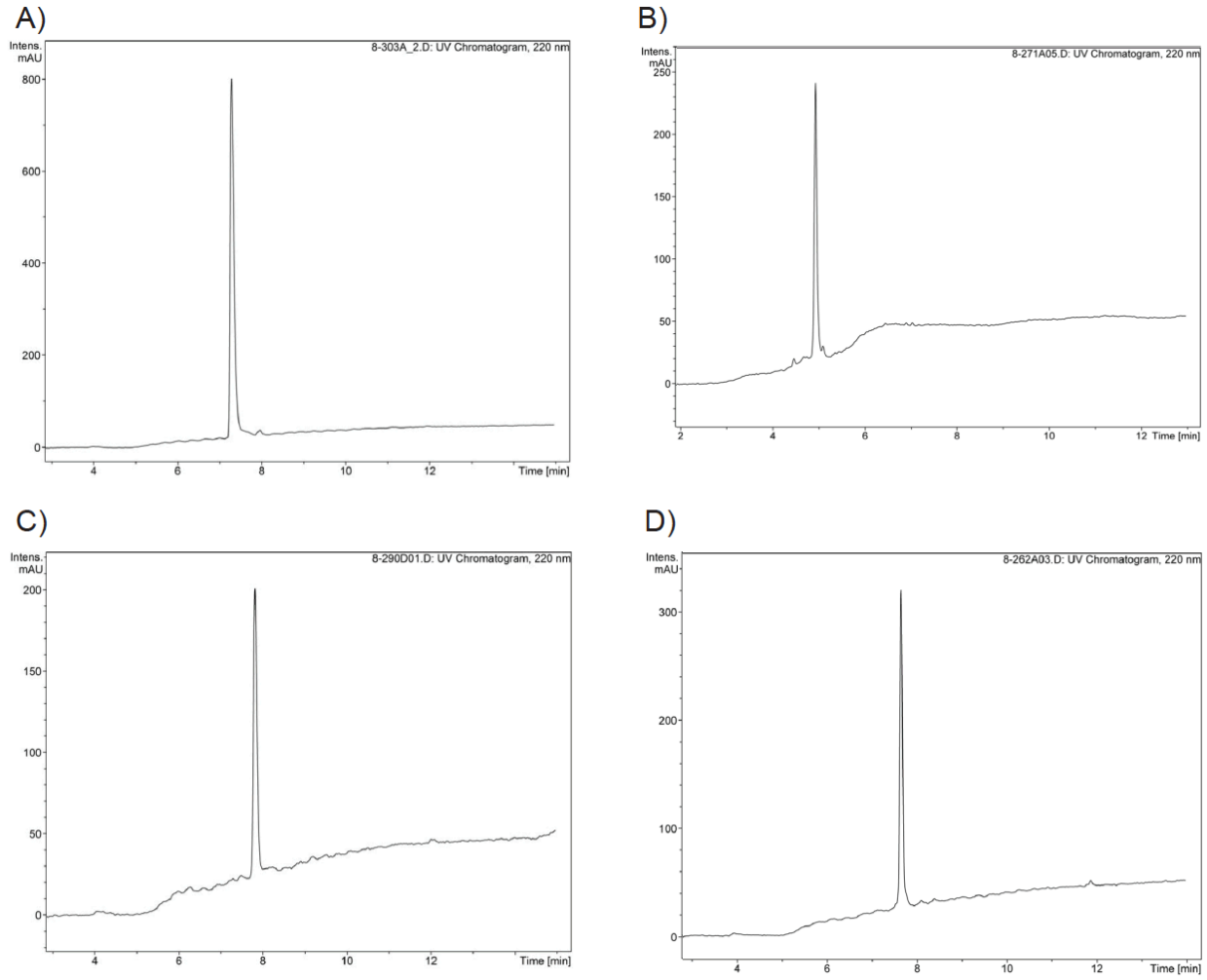

Figure S4. LC traces of Hif peptides. Traces for A) Ac-ELGRALDQ-NH_2, B) E^O-HBS XELG*RALDQ -NH_2, C) Z^O-HBS XELG*RALDQ-NH_2, and D) E^O-HBS^{DM} XELG*RALDQ-NH_2.

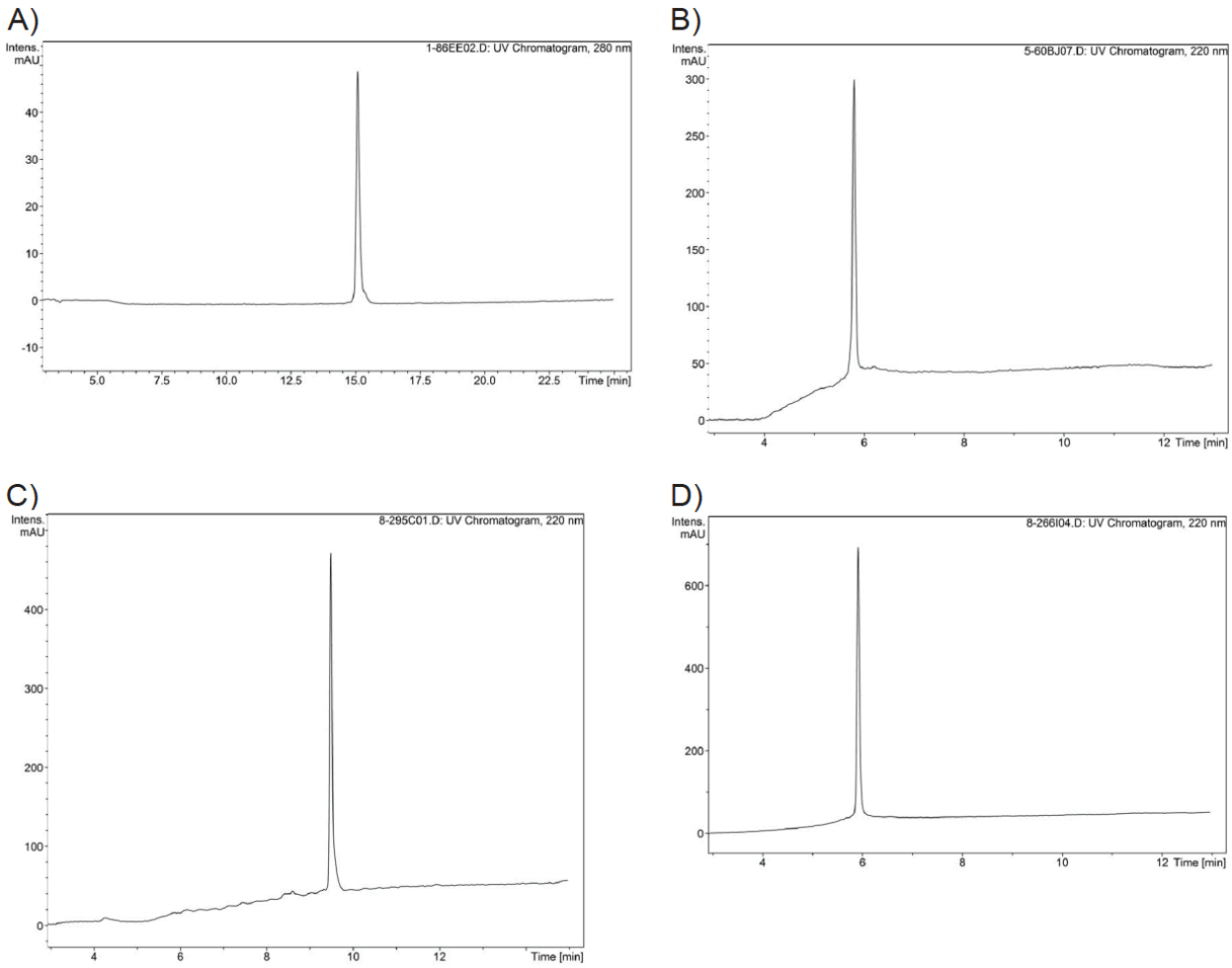

Figure S5. LC traces of p53 peptides. Traces for A) Ac-QEGFSDLWKLLS-NH_2, B) E^O-HBS XQEG*FSDLWKLLS-NH_2, C) Z^O-HBS XQEG*FSDLWKLLS-NH_2, and D) E^O-HBS^{DM} XQEG*FSDLWKLLS-NH_2.

Linker Synthesis

Synthesis of HBS peptides via lactam bond closure was required for installation of a hexenoate linker featuring the desired alkene stereochemistry and position as well as orthogonal protection of the hexenoate carboxylic acid. For E^O and Z^O-HBS derivatives, the accessible *E* and *Z* isomers of 1,4-dibromo-2-butene provided a facile method to installing the desired alkene stereochemistry at the C-O bond position. Weak acid-labile phenyl isopropyl esters were selected for orthogonal carboxylate protection due to the ability to remove them in the presence of commonly-used strong acid-labile amino acid protecting groups.[3] α-Alkylation of phenyl isopropyl acetate and isobutyrate derivatives[4] to the desired dibromoalkene yielded the desired 6-bromo-4-hexenoate linkers with or without α-dimethyl groups respectively[5]. The 4-bromohexenoate compounds could not be characterized by HRMS due to their instability under the MS conditions. Nosyl-glycine esters were N-alkylated to these bromohexenoates[6] and hydrolyzed to yield four different N-alkylated glycine residues (Figure S6) that could be easily attached to a growing peptide chain via standard peptide coupling techniques.

Installation of a *Z*-alkene at the C-N position is much more challenging and laborious due to the necessity of installing Cα-tetrasubstitution to prevent isomerization. The proximity of the desired alkene along the C3-C4 bond to the α-dimethyl group limits the utility of a number of alkene-producing reactions such as metathesis. Fortuitously, an existing synthesis for a similar compound has been previously reported which utilized a Wittig reaction on methyl 3-oxo-2,2-dimethylpropanoate to attain the desired *Z* alkene at the C3-C4 position in excellent yields[7]. This Wittig reaction was modified to utilize an azidoalkyl phosphonium salt[8] to provide the desired alkene and reduction of the azide to an amine[9] followed by nosyl protection, alkylation to

bromoacetate, and ester deprotection provided the desired N-alkylated glycine with a 3-hexenoate linker (Figure S7).

Unfortunately, phenyl isopropyl 3-oxo-2,2-dimethylpropanoate was challenging to synthesize, prone to degradation, and the protecting group difficult to maintain throughout the remainder of the synthesis. Ultimately, the accessibility and relative orthogonality of methyl esters with most amino acid protection was settled upon as a viable ester protecting group.

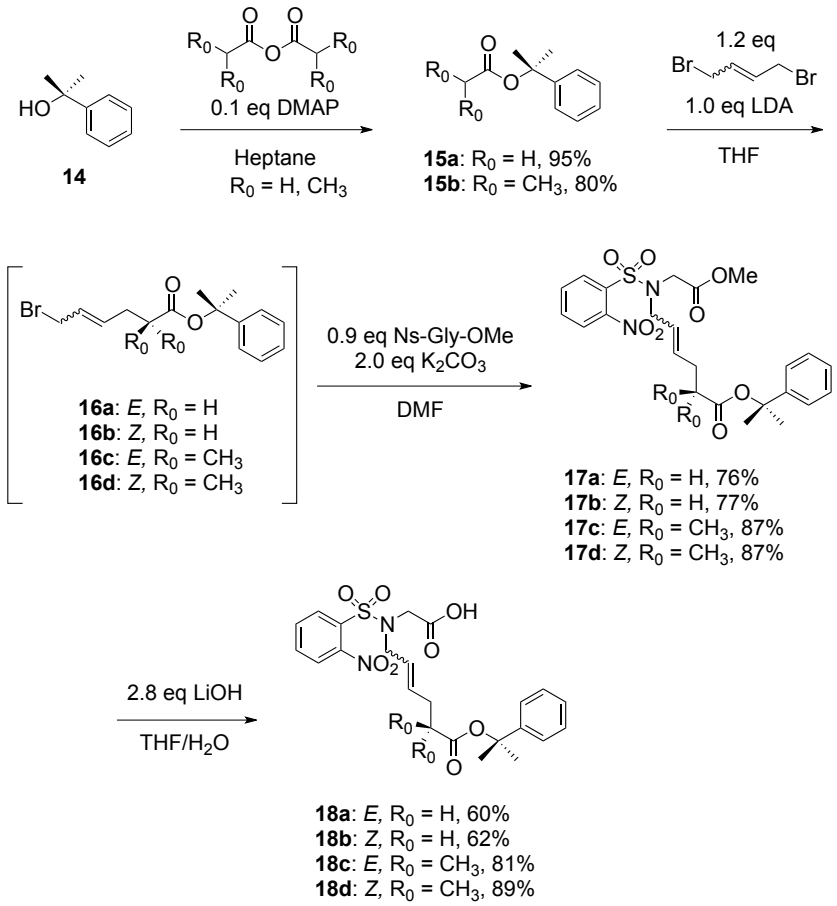

Figure S6. Synthesis of E^O/Z^O-HBS and E^O/Z^O-HBS^{DM} linkers.

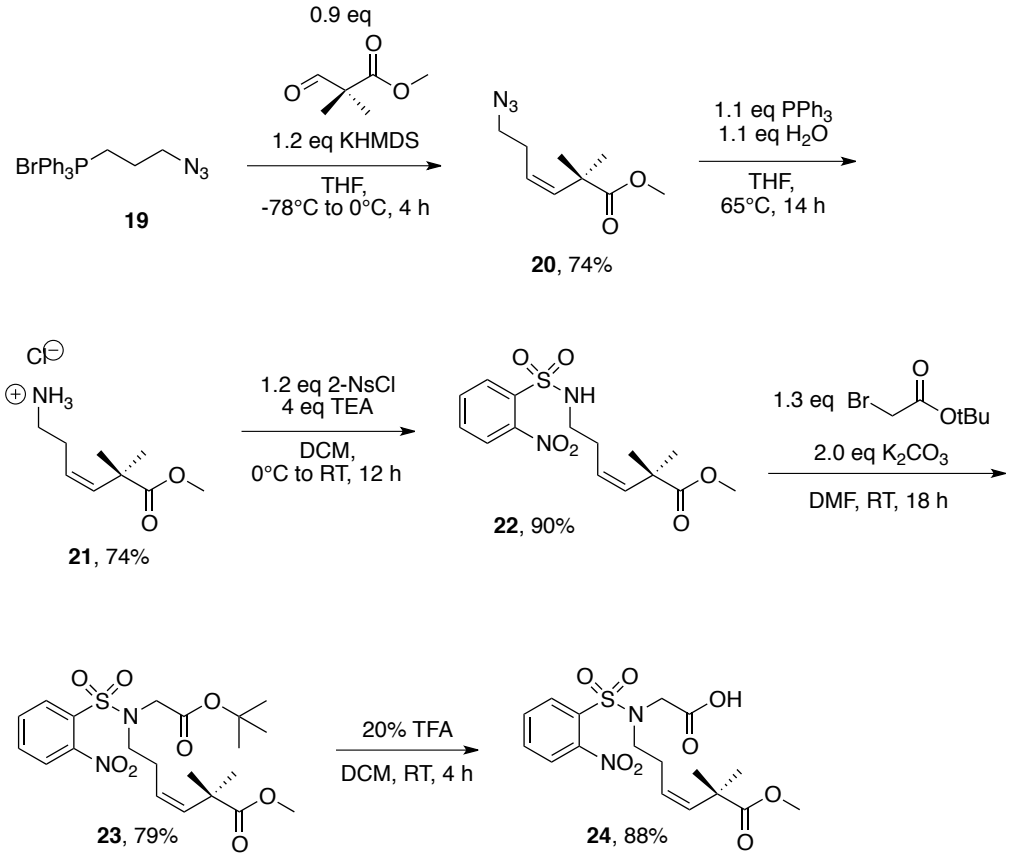

Figure S7. Synthesis of Z^N-HBS^{DM} linker.

Linker Synthesis Procedures and Analytical Data.

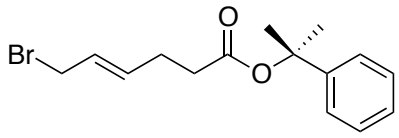

(*E*)-2-phenyl-2-propyl 6-bromo-4-hexenoate (16a). Acetate (**15a**, 11.6 mmol) was dissolved in dry THF (15 mL) and cooled to -78 °C. LDA (12.0 mmol) was added slowly and the resulting mixture was stirred at -78 °C for 30 min. In a separate flask, *E*-1,4-dibromo-2-butene (16.5 mmol) was dissolved in dry THF (20 mL) and the solution cooled to -78 °C. The chilled enolate solution was transferred into the dibromoalkene flask via cannula and the reaction mixture was stirred at -78 °C. After 20 min, the mixture was warmed to 22 °C over one hour and stired at 22 °C for another 2 h. The reaction mixture was diluted with 100 mL ethyl ether and washed with saturated aqueous NH_4Cl (2x, 50 mL). The organic layer was washed with brine (50 mL), dried over anhyd. $MgSO_4$, and filtered. The solvent was removed under vacuum. The residue was purified via column chromatography (hexanes to 1% EtOAc/hexanes to 5% EtOAc/hexanes).[5] The desired product was isolated as a clear oil (1.87 g, 6.01 mmol). 52% yield. Rf = 0.34 (1:33 EtOAc: hexanes); IR (CH_2Cl_2): 3089, 3061, 3028, 2979, 2933, 1731, 1661, and 1603 cm^{-1}; ^1H NMR ($CDCl_3$, 400 MHz): δ 1.78 (s, 6H), 2.36-2.41 (m, 4H), 3.92-3.94 (d, 2H), 5.71-5.78 (m, 2H), 7.24-7.26 (m, 1H), 7.32-7.37 (m, 4H); ^{13}C NMR ($CDCl_3$, 100 MHz): δ 27.3, 28.6, 32.9, 34.4, 81.7, 124.2, 127.0, 127.4, 128.3, 134.2, 145.8, and 171.3. LRMS (ESI) m/z: $[M+H]^+$ Calcd for $C_{15}H_{20}O_2Br$ 311.1; Found 311.1.

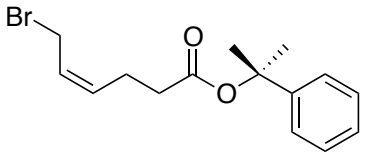

(*Z*)-2-phenyl-2-propyl 6-bromo-4-hexenoate (16b). See procedure for **16a**. Pale yellow oil (4.55 g, 14.7 mmol). 74% yield. Rf = 0.52 (1:19 EtOAc: hexanes); IR (CH_2Cl_2): 3089, 3062, 3027, 2979, 2954, 2924, 2854, 1733, 1649, and 1603 cm^{-1}; ^1H NMR ($CDCl_3$, 400 MHz): δ 1.78 (s, 6H), 2.42-2.44 (m, 4H), 3.97-3.99 (d, 2H), 5.54-5.60 (m, 1H, J = 10.4 Hz), 5.74-5.81 (m, 1H, J = 10.4 Hz), 7.24-7.27 (m, 1H), 7.32-7.38 (m, 4H); ^{13}C NMR ($CDCl_3$, 100 MHz): δ 22.4, 26.8, 28.6, 34.5, 81.8, 124.3, 126.7, 127.0, 128.3, 133.4, 145.7, and 171.3. LRMS (ESI) m/z: $[M+H]^+$ Calcd for $C_{15}H_{20}O_2Br$ 311.1; Found 311.1.

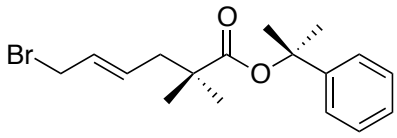

(*E*)-2-phenyl-2-propyl 6-bromo-2,2-dimethyl-4-hexenoate (16c). See procedure for **16a**, with **15b** replacing **15a**. Pale yellow oil (0.71 g, 2.09 mmol). 50% yield. Rf = 0.33 (1:27 EtOAc: hexanes); IR: 3090, 3061, 3034, 2978, 2932, 2873, 1725, 1659, 1604, and 1584 cm^{-1}; ^1H NMR ($CDCl_3$, 400 MHz): δ 1.18 (s, 6H), 1.78 (s, 6H), 2.31-2.32 (d, 2H), 3.93-3.94 (d, 2H), 5.68-5.80 (m, 2H), 7.24-7.28 (m, 1H), 7.32-7.38 (m, 4H); ^{13}C NMR ($CDCl_3$, 150 MHz): δ 24.9, 28.5, 32.9, 42.7, 42.8, 81.4, 124.2, 127.0, 128.2, 129.5, 132.0, 145.9, and 175.6. LRMS (ESI) m/z: $[M+H]^+$ Calcd for $C_{17}H_{24}O_2Br$ 339.1; Found 339.1.

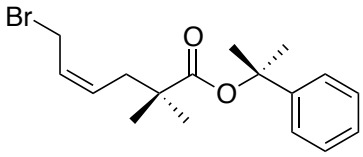

(*Z*)-2-phenyl-2-propyl 6-bromo-2,2-dimethyl-4-hexenoate (16d). See procedure for **16a**, with **15b** replacing **15a**. Pale yellow oil; 69% yield. Rf = 0.39 (1:14 EtOAc: hexanes); IR: 3090, 3061, 3028, 2978, 2932, 2872, 1725, 1648, 1603, and 1584 cm^{-1}; ^{1}H NMR (CD_2Cl_2, 400 MHz): δ 1.20 (s, 6H), 1.74 (s, 6H), 2.38-2.40 (d, 2H), 4.00-4.02 (d, 2H), 5.55-5.61 (m, 1H, J = 10.8 Hz), 5.81-5.88 (m, 1H, J = 10.8 Hz), 7.24-7.27 (m, 1H), 7.33-7.35 (m, 4H); ^{13}C NMR (CD_2Cl_2, 100 MHz): δ 19.1, 25.1, 27.6, 28.6, 28.8, 37.5, 42.8, 81.6, 124.6, 127.2, 127.9, 128.5, 131.4, 146.5, and 175.7. LRMS (ESI) m/z: $[M+H]^+$ Calcd for $C_{17}H_{24}O_2Br$ 339.1; Found 339.1.

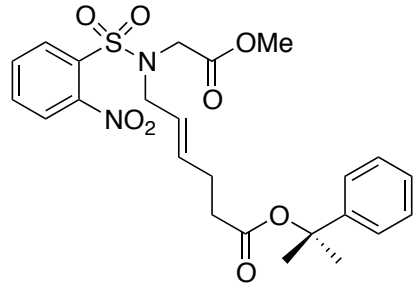

2-Nosyl-*N*-((*E*)-2-phenyl-2-propyl 4-hexenoate) glycine methyl ester (17a). Hexenoate **16a** (2.04 g, 6.57 mmol) and 2-nosyl glycine methyl ester (1.64 g, 5.97 mmol) were dissolved in DMF (20 mL). Potassium carbonate (1.82g, 13.1 mmol) was added and the reaction stirred overnight at room temperature. The reaction was diluted in ethyl acetate (100 mL) and washed sequentially with water (1x, 30 mL), 10% citric acid (30 mL, 1x), saturated $NaHCO_3$ (1x, 30 mL), and brine (1x, 50 mL) before drying over $MgSO_4$. The organic layer was filtered and evaporated under vacuum. Column chromatography on silica (10-40% ethyl acetate in hexanes) yielded **17a** as a yellow oil (2.29 g, 4.54 mmol). 76% yield. Rf = 0.29 (1:2 EtOAc: hexanes); IR:

3090, 3061, 2981, 2952, 1731, 1590, and 1542 cm^{-1}; ^1H NMR ($CDCl_3$, 400 MHz): δ 1.76 (s, 6H), 2.31-2.35 (m, 4H), 3.65 (s, 3H), 3.97-3.99 (d, 2H), 4.10 (s, 2H), 5.36-5.44 (m, 1H, J = 15.2 Hz), 5.60-5.67 (m, 1H, J = 15.2 Hz), 7.23-7.27 (m, 1H), 7.32-7.35 (m, 4H), 7.62-7.65 (m, 1H), 7.68-7.71 (m, 2H), 8.08-8.10 (m, 1H); ^{13}C NMR ($CDCl_3$, 100 MHz): δ 27.3, 28.6, 34.4, 46.7, 50.2, 52.5, 81.7, 124.2, 124.4, 127.1, 128.3, 130.9, 131.7, 133.5, 135.4, 145.7, 148.0, 169.2, and 171.2. HRMS (APCI) m/z: $[M+NH_4]^+$ Calcd for $C_{24}H_{32}N_3O_8S$ 522.1905; Found 522.1907.

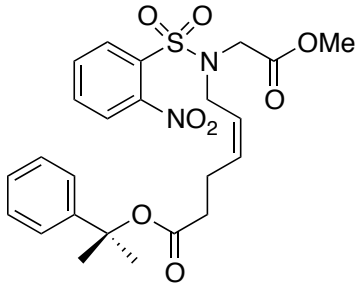

2-Nosyl-*N*-((*Z*)-2-phenyl-2-propyl 4-hexenoate) glycine methyl ester (17b). See procedure for **17a**. Yellow oil (0.67 g, 1.33 mmol). 77% yield. Rf = 0.27 (1:2 EtOAc: hexanes); IR: 3090, 3062, 3024, 2981, 2952, 1731, 1590, and 1542cm^{-1}; ^1H NMR ($CDCl_3$, 400 MHz δ 1.75 (s, 6H), 2.23-2.28 (q, 2H), 2.32-2.36 (t, 2H), 3.61 (s, 3H), 4.06 (s, 2H), 4.08-4.10 (d, 2H), 5.33-5.40 (m, 1H, J = 10.8 Hz), 5.58-5.64 (m, 1H, J = 10.8 Hz), 7.24-7.27 (m, 1H), 7.32-7.33 (d, 4H), 7.64-7.65 (m, 1H), 7.65-7.71 (m, 2H), 8.07-8.10 (m, 1H); ^{13}C NMR (CD_2Cl_2, 100 MHz): δ 22.4, 28.7, 34.5, 44.8, 46.9, 52.2, 81.8, 124.2, 124.4, 127.0, 128.3, 130.9, 131.7, 133.4, 133.5, 134.3, 145.7, 147.9, 169.4, and 171.1. HRMS (APCI) m/z: $[M+NH_4]^+$ Calcd for $C_{24}H_{32}N_3O_8S$ 522.1905; Found 522.1910.

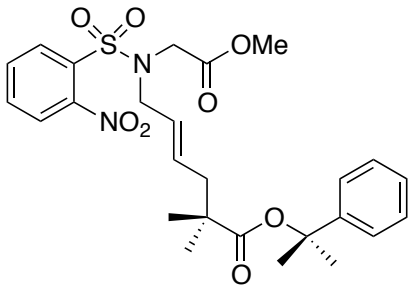

2-Nosyl-*N*-((*E*)-2-phenyl-2-propyl 2,2-dimethyl-4-hexenoate) glycine methyl ester (17c). See procedure for **17a**. Pale yellow oil (0.86 g, 1.62 mmol). 87% yield. Rf = 0.42 (1:2 EtOAc: hexanes); IR: 3479 (broad), 3093, 3056, 2984, 2946, 2878, 1763, 1722, 1590, and 1544 cm^{-1}; ^1H NMR ($CDCl_3$, 400 MHz δ 1.13 (s, 6H), 1.75 (s, 6H), 2.25-2.27 (d, 2H), 3.64 (s, 3H), 3.98-4.00 (d, 2H), 4.11 (s, 2H), 5.38-5.45 (m, 1H, J = 15.2 Hz), 5.53-5.60 (m, 1H, J = 15.2 Hz), 7.24-7.26 (m, 1H), 7.33-7.34 (m, 4H), 7.62-7.65 (m, 1H), 7.65-7.71 (m, 2H), 8.07-8.10 (m, 1H); ^{13}C NMR (CD_2Cl_2, 100 MHz): δ 24.9, 28.4, 42.5, 42.9, 46.7, 50.2, 52.2, 81.4, 124.1, 124.2, 126.6, 127.0, 128.2, 130.9, 131.8, 133.1, 133.5, 133.5, 145.8, 147.9, 169.2, and 175.5. HRMS (APCI) m/z: $[M+NH_4]^+$ Calcd for $C_{26}H_{36}N_3O_8S$ 550.2218; Found 550.2223.

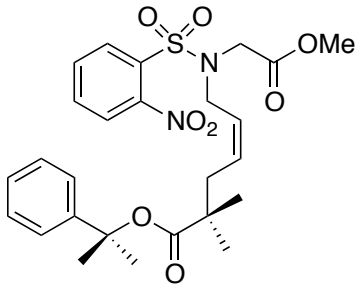

2-Nosyl-*N*-((*Z*)-2-phenyl-2-propyl 2,2-dimethyl-4-hexenoate) glycine methyl ester (17d). See procedure for **17a**. Yellow oil. 87% yield. Rf = 0.36 (1:2 EtOAc: hexanes); IR (CH_2Cl_2): 3092, 3064, 3025, 2979, 2875, 1751, 1723, 1590, and 1543 cm^{-1}; ^1H NMR ($CDCl_3$, 400 MHz): δ 1.15 (s, 6H), 1.75 (s, 6H), 2.22-2.24 (d, 2H), 3.64 (s, 3H), 4.10-4.11 (m, 4H), 5.39-5.46 (m, 1H, J = 10.8 Hz), 5.60-5.67 (m, 1H, J = 10.8 Hz), 7.24-7.26 (m, 1H), 7.32-7.33 (m, 4H), 7.62-7.65 (m,

1H), 7.65-7.71 (m, 2H), 8.07-8.10 (m, 1H); ^{13}C NMR ($CDCl_3$, 100 MHz): δ 25.1, 28.6, 37.5, 42.7, 45.0, 47.0, 52.3, 81.6, 124.3, 124.4, 125.5, 127.2, 128.4, 131.1, 131.9, 132.3, 133.6, 133.7, 145.9, 148.1, 169.5, and 175.6. HRMS (APCI) m/z: $[M+Na]^+$ Calcd for $C_{26}H_{32}N_2O_8SNa$ 555.1772; Found 555.1773.

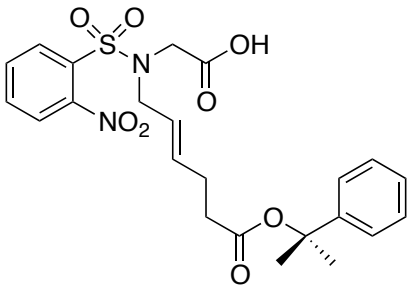

2-Nosyl-*N*-((*E*)-2-phenyl-2-propyl 4-hexenoate) glycine (18a). Methyl ester (**17a**, 2.26 g, 4.48 mmol) was dissolved in 20 mL THF and cooled to 4 °C. Lithium hydroxide monohydrate (0.53 g, 12.6 mmol) was dissolved in 20 mL water and cooled to 4 °C. The chilled aqueous base was then added to the chilled THF solution and the reaction stirred for 18 h at 4 °C. The THF was removed under vacuum and washed with ethyl ether (1x, 20 mL). The aqueous layer was acidified with chilled 10% citric acid (20 mL) before extracting with ethyl acetate (3x, 20 mL). The combined ethyl acetate layers were washed with brine (1x, 20 mL) and dried over $MgSO_4$, filtered, and the solvent removed under vacuum. The product was isolated without additional purification as a yellow oil (1.31 g, 2.67 mmol). 60% yield. Rf = 0.29 (1:1 EtOAc: hexanes w/ 0.1% AcOH); IR: 3498 (broad), 3091, 3060, 3025, 2981, 2934, 1727, 1655, 1591, and 1541 cm^{-1}; ^{1}H NMR ($CDCl_3$, 400 MHz δ 1.76 (s, 6H), 2.29-2.32 (t, 2H), 2.34-2.38 (m, 2H), 3.95-3.97 (d, 2H), 4.09 (s, 2H), 5.33-5.41 (m, 1H, J = 15.6 Hz), 5.61-5.68 (m, 1H, J = 15.6 Hz), 7.22-7.27 (m, 1H), 7.31-7.37 (m, 4H), 7.61-7.65 (m, 1H), 7.66-7.70 (m, 2H), 8.03-8.06 (m, 1H), 9.46 (s, 1H); ^{13}C NMR ($CDCl_3$, 100 MHz): δ 27.3, 28.6, 34.4, 46.7, 50.2, 82.0, 124.3, 124.4, 127.1, 128.3,

130.8, 132.0, 133.2, 133.9, 135.6, 145.7, 147.8, 171.7, and 174.0. HRMS (APCI) m/z: $[M+Na]^+$ Calcd for $C_{23}H_{26}N_2O_8SNa$ 513.1302; Found 513.1302.

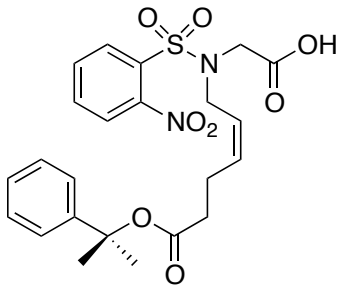

2-Nosyl-*N*-((*Z*)-2-phenyl-2-propyl 4-hexenoate) glycine (18b). Orange oil (0.591 g, 12.1 mmol), 62% yield. Rf = 0.28 (4:1 EtOAc: hexanes); IR (CH_2Cl_2): 3090, 3023, 2980, 2934, 1721, 1590, 1541, and 1496 cm^{-1}; ^1H NMR ($CDCl_3$, 400 MHz): δ 1.75 (s, 6H), 2.25-2.28 (m, 2H), 2.33-2.37 (m, 2H), 4.05-4.06 (d, 4H), 5.32-5.38 (m, 1H, J = 10.8 Hz), 5.57-5.64 (m, 1H, J = 10.8 Hz), 7.23-7.27 (m, 1H), 7.32-7.33 (d, 4H), 7.61-7.70 (m, 3H), 8.04-8.06 (m, 1H), 8.946 (s, 1H); ^{13}C NMR ($CDCl_3$, 100 MHz): δ 22.5, 28.6, 34.5, 44.9, 46.8, 81.9, 124.2, 124.3, 124.3, 127.1, 128.3, 128.7, 130.9, 131.8, 133.2, 133.7, 134.4, 145.6, 147.8, 171.4, and 173.6. HRMS (APCI) m/z: $[M+NH_4]^+$ Calcd for $C_{23}H_{29}N_3O_8S$ 508.1748; Found 508.1745.

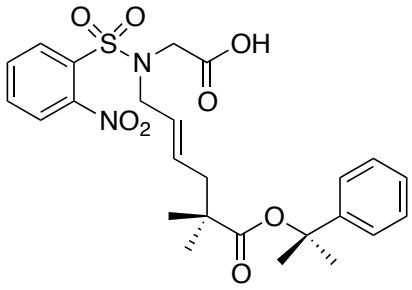

2-Nosyl-*N*-((*E*)-2-phenyl-2-propyl 2,2-dimethyl-4-hexenoate) glycine (18c). White powder (0.67 g, 1.29 mmol). 81% yield. Rf = 0.16 (1:1 EtOAc: hexanes); IR (CH_2Cl_2): 3479 (broad), 3093, 3056, 2983, 2945, 2878, 1763, 1722, 1590, and 1544 cm^{-1}; ^1H NMR ($CDCl_3$, 400 MHz δ 1.13 (s, 6H), 1.75 (s, 6H), 2.25-2.26 (d, 2H), 3.96-3.97 (d, 2H), 4.11 (s, 2H), 5.35-5.42 (m, 1H, J

= 15.6 Hz), 5.54-5.62 (m, 1H, *J* = 15.6 Hz), 7.24-7.27 (m, 1H), 7.30-7.34 (m, 4H), 7.63-7.65 (m, 1H), 7.67-7.72 (m, 2H), 8.05-8.07 (m, 1H); ^{13}C NMR ($CDCl_3$, 100 MHz): δ 24.9, 28.4, 42.6, 42.9, 46.5, 50.2, 81.5, 124.2, 124.4, 126.4, 127.1, 128.3, 130.8, 131.8, 133.2, 133.3, 133.7, 135.6, 145.7, 147.8, 173.8, and 175.6. HRMS (APCI) m/z: $[M+Na]^+$ Calcd for $C_{25}H_{30}N_2O_8SNa$ 541.1615; Found 541.1606.

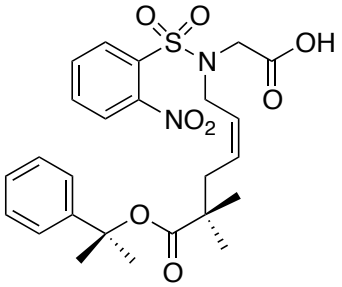

2-Nosyl-*N*-((*Z*)-2-phenyl-2-propyl 2,2-dimethyl-4-hexenoate) glycine (18d). Orange oil. 89% yield. Rf = 0.17 (1:1 EtOAc: hexanes); IR (CH_2Cl_2): 3026, 2978, 2934 (all broad), 1722, 1590, and 1542 cm^{-1}; ^{1}H NMR ($CDCl_3$, 400 MHz): δ 1.15 (s, 6H), 1.74 (s, 6H), 2.21-2.23 (d, 2H), 4.05-4.07 (m, 4H), 5.37-5.43 (m, 1H, *J* = 11.2 Hz), 5.59-5.65 (m, 1H, *J* = 11.2 Hz), 7.22-7.26 (m, 1H), 7.32-7.33 (d, 4H), 7.63-7.70 (m, 3H), 8.04-8.07 (m, 1H), 9.45 (s, 1H); ^{13}C NMR ($CDCl_3$, 100 MHz): δ 25.0, 28.4, 37.4, 42.6, 44.9, 47.1, 81.6, 124.2, 124.3, 125.2, 127.0, 128.3, 130.9, 131.9, 132.1, 133.2, 133.7, 145.8, 147.8, 174.2, and 175.6. HRMS (APCI) m/z: $[M+Na]^+$ Calcd for $C_{25}H_{30}N_2O_8SNa$ 541.1615; Found 541.1622.

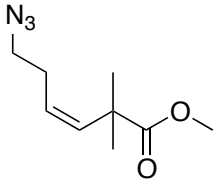

(*Z*)-methyl 6-azido-2,2-dimethyl-3-hexenoate (20). Synthesis was adapted from a previously-reported Wittig reaction using methyl 2,2-dimethyl-3-oxopropionate.[7] 3-Azidopropyl-triphenylphosphonium bromide salt[8a, 8d] (0.985 g, 2.3 mmol) was added to a dry 100 mL flask

with stir bar and purged with N_2. The flask was charged with 20 mL dry THF and the suspension chilled to -78 °C under nitrogen atmosphere. While stirring, a 0.63 M potassium bis(trimethylsilyl)amide in THF solution (4 mL, 2.5 mmol) was added dropwise to the reaction flask over 10 min. The reaction was stirred for 1 h at -78 °C, after which methyl 2,2-dimethyl-3-oxopropionate (0.262 g, 2.0 mmol) was added to the solution. The reaction was stirred at -78 °C for another hour before warming to 22 °C and stirring 1 h. The reaction was quenched with 10 mL methanol and then diluted with 40 mL ethyl ether. The organic layer was washed with saturated ammonium chloride (1x, 10 mL) and brine (1x, 10 mL). The organic layer was dried over anhyd. $MgSO_4$, filtered, and the solvent removed under vacuum. Product was purified using column chromatography on silica (mobile phase: pentane → 10% ethyl ether in pentane), the solvent evaporated, and product isolated as a pale yellow oil. 74% yield. R_f = 0.26 (1:9 Et_2O: hexanes); IR: 3013, 2976, 2951, 2875, 2090, 1728, and 1649 cm^{-1}; ^1H NMR ($CDCl_3$, 400 MHz): δ 1.35 (s, 6H), 2.23-2.29 (q, 2H), 3.25-3.28 (t, 2H), 3.70 (s, 3H), 5.30-5.37 (m, 1H, J = 11.2 Hz), 5.52-5.56 (m, 1H, J = 11.2 Hz); ^{13}C NMR ($CDCl_3$, 100 MHz): δ 27.1, 27.7, 43.0, 50.7, 52.1, 126.8, 137.2, and 177.7. HRMS (APCI) m/z: $[M+Na]^+$ Calcd for $C_9H_{15}N_3O_2Na$ 220.1056; Found 220.1046.

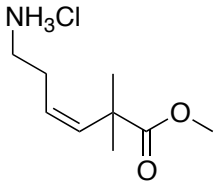

(*Z*)-methyl 6-amino-2,2-dimethyl-3-hexenoate hydrochloride salt (21). (*Z*)-6-azido-2,2-dimethyl-3-hexenoate methyl ester (**20,** 0.277 g, 1.4 mmol) and triphenylphosphine (0.405 g, 1.55 mmol) were added to a dry 25 mL flask containing 10 mL THF.[9] A condenser was attached, water (0.029 mL, 1.67 mmol) added, and the reaction stirred at 22 °C for 30 min. The reaction

was heated to reflux and stirred 12 h. Reaction was cooled to 22 °C, diluted in 30 mL ethyl ether and extracted with 1 M HCl (2x, 20 mL). The combined aqueous layers were washed with 20 mL ethyl ether, frozen, and lyophilized. Product was isolated as a white solid (0.214 g, 1.03 mmol). 74% yield. IR: 3017, 2971, 2951 (all broad), 1725, 1593, 1573, and 1521 cm^{-1}; ^{1}H NMR (d_6-DMSO, 400 MHz): δ 1.27 (s, 6H), 2.19-2.25 (q, 2H), 2.71-2.76 (m, 2H), 3.65 (s, 3H), 5.27-5.33 (m, 1H, J = 11.6 Hz), 5.47-5.51 (m, 1H, J = 11.6 Hz), 8.09 (s, 3H); ^{13}C NMR (d_6-DMSO, 100 MHz): δ 26.1, 27.2, 38.6, 42.9, 52.5, 126.3, 137.1, and 177.2. HRMS (APCI) m/z: $[M+Na]^+$ Calcd for $C_9H_{18}NO_2$ 172.1332; Found 172.1334.

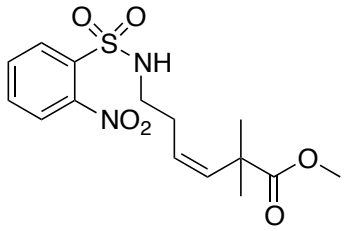

(*Z*)-(*N*-2-Nosyl)-6-amino-2,2-dimethyl-3-hexenoic acid methyl ester (22). The hydrochloride salt of (*Z*)-6-amino-2,2-dimethyl-3-hexenoate methyl ester (0.2 g, 0.966 mmol) was suspended in 5 mL dry DCM in a dry 25 mL flask. A stir bar and 2-nitrobenzene sulfonyl chloride (0.257 g, 1.16 mmol) were added, a dropping funnel attached, and triethylamine (0.3 mL, 2.15 mmol) added to to funnel. The reaction was stirred and cooled in an ice bath to 4 °C under a nitrogen atmosphere, after which was base slowly added to the reaction over 10 min. Stirring was continued at 4 °C for 1.5 h, the reaction warmed to 22 °C and stirred 3 h more. DCM (10 mL) was added and the reaction transferred to a separatory funnel. The organic layer was washed with 1M HCl (20 mL, 1x) and brine (20 mL, 1x), dried over $MgSO_4$, filtered, and the solvent removed under vacuum. Column chromatography on silica (mobile phase 20-60% DCM in hexanes, then hexane wash followed by 33-40% ethyl acetate in hexanes) yielded a white solid (0.31 g, 0.87 mmol). 90% yield. Rf = 0.22 (1:2 EtOAc: hexanes); IR (CH_2Cl_2): 3054, 3006,

2987, 2306, 1729, and 1545 cm^{-1}; ^1H NMR ($CDCl_3$, 400 MHz): δ 1.32 (s, 6H), 2.21-2.27 (q, 2H), 3.09-3.14 (q, 2H), 3.71 (s, 3H), 5.17-5.24 (m, 1H, J = 11.6 Hz), 5.34-5.37 (t, 1H), 5.52-5.55 (m, 1H, J = 11.6 Hz), 7.74-7.77 (m, 1H), 7.86-7.89 (m, 2H), 8.14-8.16 (m, 1H); ^{13}C NMR ($CDCl_3$, 100 MHz): δ 27.2, 28.0, 43.0, 43.2, 52.3, 125.4, 126.5, 131.1, 132.8, 133.5, 133.6, 137.9, 148.1, and 177.7. HRMS (APCI) m/z: $[M+Na]^+$ Calcd for $C_{15}H_{20}N_2O_6SNa$ 379.0934; Found 379.0946.

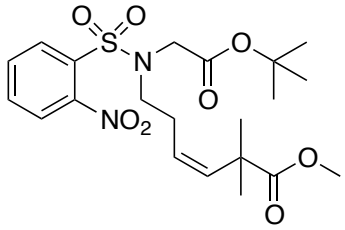

2-Nosyl-*N*-((*Z*)-methyl 2,2-dimethyl-3-hexenoate) glycine t-butyl ester (23). Sulfonamide (**23**, 0.85 mg, 2.39 mmol) was dissolved in 20 mL DMF along with t-butyl bromoacetate (0.59 mg, 3.05 mmol) and potassium carbonate (0.66 g, 4.77 mmol). The reaction was stirred for 24 h at 22 °C. Water (50 mL) was added and extracted with EtOAc (50 mL, 3x). The combined organic layers were washed with water (50 mL, 2x) and brine (50 mL) and the combined aqueous layers extracted with ethyl ether (50 mL, 2x). The combined ether layers were washed with brine (50 mL) and added to the ethyl acetate layers. The combined ethyl acetate and ethyl ether solution was dried over $MgSO_4$, filtered, and the solvent removed under vacuum.[6] Column chromatography on silica (10-30% ethyl acetate in hexanes) yielded a yellow oil (0.884 g, 1.88 mmol). 79% yield. Rf = 0.27 (1:4 EtOAc: hexanes); IR: 3096, 2978, 2950, 1726, 1590, and 1543 cm^{-1}; ^1H NMR ($CDCl_3$, 400 MHz): δ 1.30 (s, 6H), 1.36 (s, 9H), 2.22-2.28 (q, 2H), 3.37-3.41 (q, 2H), 3.68 (s, 3H), 4.06 (s, 2H), 5.21-5.27 (m, 1H, J = 11.6 Hz), 5.45-5.48 (m, 1H, J = 11.6 Hz), 7.58-7.60 (m, 1H), 7.67-7.69 (m, 2H), 8.06-8.08 (m, 1H); ^{13}C NMR ($CDCl_3$, 100 MHz): δ 26.7, 27.1, 27.9, 43.0, 47.6, 48.4, 52.2, 82.3, 124.0, 126.6, 130.9, 131.7, 133.4, 133.5,

137.0, 147.9, 167.6, and 177.6. HRMS (APCI) m/z: $[M+Na]^+$ Calcd for $C_{21}H_{30}N_2O_8SNa$ 493.1615; Found 493.1620.

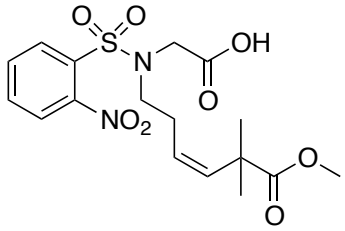

2-Nosyl-*N*-((*Z*)-methyl 2,2-dimethyl-3-hexenoate) glycine (24. 2-Nosyl glycine t-butyl ester (0.88 g, 1.87 mmol) was dissolved in 25 mL 20% TFA in DCM and stirred for 4 h at 22 °C. The solvent was removed under vacuum and the residue dissolved in 20 mL ethyl ether, extracted with 1% aqueous sodium bicarbonate solution (3x, 40 mL). The aqueous layer was acidified with 6 M aqueous HCl to pH 1 and extracted with with 50 mL chloroform (3x). The chloroform layer was washed with saturated brine solution (1x, 50 mL), dried over $MgSO_4$, filtered, and the solvent removed under vacuum. Product was isolated without further purification as a yellow oil (0.68 g, 1.64 mmol). 93% yield. Rf = 0.12 (3:2 EtOAc: hexanes w/ 0.1% AcOH); IR: 3098, 2977, 2952 (all broad), 1723, 1590, and 1543 cm^{-1}; ^1H NMR ($CDCl_3$, 400 MHz): δ 1.31 (s, 6H), 2.23-2.29 (q, 2H), 3.37-3.41 (q, 2H), 3.68 (s, 3H), 4.22 (s, 2H), 5.20-5.26 (m, 1H, J = 11.6 Hz), 5.45-5.49 (m, 1H, J = 11.6 Hz), 7.64-7.66 (m, 1H), 7.69-7.75 (m, 2H), 8.06-8.08 (m, 1H), 8.65 (s, 1H); ^{13}C NMR ($CDCl_3$, 100 MHz): δ 26.7, 27.1, 43.0, 47.6, 47.8, 52.2, 124.3, 126.2, 130.9, 131.8, 133.1, 133.7, 137.3, 147.8, 173.6, and 177.7. HRMS (APCI) m/z: $[M+Na]^+$ Calcd for $C_{17}H_{22}N_2O_8SNa$ 437.0989; Found 437.0993.

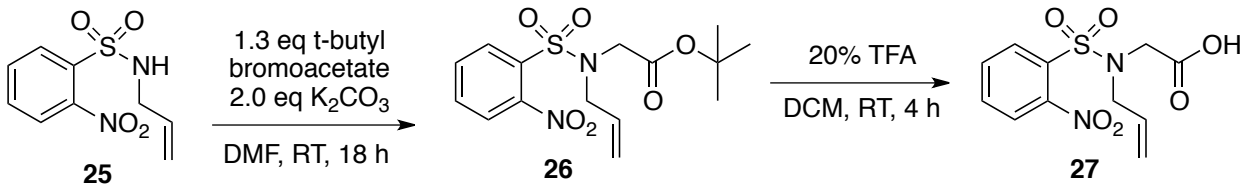

Figure S8. Synthesis of 2-Ns-*N*-Allylglycine.

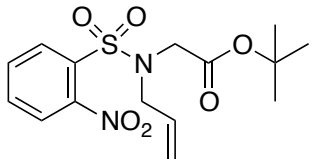

2-Nosyl *N*-allylglycine t-butyl ester (26). 2-Nosyl allylamine[10] (**25**, 4.06 g, 16.7 mmol) and t-butyl bromoacetate (4.14 g, 21.2 mmol) were dissolved in DMF (50 mL). Potassium carbonate (4.89 g, 35.4 mmol) was added and the reaction stirred overnight at 22 °C. Allylamine (2 mL, 26.7 mmol) was added and the reaction stirred one hour at 22 °C. Reaction was diluted in ethyl ether (100 mL) and washed with water (100 mL). The organic layer was washed with 1 M HCl (50 mL, 3x), saturated $NaHCO_3$ (50 mL), and brine (50 mL) before drying over $MgSO_4$. The organic layer was filtered and evaporated under vacuum. The product was recrystallized from ethyl ether and pet ether to produce **26** (5.03 g, 85%) as white crystals. IR (CH_2Cl_2): 1742, 1547, and 1370 cm^{-1}; ^1H NMR ($CDCl_3$, 400 MHz): δ 1.38 (s, 9H), 4.04-4.06 (m, 4H), 5.25-5.20 (m, 2H), 5.70-5.80 (m, 1H), 7.62-7.65 (m, 1H), 7.66-7.71 (m, 2H), 8.08-8.11 (m, 1H); ^{13}C NMR ($CDCl_3$, 100 MHz): δ 28.1, 48.0, 51.2, 82.4, 120.3, 124.3, 131.2, 131.9, 132.3, 133.6, 133.9, 148.2, and 167.8. HRMS (APCI) m/z: $[M+Na]^+$ Calcd for $C_{15}H_{20}N_2O_6SNa$ 379.0940; Found 379.0946.

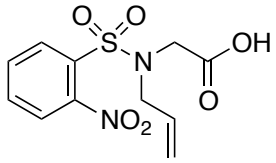

2-Nosyl *N*-allylglycine (27). Protected *N*-allylglycine (6.63 g, 18.6 mmol) was dissolved in DCM (40 mL) in a 250 mL flask and TFA (10 mL) was added. Reaction was stirred at room temperature and monitored with TLC. After 2 hours, more TFA (2 mL) was added and the reaction stirred for 2 hours more at 22 °C. The solvent was removed under vacuum and the product recrystallized from ethyl acetate and hexanes to yield **27** (5.47 g, 98%) as white crystals.

IR (CH_2Cl_2): 3006, 2090, 1731, 1546, 1371, 1275, and 1267 cm^{-1}; ^1H NMR (CD_3CN, 400 MHz): δ 3.99-4.01 (d, 2H), 4.07 (s, 2H), 5.17-5.24 (m, 2H), 5.67-5.76 (m, 1H), 7.71-7.75 (m, 1H), 7.76-7.82 (m, 2H), 8.05-8.08 (m, 1H); ^{13}C NMR (CD_3CN, 100 MHz): δ 46.8, 50.7, 118.9, 124.0, 130.5, 131.8, 132.0, 132.9, 133.9, 147.9, and 170.6. HRMS (APCI) m/z: $[M+Na]^+$ Calcd for $C_{11}H_{12}N_2O_6SNa$ 323.0314; Found 323.0310.

Circular Dichroism Studies

CD spectra were recorded on AVIV 202SF CD spectrometer equipped with a temperature controller using 1 mm length cells and a scan speed of 0.5 nm/sec. The spectra were averaged over 10 scans with the baseline subtracted from analogous conditions as that for the samples. The samples were prepared in 0.1X phosphate buffered saline (13.7 mM NaCl, 1 mM phosphate, 0.27 mM KCl, pH 7.4), with the final peptide concentration of 100 μM. The concentrations of peptides were determined by the UV absorption of the tyrosine (AKG sequences) or tryptophan residue (p53) at 280 nm or by mass (Hif). The helix content of the α-peptides were determined from the mean residue CD at 222 nm, $[\theta]_{222}$ (deg cm^2 $dmol^{-1}$) corrected for the number of amino acids. Percent helicity was calculated from the ratio $[\theta]222/[\theta]max$, where $[\theta]max = (-44000 + 250T)(1 - k/n)$, with k = 4.0 and n = number of residues. Trifluoroethanol was titrated in for each peptide to attain measurements of helicity in PBS, 10% TFE, 20% TFE, 30% TFE, and 40% TFE for all peptides.

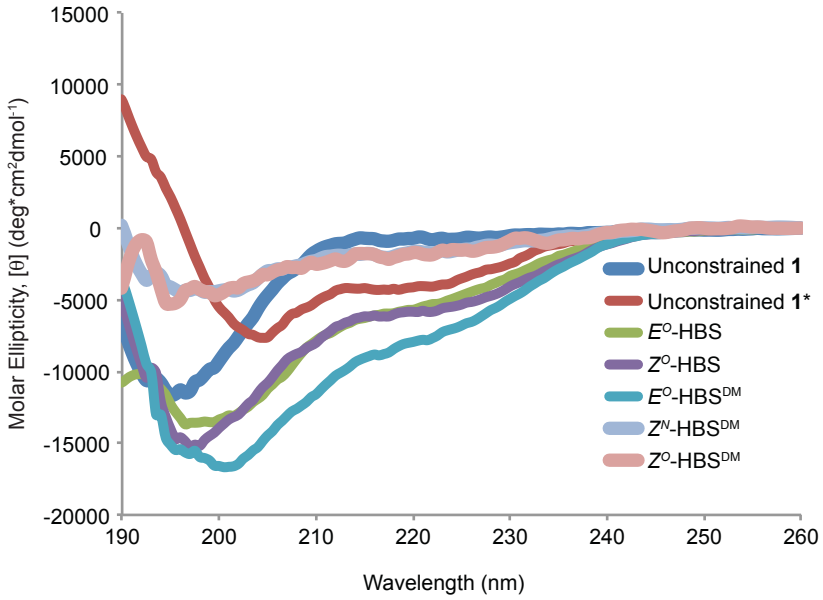

Figure S9. Circular dichroism curves for unconstrained **1** (Ac-AKGAAAAAKAY-NH_2) and HBS derivatives (XAKGAAAAAKAY-NH_2) in 0.1X PBS, pH = 7.6 at 25 °C. *Denotes unconstrained **1** in 30% 2,2,2-trifluoroethanol (TFE) in 0.1X PBS. All other curves were taken in the absence of 2,2,2-trifluoroethanol.

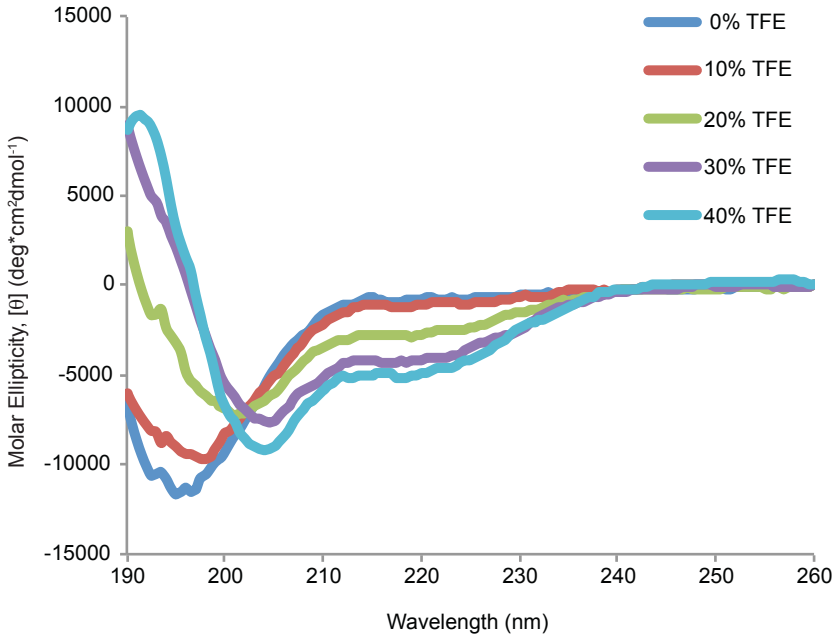

Figure S10. Circular dichroism curves for unconstrained **1** (Ac-AKGAAAAAKAY-NH_2) in 0.1X PBS, pH = 7.6 at 25 °C with increasing amounts of TFE.

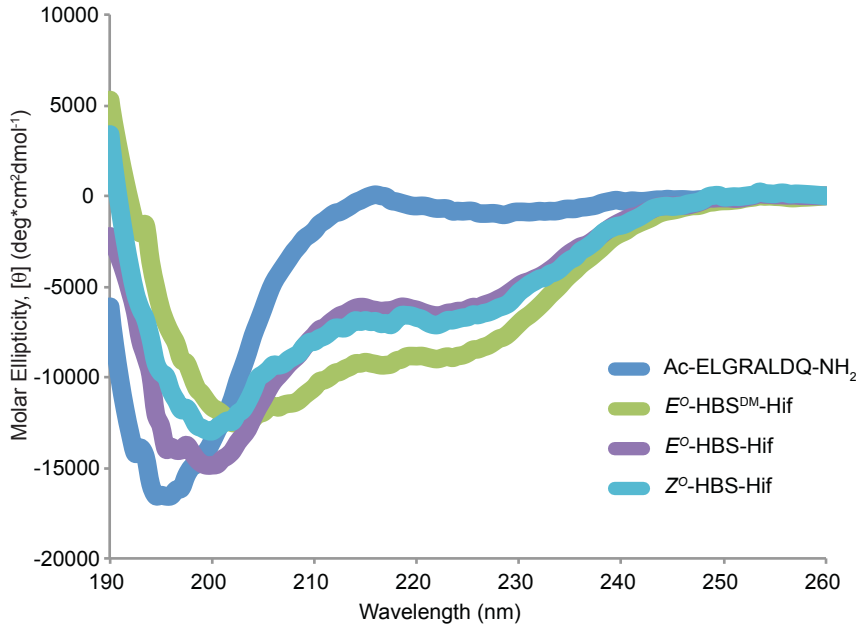

Figure S11. Circular dichroism curves for unconstrained Hif peptide and Hif HBS derivatives in 0.1X PBS, pH = 7.6 at 25 °C.

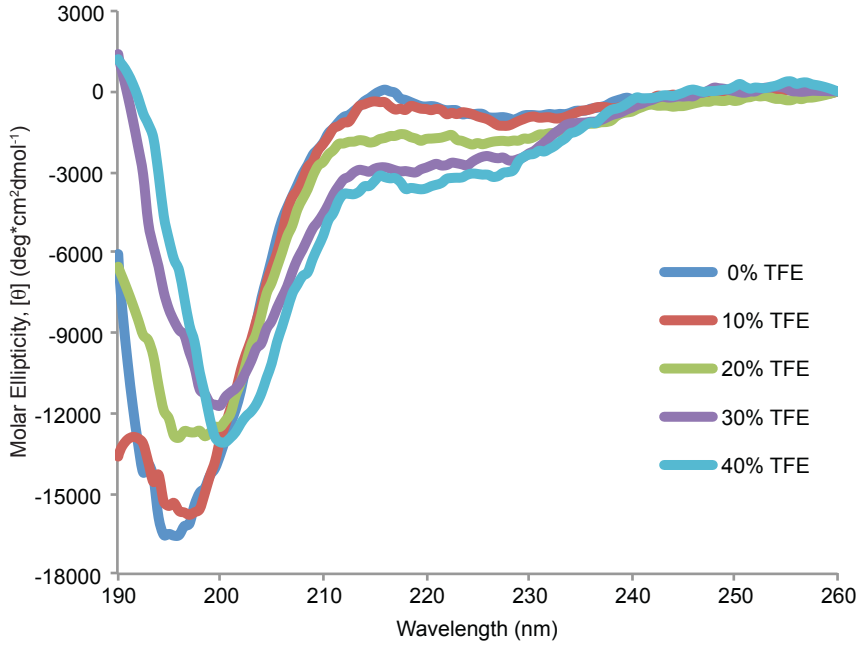

Figure S12. Circular dichroism curves for unconstrained Hif (Ac-ELGRALDQ-NH_2) in 0.1X PBS, pH = 7.6 at 25 °C with increasing amounts of TFE.

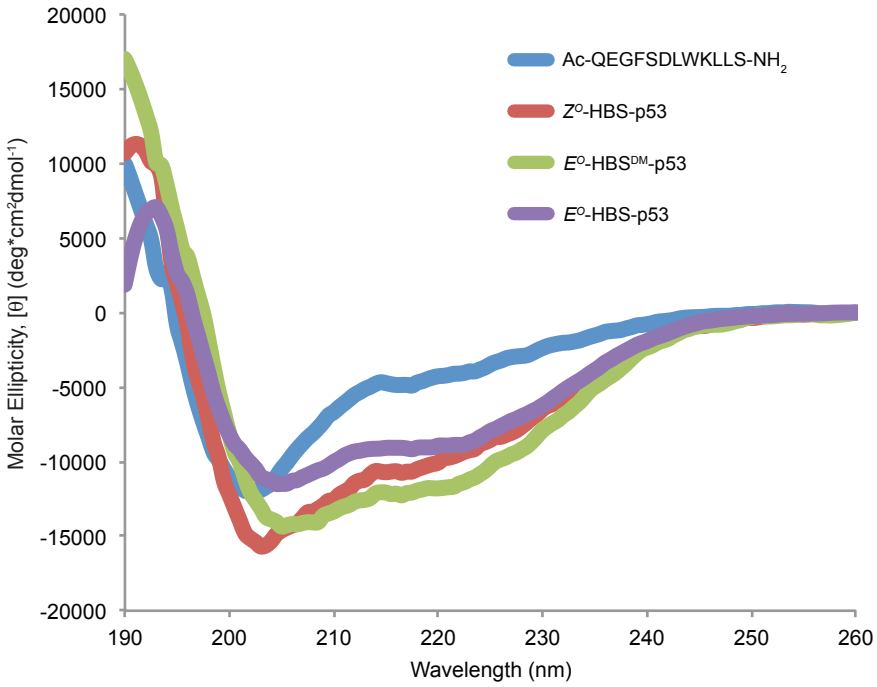

Figure S13. Circular dichroism curves for unconstrained p53 peptide and p53 HBS derivatives in 0.1X PBS, pH = 7.6 at 25 °C.

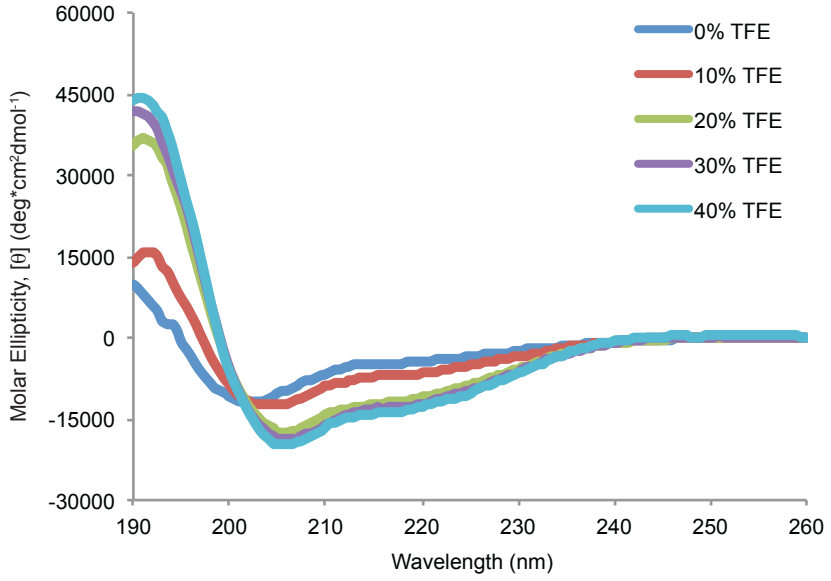

Figure S14. Circular dichroism curves for unconstrained p53 (Ac-QEGFSDLWKLLS-NH_2) in 0.1X PBS, pH = 7.6 at 25 °C with increasing amounts of TFE.

Computational Methods and Results

Computational analysis of each type of HBS macrocycle was employed to understand the superiority of the E^{O}-HBS^{DM} in spite of its poor mimicry of the natural helical hydrogen bond architecture. Additionally, computational assessment was used to investigate the relative incompatibility of HBS *Z*-alkenes and α-dimethyl substitution. All computations were performed using the Macromodel 2015 software package.

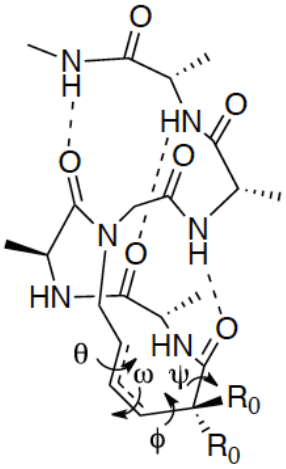

Figure S15. Structure of HBS XAAG*AA-NHMe pentamer utilized for computational studies. Intramolecular *i* to *i+4* hydrogen bonds highlighted by dashed lines. Conformational search on each HBS derivative illuminates the different dihedral combinations (ψ, ϕ, ω, and θ) that accommodate each alkene while maintaining the first three hydrogen bonds.

First, analysis of short HBS peptides was used to determine how different combinations of alkene stereochemistry and position are accommodated into a helix-nucleating HBS macrocycle. Using a short, two-turn HBS peptide (XAAG*AA-NHMe, Figure S15), conformational searches were performed using rigid (2.0 ± 0.5 Å) and flexible (2.5 ± 0.5 Å) hydrogen bond constraints. In total, three different scans were used: 1) Rigid restriction of the second and third *i* to *i+4* hydrogen bonds to assess breaking of the first hydrogen bond, 2) rigid restriction of the first and third *i* to *i+4* hydrogen bonds to determine stability of the second hydrogen bond, and 3) flexible restriction of all three helical hydrogen bonds. Conformational searches illustrated that alkenes are incorporated in different manners while maintaining the

desired helical hydrogen-bonding pattern. Analysis of E^O-HBS and E^O-HBS^{DM} derivatives revealed four and three different combinations of dihedral angles capable of nucleating a helix while Z^O-HBS, Z^O-HBS^{DM}, and Z^N-HBS^{DM} all featured only one helical dihedral combination (Table S2 and Figures S16 and S17). Notably, many of these combinations stray from the standard dihedral angles for helices (Table S2).

To effectively compare each of these dihedral combinations, HBS linkers were excised from their macrocycles and converted to simple hydrocarbons. Octadienes were employed to cover all carbons within the hexenamide linkers while also replacing the amide portion of the linker with a trans-alkene isostere (Figure S18). This provided a very simple system to compare the relative stability of each set of helix-inducing dihedrals. Coordinate scans on each dihedral angle provided relative stabilities for each set of dihedrals. Intriguingly, the lowest energy dihedral combination belonged to E^O-HBS^{DM}, consistent with the experimental data showing that the E^O-HBS^{DM} macrocycle produces the most helical sequences. Meanwhile, E^O-HBS and Z^O-HBS hydrocarbon analogues featured comparable low energy dihedral combinations while dimethylated linkers featuring *Z*-alkenes produced much higher relative energies (Table S2). These computations therefore corroborate the previously observed experimental trends.

Table S2. Dihedral angle combinations that accommodate each alkene while maintaining helical intramolecular hydrogen bonds and the relative energies of each set of rotamers.

Macrocycle	Figure	ψ	ϕ	ω	θ	Rotamer ΔΔG (kcal/mol)
α-Helical Turn	NA	-45°	-60°	≈ 0°	-26°	NA
E^O-HBS	S9A	-115.1° ± 9.62°	53.1° ± 0.14°	-115.6° ± 9.4°	≈ 180°	0.51
	S9B	-141.6° ± 0.35°	57.9° ± 0.21°	14.0° ± 0.85°	≈ 180°	0.70
	S9C	-52.2° ± 0.21°	-47.4° ± 0.07°	-21.5° ± 0.21°	≈ 180°	1.58
	S9D	-67.9° ± 2.59°	-49.4° ± 0.25°	116.4° ± 2.38°	≈ 180°	1.12
E^O-HBS^{DM}	S10A	-56.4° ± 0.14°	-44.1° ± 0.07°	-15.8° ± 0.00°	≈ 180°	2.13
	S10B	-63.0° ± 0.64°	-49.7° ± 0.14°	118.2° ± 1.13°	≈ 180°	1.11
	S10C	-124.4° ± 6.93°	50.1° ± 1.41°	-124.5° ± 21.92°	≈ 180°	0.44
Z^O-HBS	S9E	-81.4° ± 2.15°	-81.8° ± 3.01°	106.6° ± 3.06°	≈ 0°	0.52
Z^O-HBS^{DM}	S10D	-73.6° ± 0.82°	-83.4° ± 1.38°	103.6° ± 2.94°	≈ 0°	1.17
Z^N-HBS^{DM}	S10E	-66.5° ± 3.61°	-55.1° ± 4.88°	≈ 0°	120.1° ± 0.21°	1.49

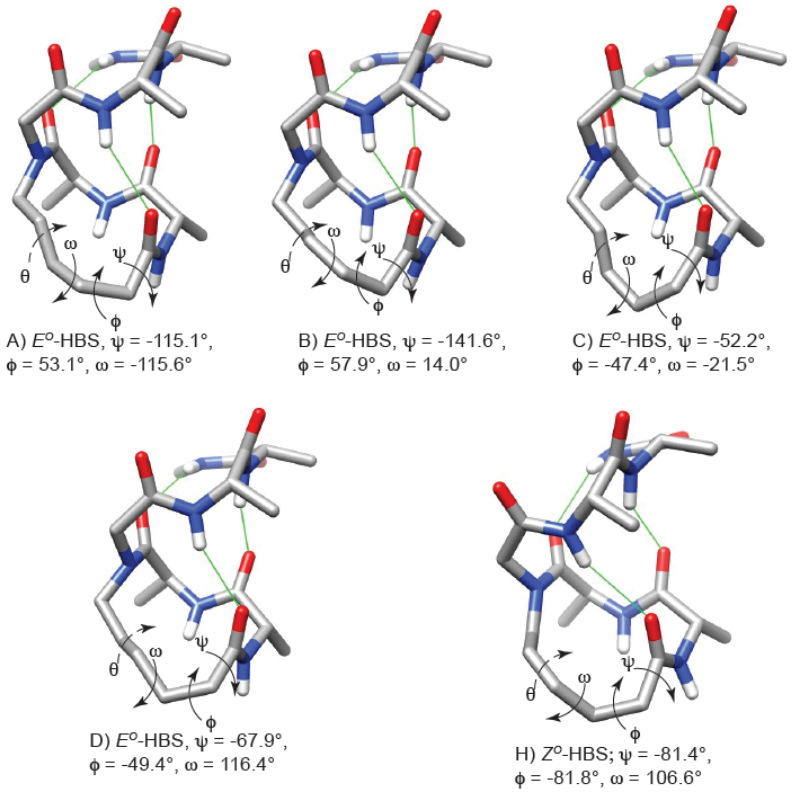

Figure S16. Calculated linker dihedral angles capable of maintaining first three helical *i* to *i+4* hydrogen bonds for E^O and Z^O-HBS linkers. Hydrogen bonds highlighted in green. Dashed θ lines indicate position of alkene bond.

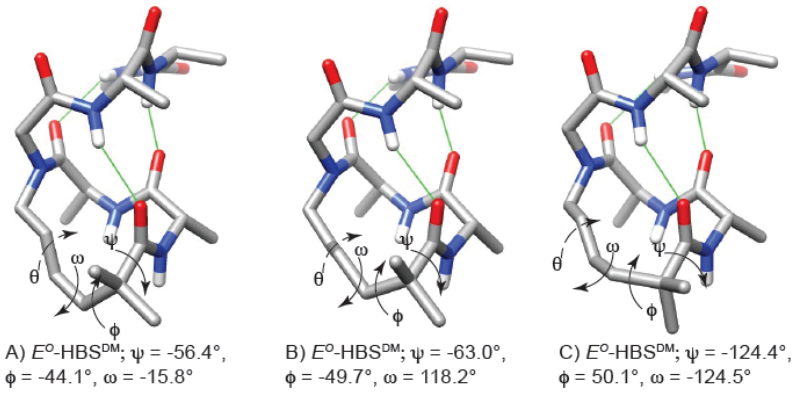

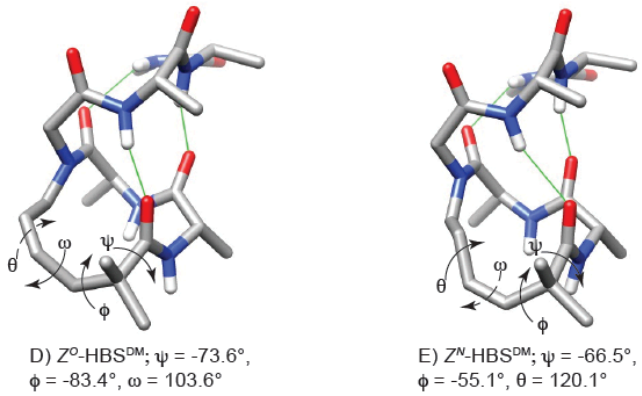

Figure S17. Calculated linker dihedral angles capable of maintaining first three helical *i* to *i+4* hydrogen bonds for E^O/Z^O-HBS^{DM} and Z^N-HBS^{DM} linkers. Hydrogen bonds highlighted in green. Dashed ω or θ lines indicate position of alkene bond.

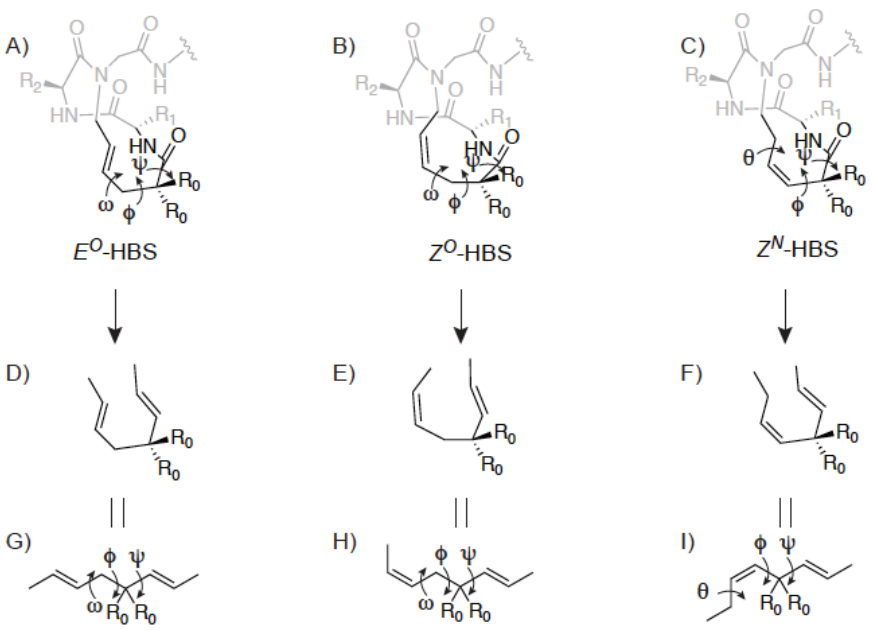

Figure S18. Structure of A) E^O, B) Z^O, and C) Z^N-HBS macrocycles with 4-hexenamide or 3-hexenamide linker portions highlighted in black. The trans amide moiety was converted to methylated *E*-alkene to produce D) *E,E*-2,6-octadiene (R_0 = H) or *E,E*-4,4-dimethyl-2,6-octadiene (R_0 = Me), E) *E,Z*-2,6-octadiene (R_0 = H) or *E,Z*-4,4-dimethyl-2,6-octadiene (R_0 = Me), and F) *E,Z*-4,4-dimethyl-2,5-octadiene (R_0 = Me). Octadiene hydrocarbons used to analyze relative rotamer energies for ψ, ϕ, and ω for E^O and Z^O (G,H) or ψ, ϕ, and θ for Z^N (I)

His6-MDM2 Expression and Purification.

Competent BL21 DE3 pLySS E. coli cells were transformed by the heat shocking the bacteria at 42° C for 1 min in media containing a pET-14B vector containing a His6-tagged MDM2 (25-117) fusion protein. Cells were grown on ampicillin containing agar places (50 mg/mL), and a single culture was used to inoculate a 100 mL overnight culture of LB media containing ampicillin (50 mg/mL). 500 mL of terrific broth (4L flask) was seeded with 50 mL of overnight culture and incubated at 30° C for until the optical density of the media is 1 at 600 nm. Induction of protein expression with 0.4 mM IPTG (Novagen) was done by incubating the flask at 30° C for an additional 4.5 hours. The cells were harvest by centrifugation at 6000 g for 20 minutes and the supernatant was discarded. The cells were resuspended in 10 mL binding buffer (50 mM NaH_2PO_4 (pH 8), 300 mM NaCl, 10 mM imidazole, 2mM β-mercaptoethanol and protease inhibitors (Roche)), and lysed by sonication in ice (15 x 7 seconds pulses). The cells were again centrifuged at 15,000 g for 20 minutes, and the resulting supernatant containing the desired MDM2 fusion protein was incubated with Ni-NTA beads (Novagen) at 4 ºC for 2 h. Beads were washed with 10 ml (x 5) with washing buffer (50 mM NaH_2PO_4 (pH 8), 300 mM NaCl, 25 mM imidazole, 2mM β-mercaptoethanol) and the protein is eluted with elution buffer (50 mM NaH_2PO_4, 300 mM NaCl, 250 mM imidazole, 2mM β-mercaptoethanol, pH 8). The resulting protein was dialyzed in 10 mM PBS (pH 7.5) with 5 mM EDTA and 0.5 mM DTT and concentrated with 3 kD MW cut-off Amicon concentrator tubes (Millipore). Purified MDM2 was characterized by SDS-PAGE analysis, snap-frozen in liquid N_2 and stored at -80 ºC until further use.

Description of His6-MDM2 binding studies.[11]

The relative affinities of peptides for N-terminal His_6-tagged MDM2 (25-117) were determined using fluorescence polarization based competitive binding assay with fluorescein labeled p53 peptide, **Flu-p53**. The polarization experiments were performed with a DTX 880 Multimode Detector (Beckman) at 25° C, with excitation and emission wavelengths at 485 nm and 535 nm, respectively. All samples were prepared in 96 well plates in 0.1% pluronic F-68 (Sigma). The binding affinity (K_D) values reported for each peptide are the averages of 3-5 individual experiments, and were determined by fitting the experimental data to a sigmoidal dose-response nonlinear regression model on GraphPad Prism 4.0. The concentration of the MDM2 protein was determined by a Bradford Assay (BioRad).

Prior to the competition experiments, the affinity of the **Flu-p53** for MDM2 (25-117) was determined by monitoring polarization of the fluorescent probe upon binding MDM2 (25-117). Addition of an increasing concentration (0 nm to 50 μM) of MDM2 (25-117) protein to a 15 nM solution of **Flu-p53** in MDM2 (25-117) dialysis buffer (10 mM PBS (pH 7.4), 5 mM EDTA and 0.5 mM DTT) and 0.1 % pluronic acid afforded the saturation-binding curve (Figure S17). The IC_{50} value obtained from this binding curve was fit into equation (**1)** to calculate the dissociation constant (K_{D1}) for the p53/MDM2 complex.

$$K_{D1} = (R_T*(1-F_{SB}) + L_{ST}*F_{SB}^2)/F_{SB}-L_{ST} \quad (\mathbf{1})$$

where:

R_T = Total concentration of MDM2 protein

L_{ST} = Total concentration of p53 fluorescent peptide

F_{SB} = Fraction of bound p53 fluorescent peptide

The K_{D1} of **Flu-p53** was determined to be 75 ± 10 nM. For competition experiments, a solution

of 300 nM MDM2 and 15 nM **Flu-p53** in MDM2 dialysis buffer (1X PBS (pH 7.4), 5 mM EDTA and 0.5 mM DTT) and 0.1 % pluronic acid was incubated at 25 ºC in a 96 well plate. After 1h appropriate concentrations of the HBS or linear peptides (1 nm to 100 μM) were added to the MDM2- **Flu-p53** solution and the resulting mixtures were incubated at 25° C for 1h before measuring the degree of dissociation of **Flu-p53** by polarization. The IC_{50} was fit into equation (**2)** to calculate the K_{D2} value of the HBS or linear peptides.

$$K_{D2} = K_{D1}*F_{SB}*((L_T/(L_{ST}*F_{SB2} - (K_{D1} + L_{ST} + R_T)*F_{SB} + R_T)) - 1/(1 - F_{SB})) \quad (2)$$

where:

K_{D1} = K_D of fluorescent probe **Flu-p53**

R_T = Total concentration of MDM2 protein

L_{ST} = total concentration of p53 fluorescent peptide

F_{SB} = Fraction of bound p53 fluorescent peptide

L_T = total concentration of HBS peptide

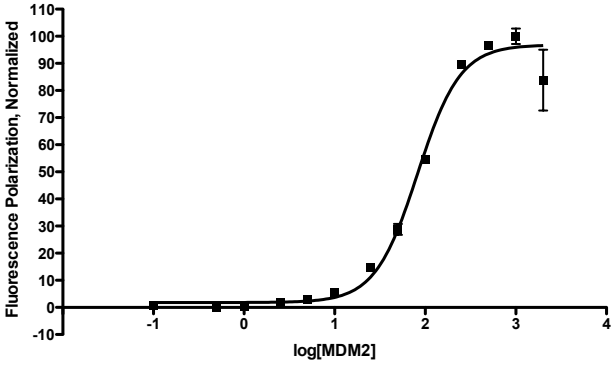

Figure S19. Saturation binding curve of **Flu-p53** with MDM2 in PBS buffer at 25 °C, K_D = 75 ± 10 nM.

^{1}H NMR Spectra

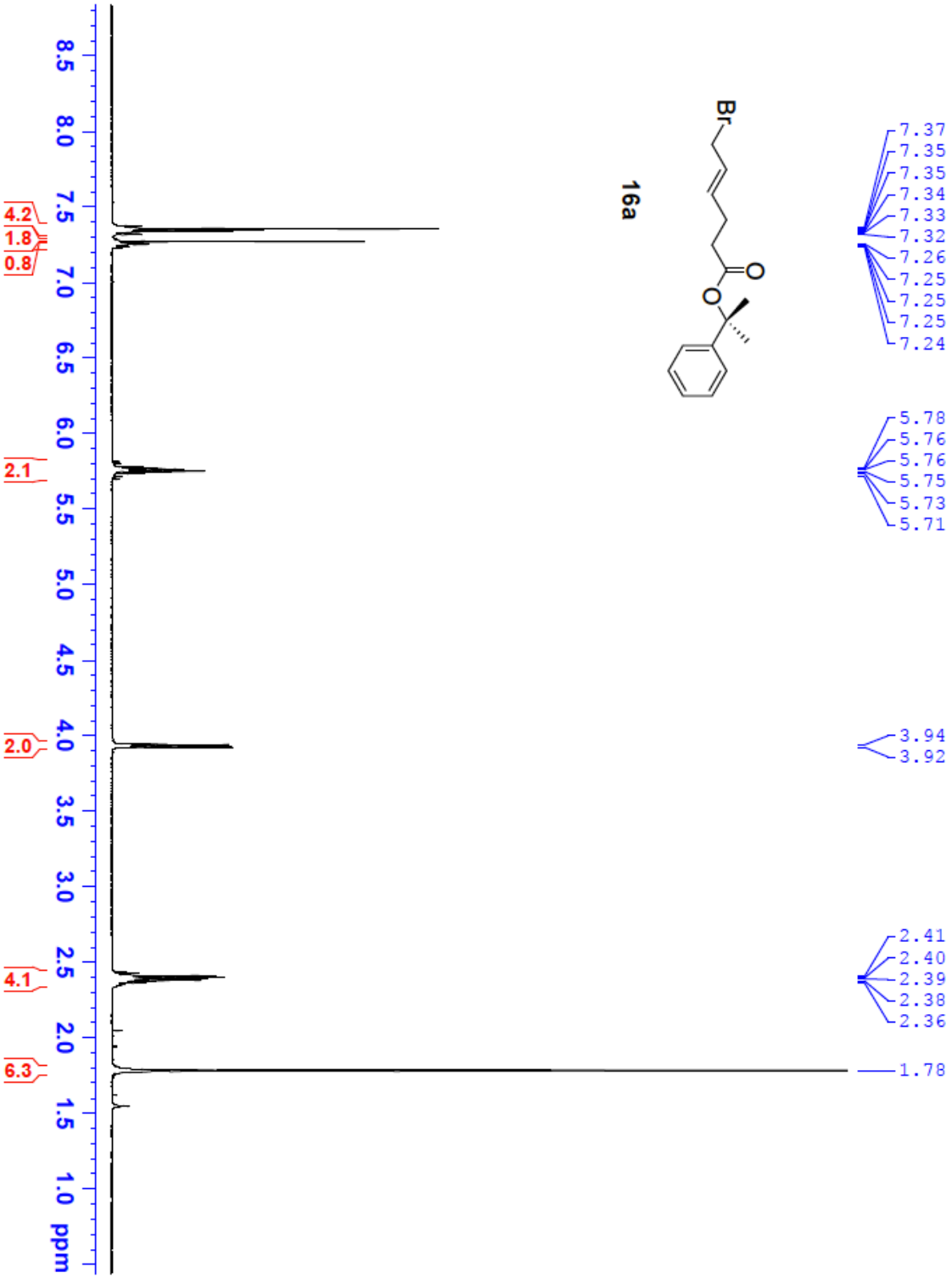

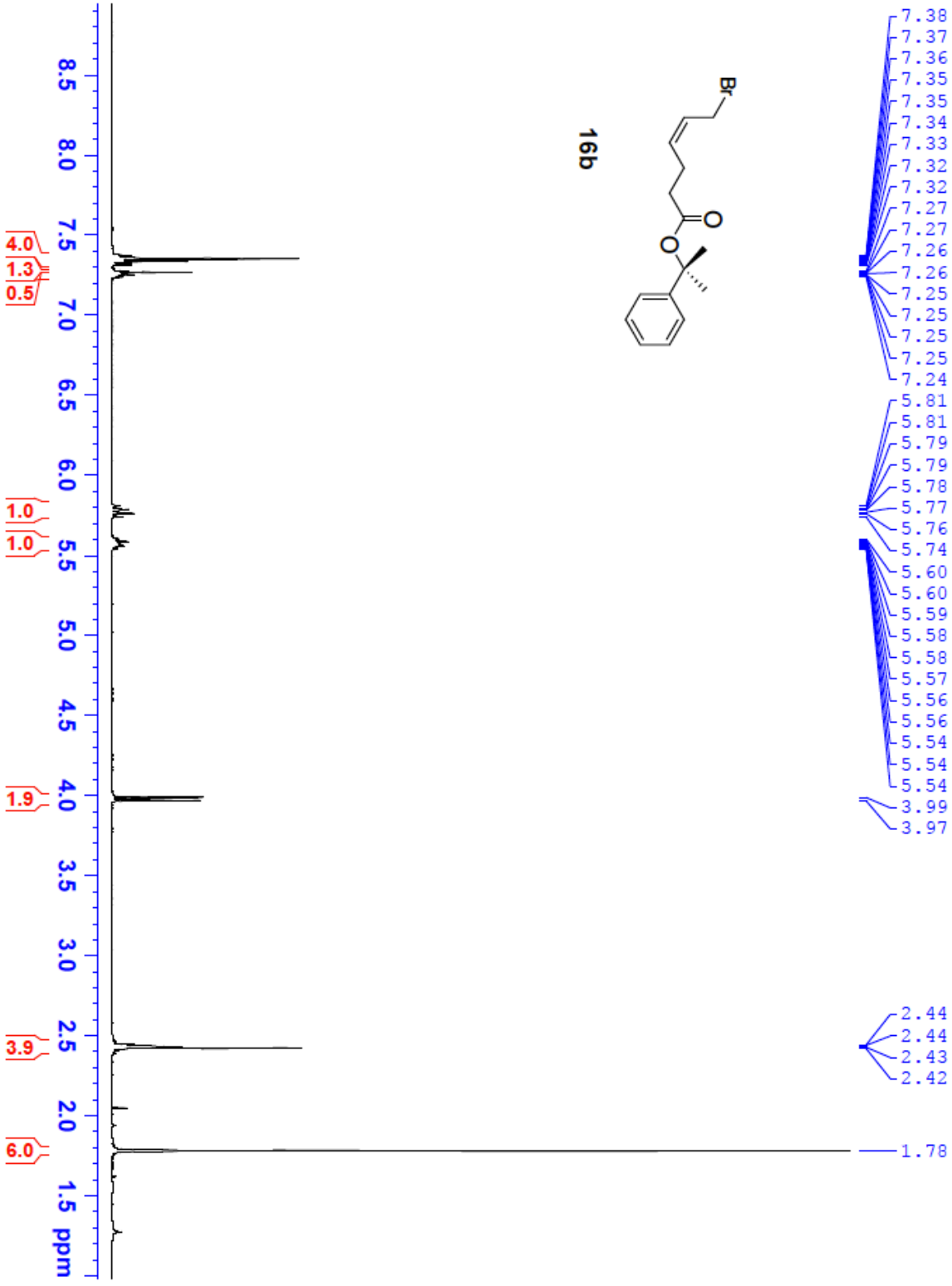
16b
Br
O
O
7.38
7.37
7.36
7.35
7.35
7.34
7.33
7.32
7.32
7.27
7.27
7.26
7.26
7.25
7.25
7.25
7.25
7.24
5.81
5.81
5.79
5.79
5.78
5.77
5.76
5.74
5.60
5.60
5.59
5.58
5.58
5.57
5.56
5.56
5.54
5.54
5.54
3.99
3.97
2.44
2.44
2.43
2.42
1.78
4.0
1.3
0.5
1.0
1.0
1.9
3.9
6.0
8.5
8.0
7.5
7.0
6.5
6.0
5.5
5.0
4.5
4.0
3.5
3.0
2.5
2.0
1.5
ppm

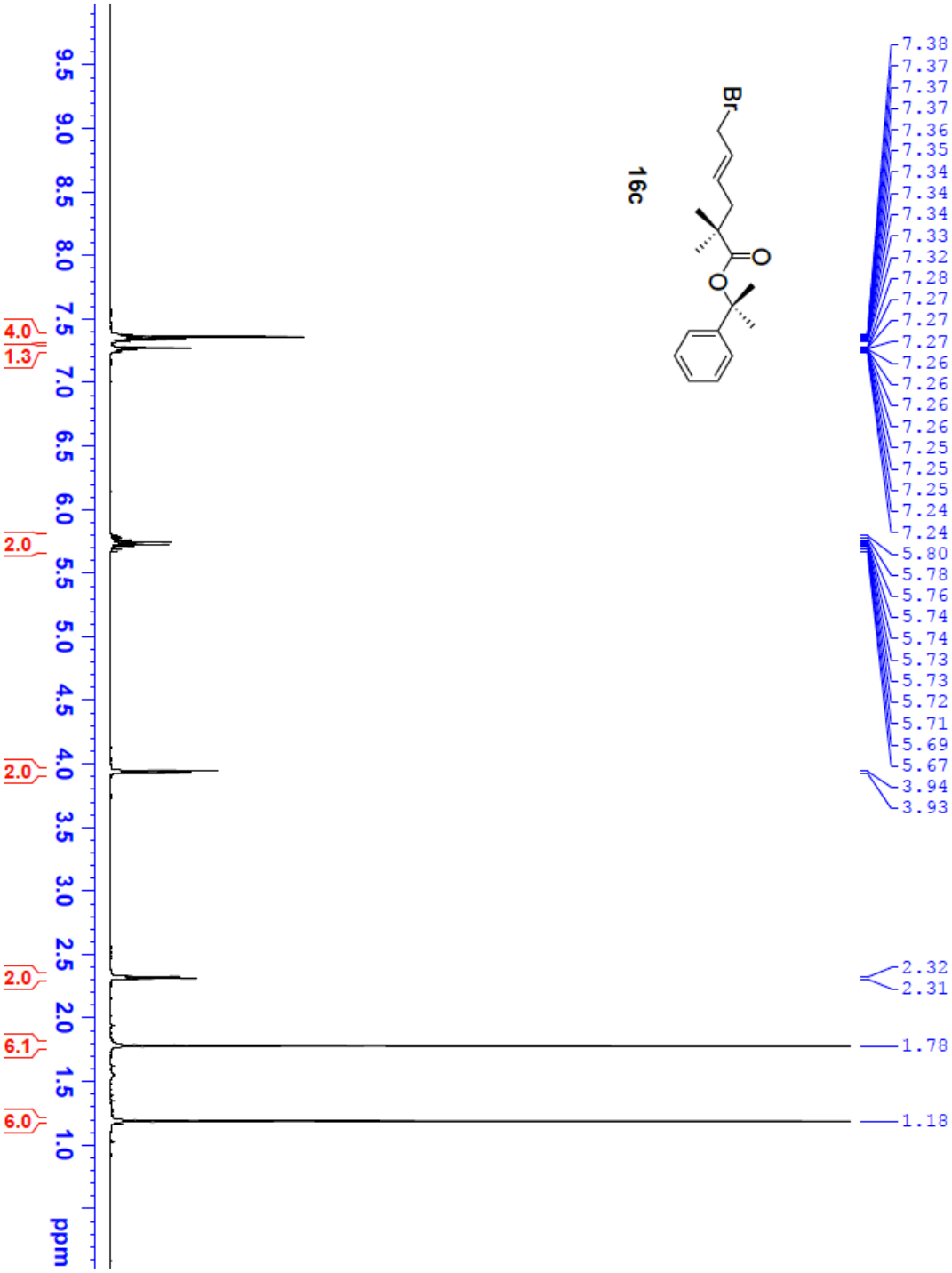
16c
Br
O
O
7.38
7.37
7.37
7.37
7.36
7.35
7.34
7.34
7.34
7.33
7.32
7.28
7.27
7.27
7.27
7.26
7.26
7.26
7.26
7.25
7.25
7.25
7.24
7.24
5.80
5.78
5.76
5.74
5.74
5.73
5.73
5.72
5.71
5.69
5.67
3.94
3.93
2.32
2.31
1.78
1.18
4.0
1.3
2.0
2.0
2.0
6.1
6.0
9.5
9.0
8.5
8.0
7.5
7.0
6.5
6.0
5.5
5.0
4.5
4.0
3.5
3.0
2.5
2.0
1.5
1.0
ppm

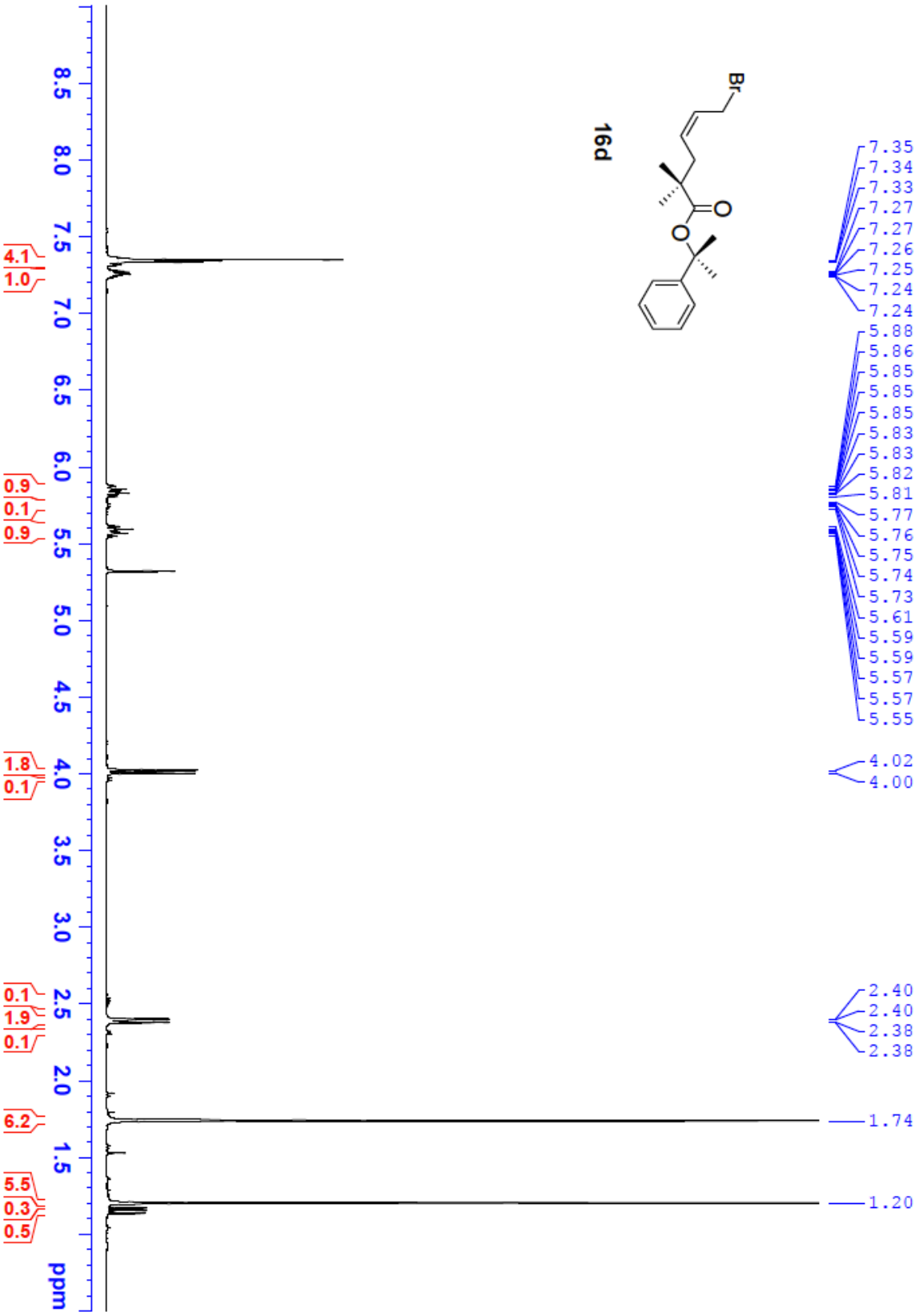
16d
Br
O
O
7.35
7.34
7.33
7.27
7.27
7.26
7.25
7.24
7.24
5.88
5.86
5.85
5.85
5.85
5.83
5.83
5.82
5.81
5.77
5.76
5.75
5.74
5.73
5.61
5.59
5.59
5.57
5.57
5.55
4.02
4.00
2.40
2.40
2.38
2.38
1.74
1.20
4.1
1.0
0.9
0.1
0.9
1.8
0.1
0.1
1.9
0.1
6.2
5.5
0.3
0.5
8.5
8.0
7.5
7.0
6.5
6.0
5.5
5.0
4.5
4.0
3.5
3.0
2.5
2.0
1.5
ppm

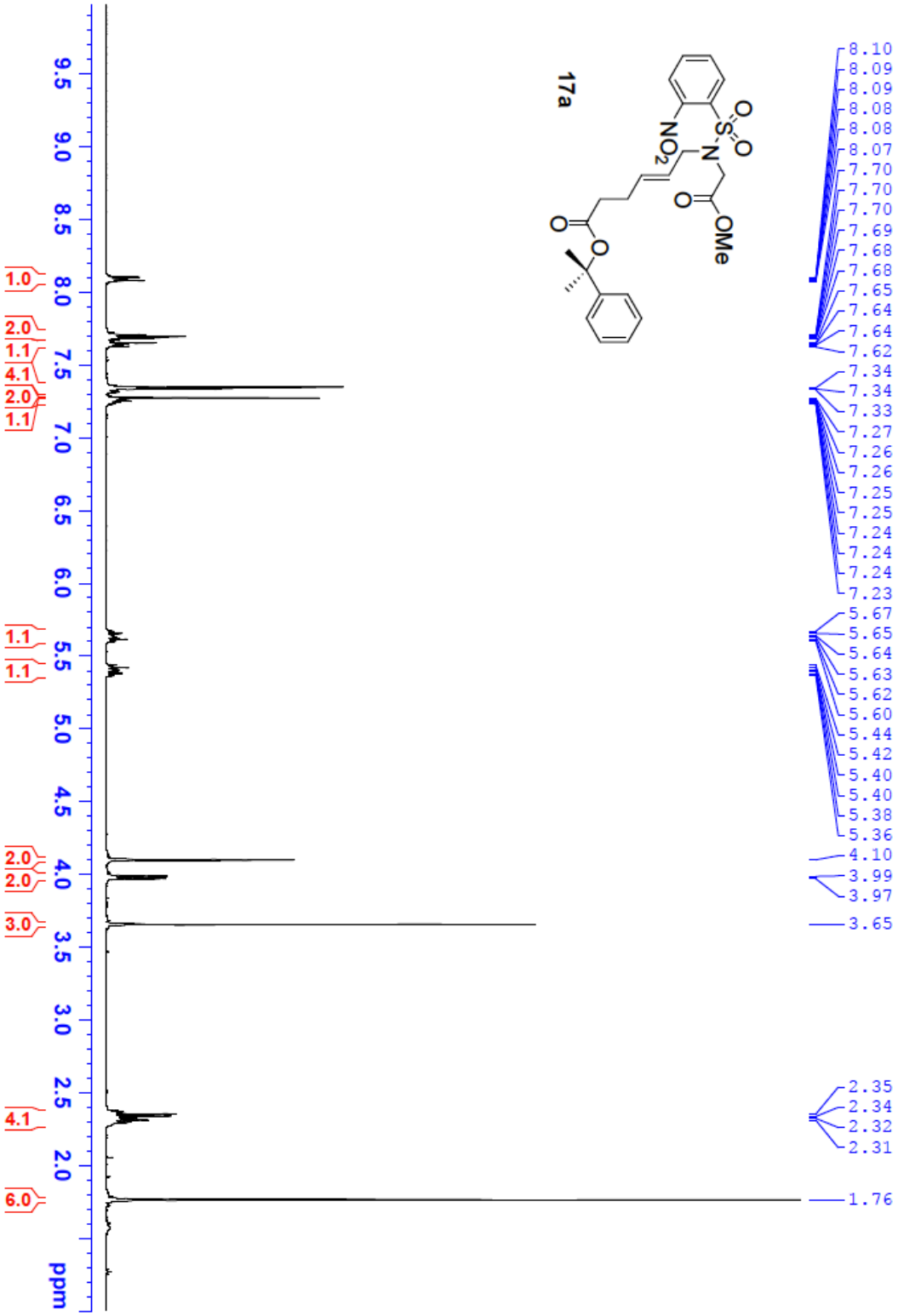
17a
8.10
8.09
8.09
8.08
8.08
8.07
7.70
7.70
7.70
7.69
7.68
7.68
7.65
7.64
7.64
7.62
7.34
7.34
7.33
7.27
7.26
7.26
7.25
7.25
7.24
7.24
7.24
7.23
5.67
5.65
5.64
5.63
5.62
5.60
5.44
5.42
5.40
5.40
5.38
5.36
4.10
3.99
3.97
3.65
2.35
2.34
2.32
2.31
1.76
1.0
2.0
1.1
4.1
2.0
1.1
1.1
1.1
2.0
2.0
3.0
4.1
6.0
ppm

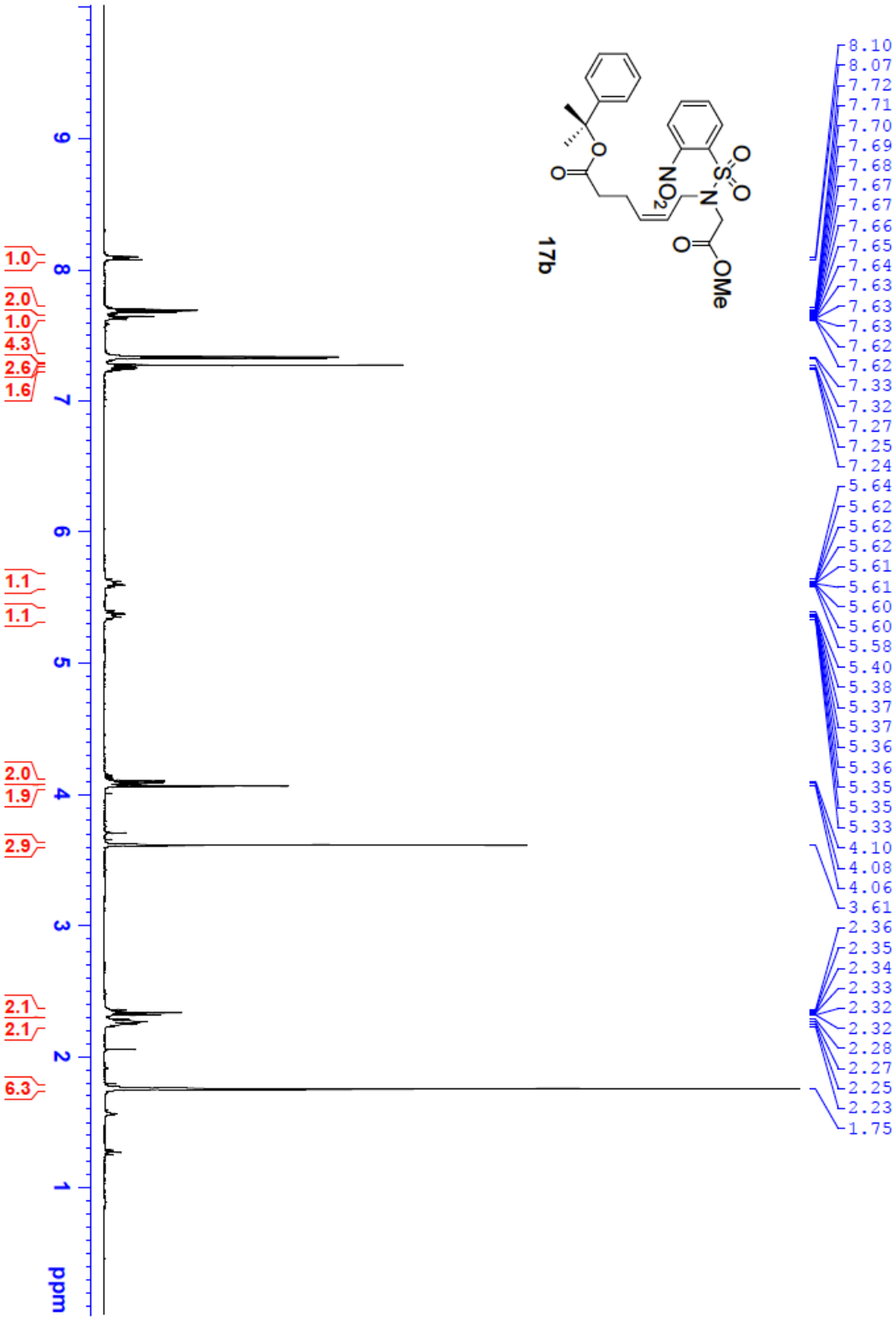
17b
8.10
8.07
7.72
7.71
7.70
7.69
7.68
7.67
7.67
7.66
7.65
7.64
7.63
7.63
7.63
7.62
7.62
7.33
7.32
7.27
7.25
7.24
5.64
5.62
5.62
5.62
5.61
5.61
5.60
5.60
5.58
5.40
5.38
5.37
5.37
5.36
5.36
5.35
5.35
5.33
4.10
4.08
4.06
3.61
2.36
2.35
2.34
2.33
2.32
2.32
2.28
2.27
2.25
2.23
1.75
1.0
2.0
1.0
4.3
2.6
1.6
1.1
1.1
2.0
1.9
2.9
2.1
2.1
6.3
ppm

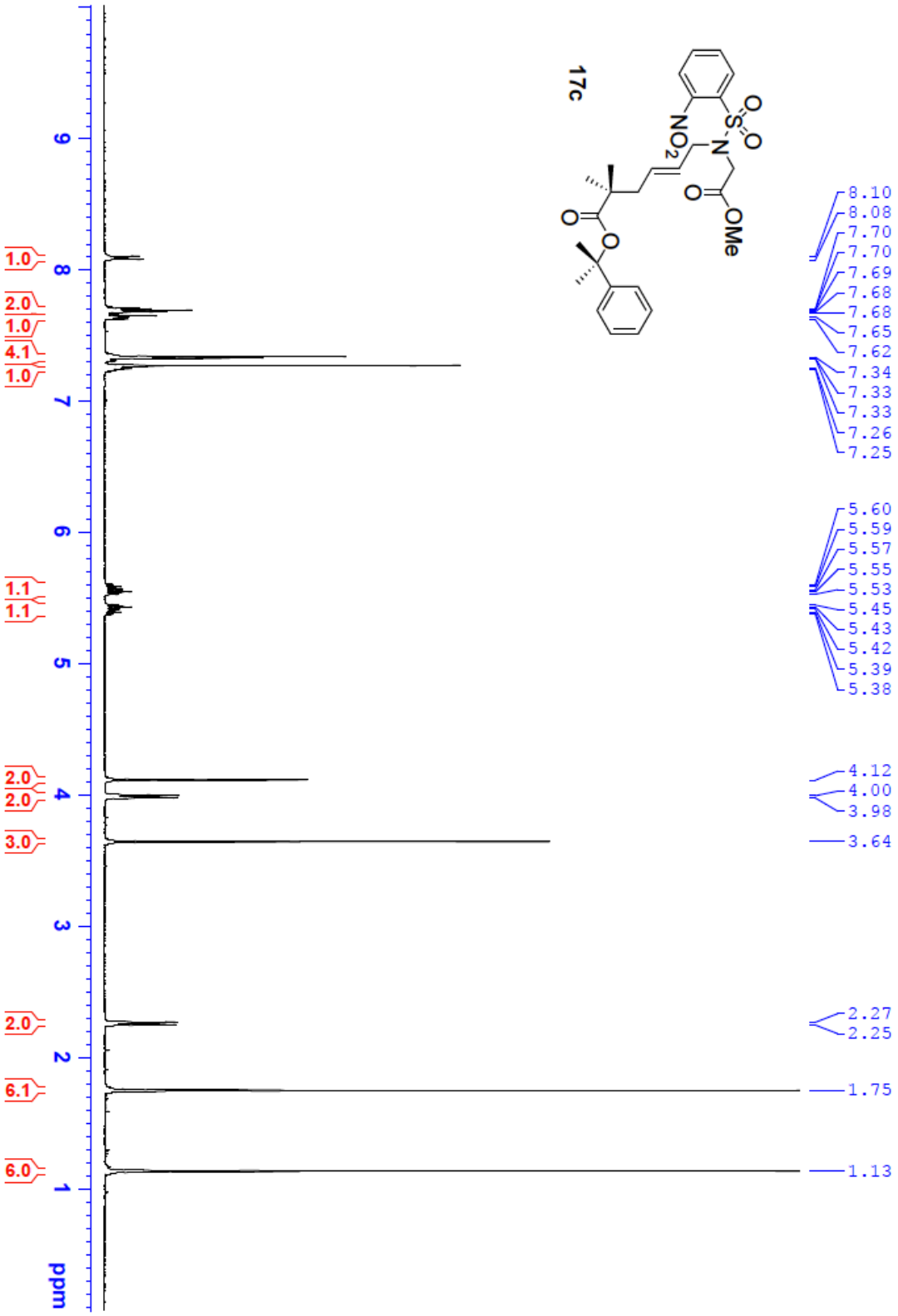
17c
NO2
S
O
O
N
O
OMe
O
O
8.10
8.08
7.70
7.70
7.69
7.68
7.68
7.65
7.62
7.34
7.33
7.33
7.26
7.25
5.60
5.59
5.57
5.55
5.53
5.45
5.43
5.42
5.39
5.38
4.12
4.00
3.98
3.64
2.27
2.25
1.75
1.13
1.0
2.0
1.0
4.1
1.0
1.1
1.1
2.0
2.0
3.0
2.0
6.1
6.0
ppm

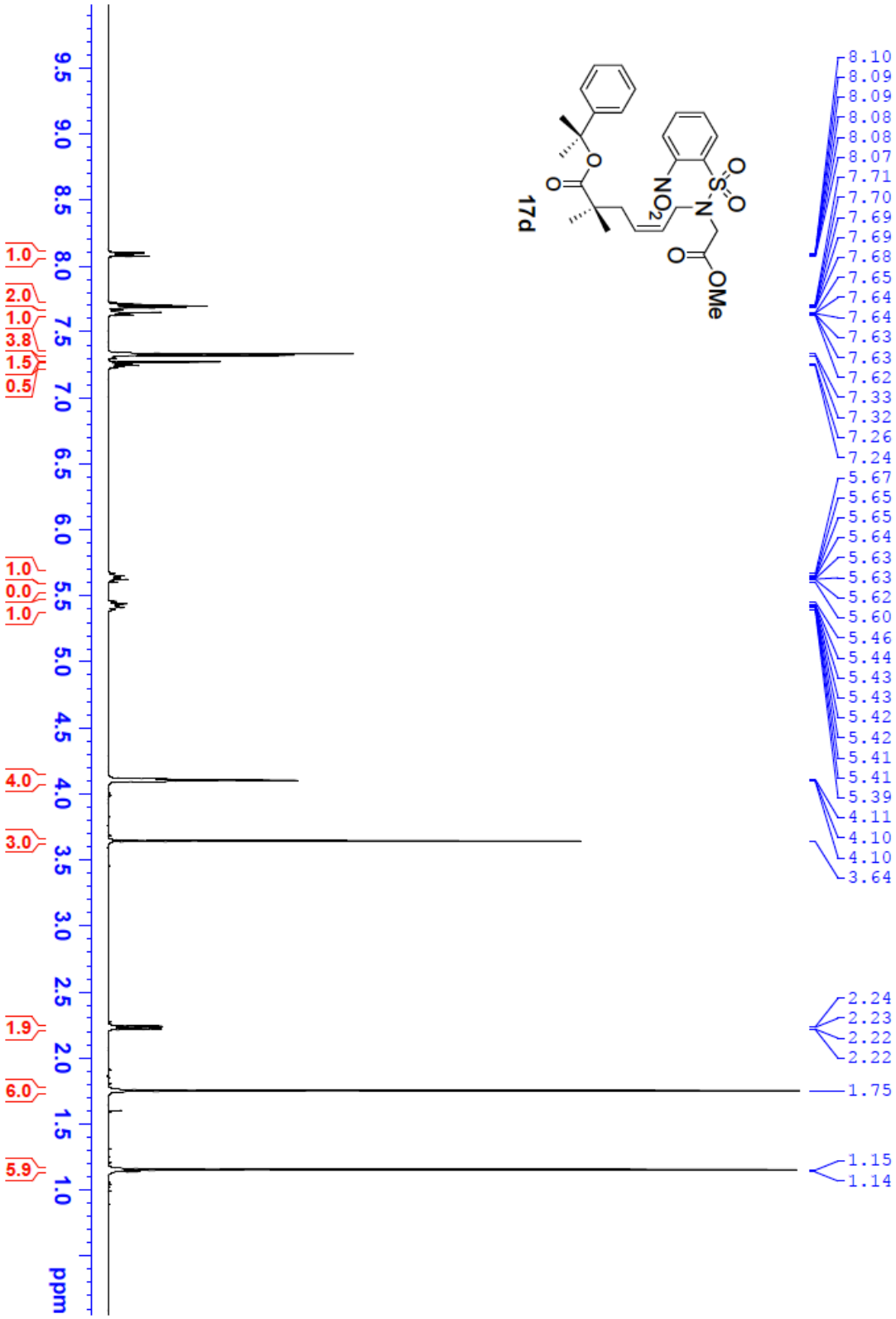
17d
8.10
8.09
8.09
8.08
8.08
8.07
7.71
7.70
7.69
7.69
7.68
7.65
7.64
7.64
7.63
7.63
7.62
7.33
7.32
7.26
7.24
5.67
5.65
5.65
5.64
5.63
5.63
5.62
5.60
5.46
5.44
5.43
5.43
5.42
5.42
5.41
5.41
5.39
4.11
4.10
4.10
3.64
2.24
2.23
2.22
2.22
1.75
1.15
1.14
1.0
2.0
1.0
3.8
1.5
0.5
1.0
0.0
1.0
4.0
3.0
1.9
6.0
5.9
ppm

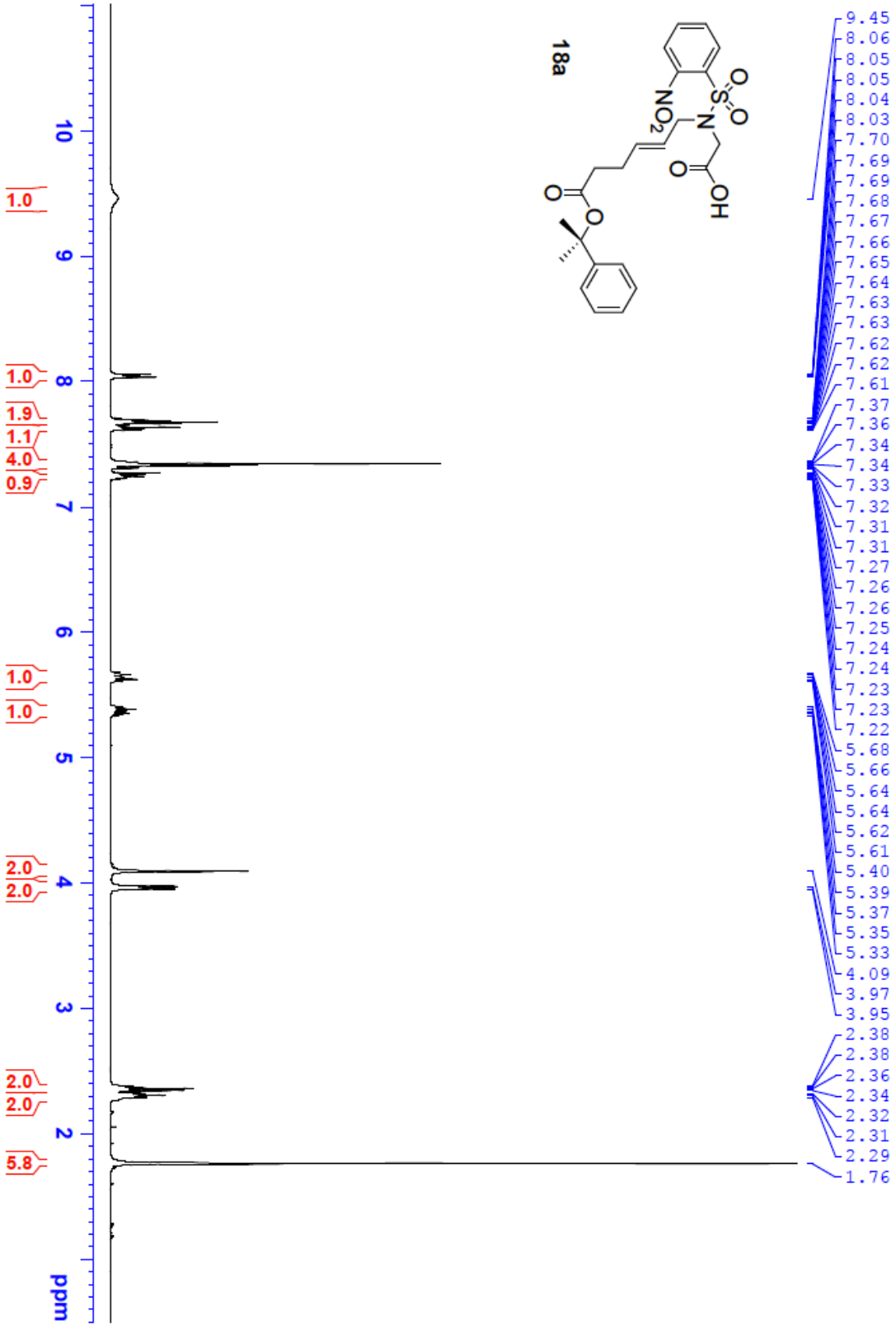
18a
9.45
8.06
8.05
8.05
8.04
8.03
7.70
7.69
7.69
7.68
7.67
7.66
7.65
7.64
7.63
7.63
7.62
7.62
7.61
7.37
7.36
7.34
7.34
7.33
7.32
7.31
7.31
7.27
7.26
7.26
7.25
7.24
7.24
7.23
7.23
7.22
5.68
5.66
5.64
5.64
5.62
5.61
5.40
5.39
5.37
5.35
5.33
4.09
3.97
3.95
2.38
2.38
2.36
2.34
2.32
2.31
2.29
1.76
1.0
1.0
1.9
1.1
4.0
0.9
1.0
1.0
2.0
2.0
2.0
2.0
5.8
ppm

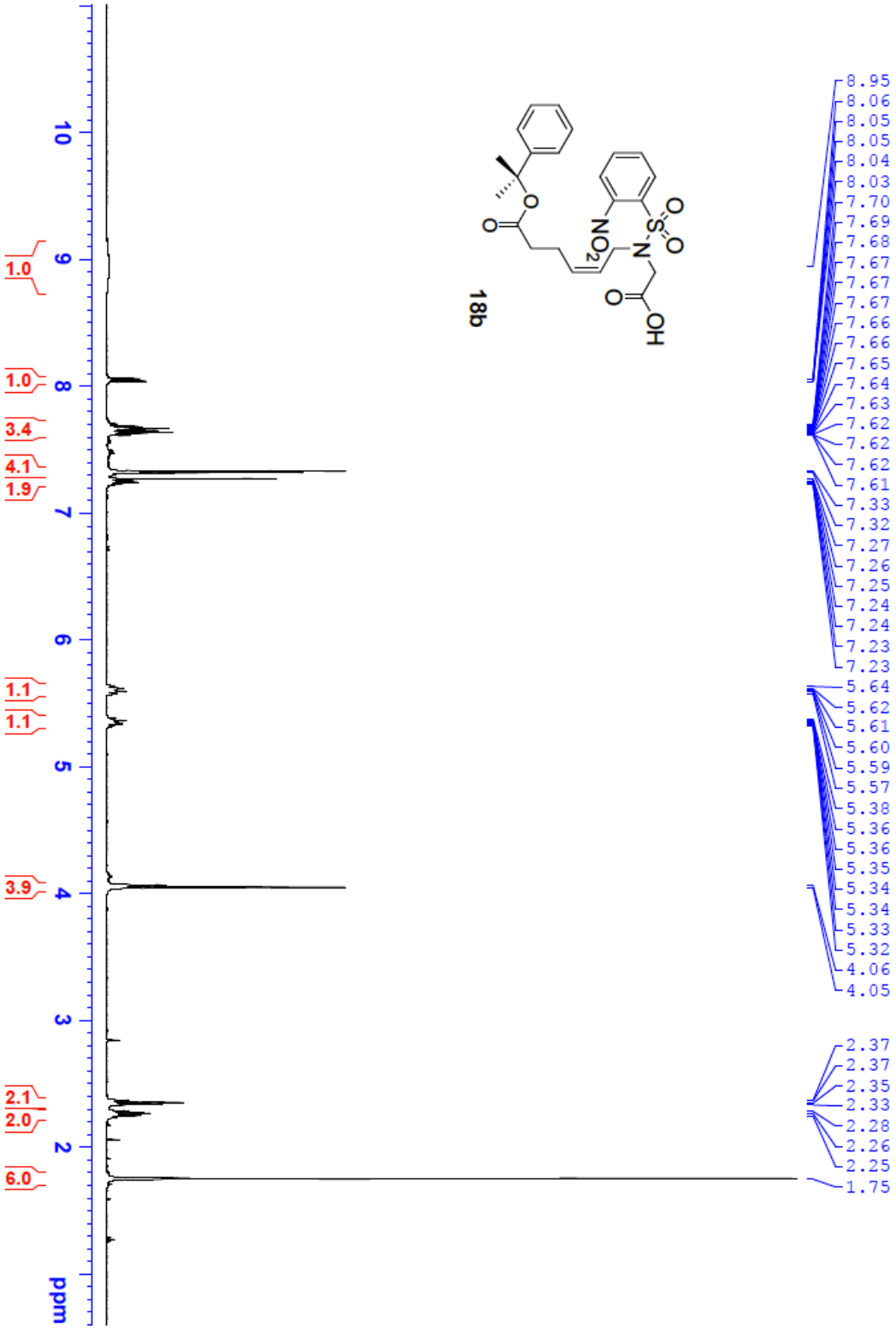
18b
8.95
8.06
8.05
8.05
8.04
8.03
7.70
7.69
7.68
7.67
7.67
7.67
7.67
7.66
7.66
7.65
7.64
7.63
7.62
7.62
7.62
7.61
7.33
7.32
7.27
7.26
7.25
7.24
7.24
7.23
7.23
5.64
5.62
5.61
5.60
5.59
5.57
5.38
5.36
5.36
5.35
5.34
5.34
5.33
5.32
4.06
4.05
2.37
2.37
2.35
2.33
2.28
2.26
2.25
1.75
1.0
1.0
3.4
4.1
1.9
1.1
1.1
3.9
2.1
2.0
6.0
ppm

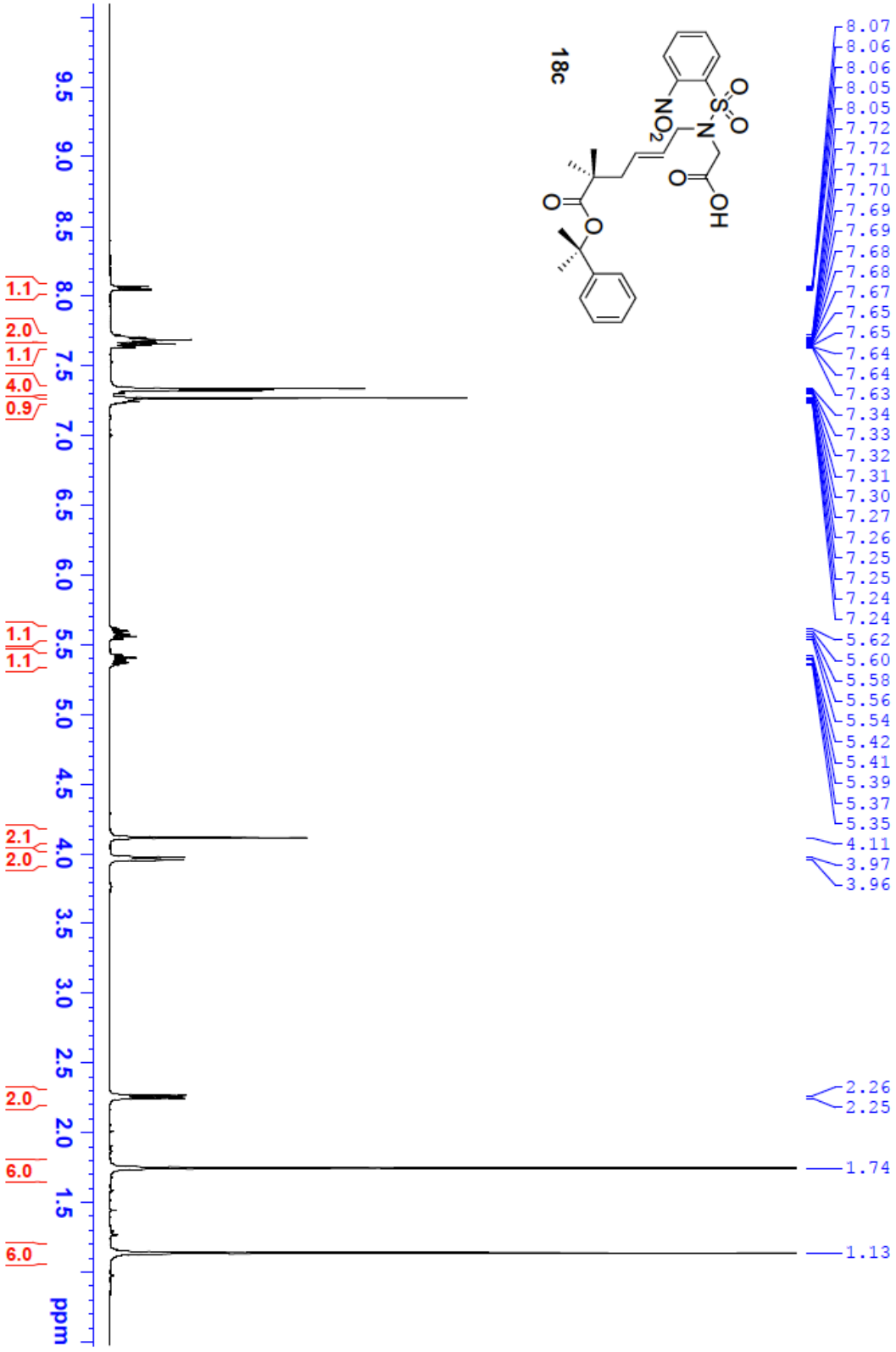
18c
8.07
8.06
8.06
8.05
8.05
7.72
7.72
7.71
7.70
7.69
7.69
7.68
7.68
7.67
7.65
7.65
7.64
7.64
7.63
7.34
7.33
7.32
7.31
7.30
7.27
7.26
7.25
7.25
7.24
7.24
5.62
5.60
5.58
5.56
5.54
5.42
5.41
5.39
5.37
5.35
4.11
3.97
3.96
2.26
2.25
1.74
1.13
1.1
2.0
1.1
4.0
0.9
1.1
1.1
2.1
2.0
2.0
6.0
6.0
ppm

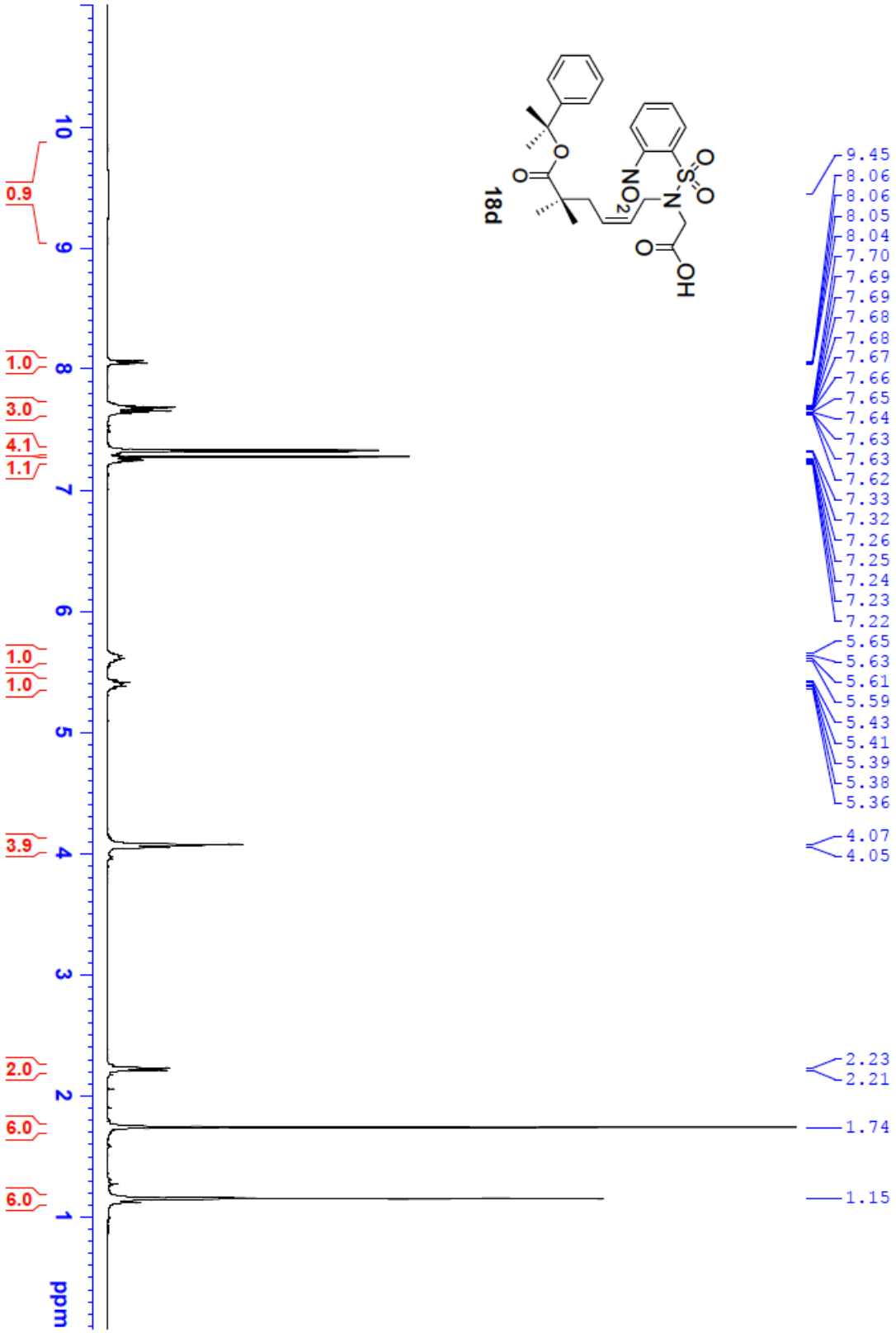
18d
9.45
8.06
8.06
8.05
8.04
7.70
7.69
7.69
7.68
7.68
7.67
7.66
7.65
7.64
7.63
7.63
7.62
7.33
7.32
7.26
7.25
7.24
7.23
7.22
5.65
5.63
5.61
5.59
5.43
5.41
5.39
5.38
5.36
4.07
4.05
2.23
2.21
1.74
1.15
0.9
1.0
3.0
4.1
1.1
1.0
1.0
3.9
2.0
6.0
6.0
ppm

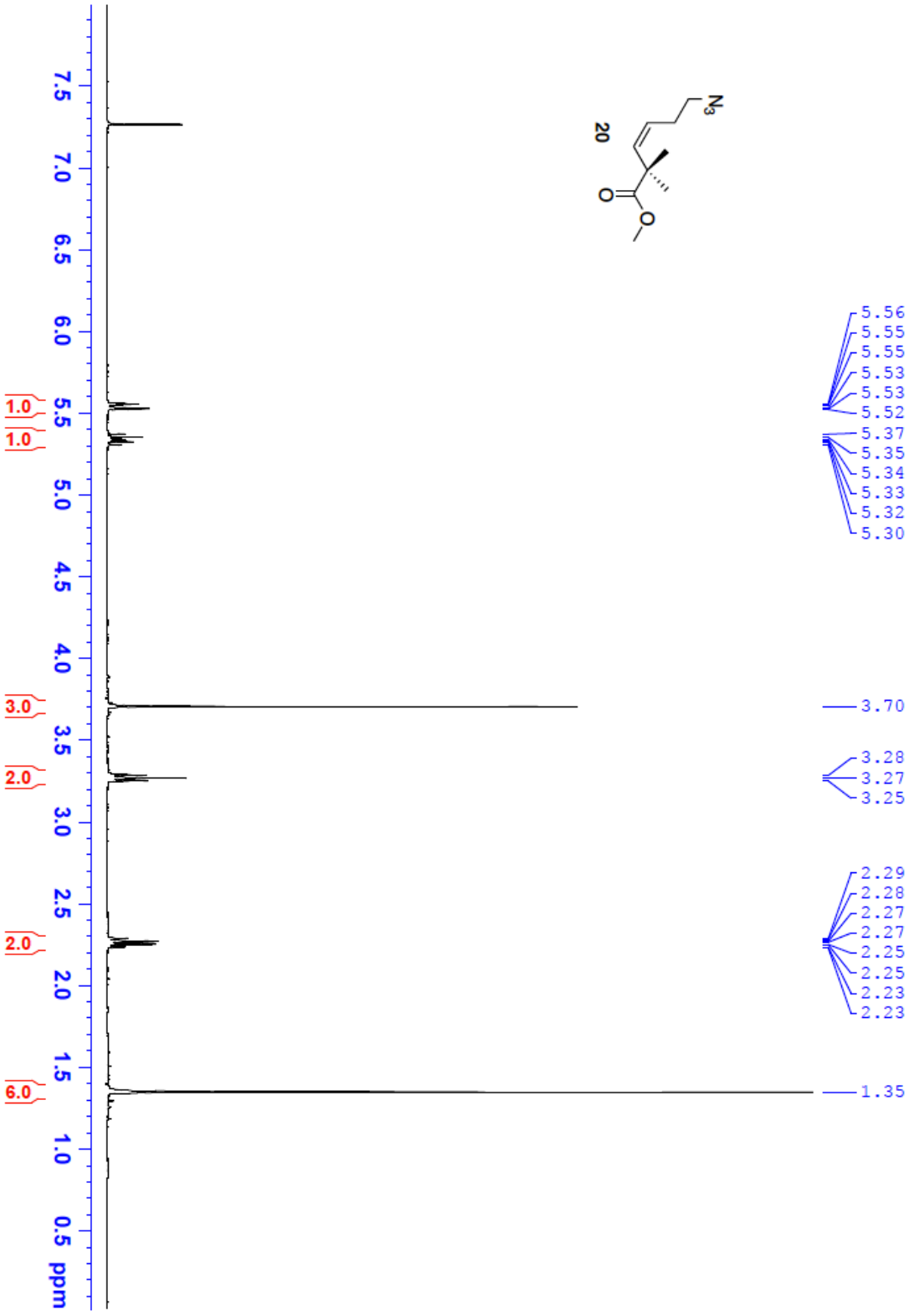
20
N3
O
O
5.56
5.55
5.55
5.53
5.53
5.52
5.37
5.35
5.34
5.33
5.32
5.30
3.70
3.28
3.27
3.25
2.29
2.28
2.27
2.27
2.25
2.25
2.23
2.23
1.35
1.0
1.0
3.0
2.0
2.0
6.0
7.5
7.0
6.5
6.0
5.5
5.0
4.5
4.0
3.5
3.0
2.5
2.0
1.5
1.0
0.5
ppm

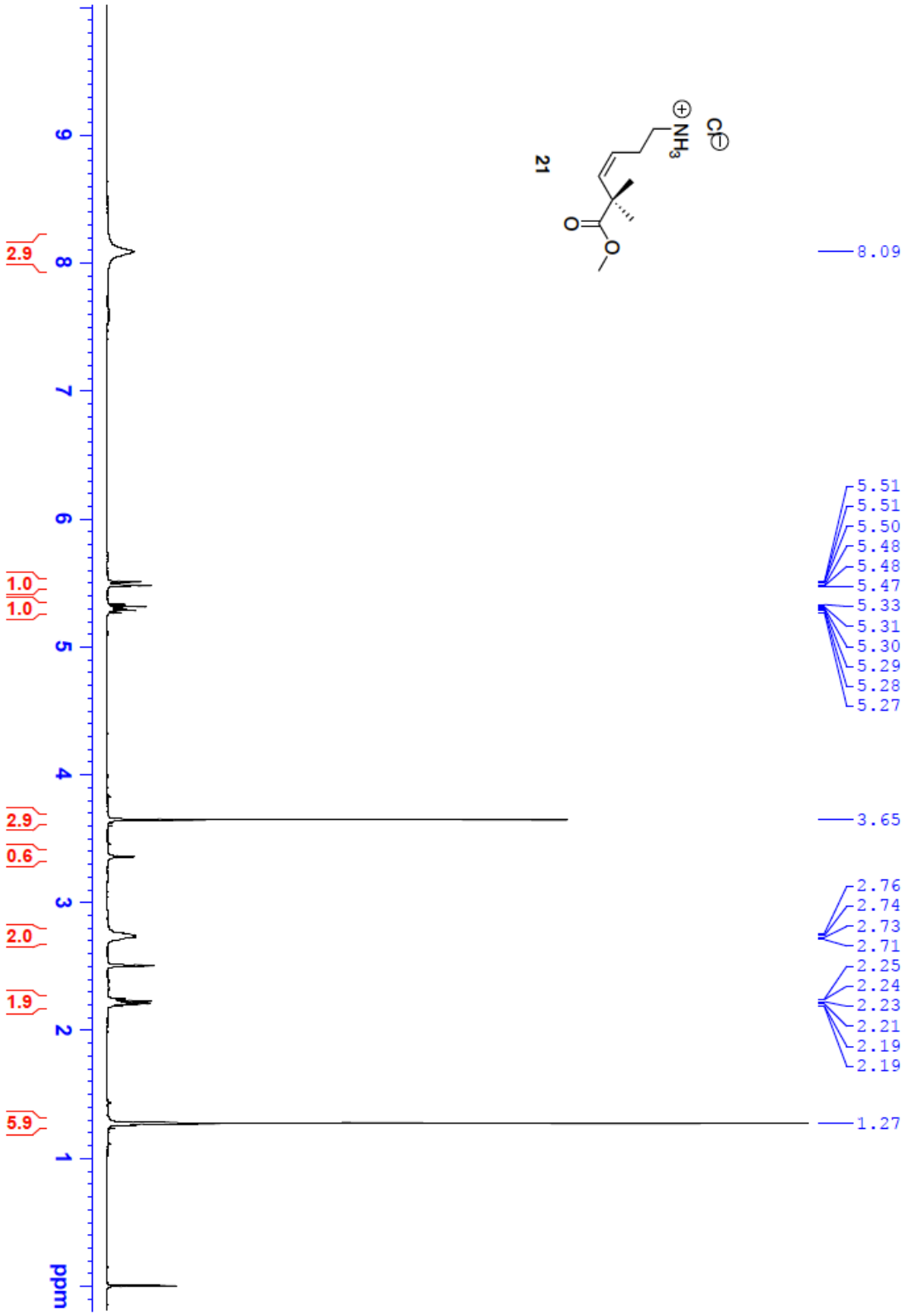
21
⊕NH3
Cl⊖
8.09
5.51
5.51
5.50
5.48
5.48
5.47
5.33
5.31
5.30
5.29
5.28
5.27
3.65
2.76
2.74
2.73
2.71
2.25
2.24
2.23
2.21
2.19
2.19
1.27
2.9
1.0
1.0
2.9
0.6
2.0
1.9
5.9
ppm

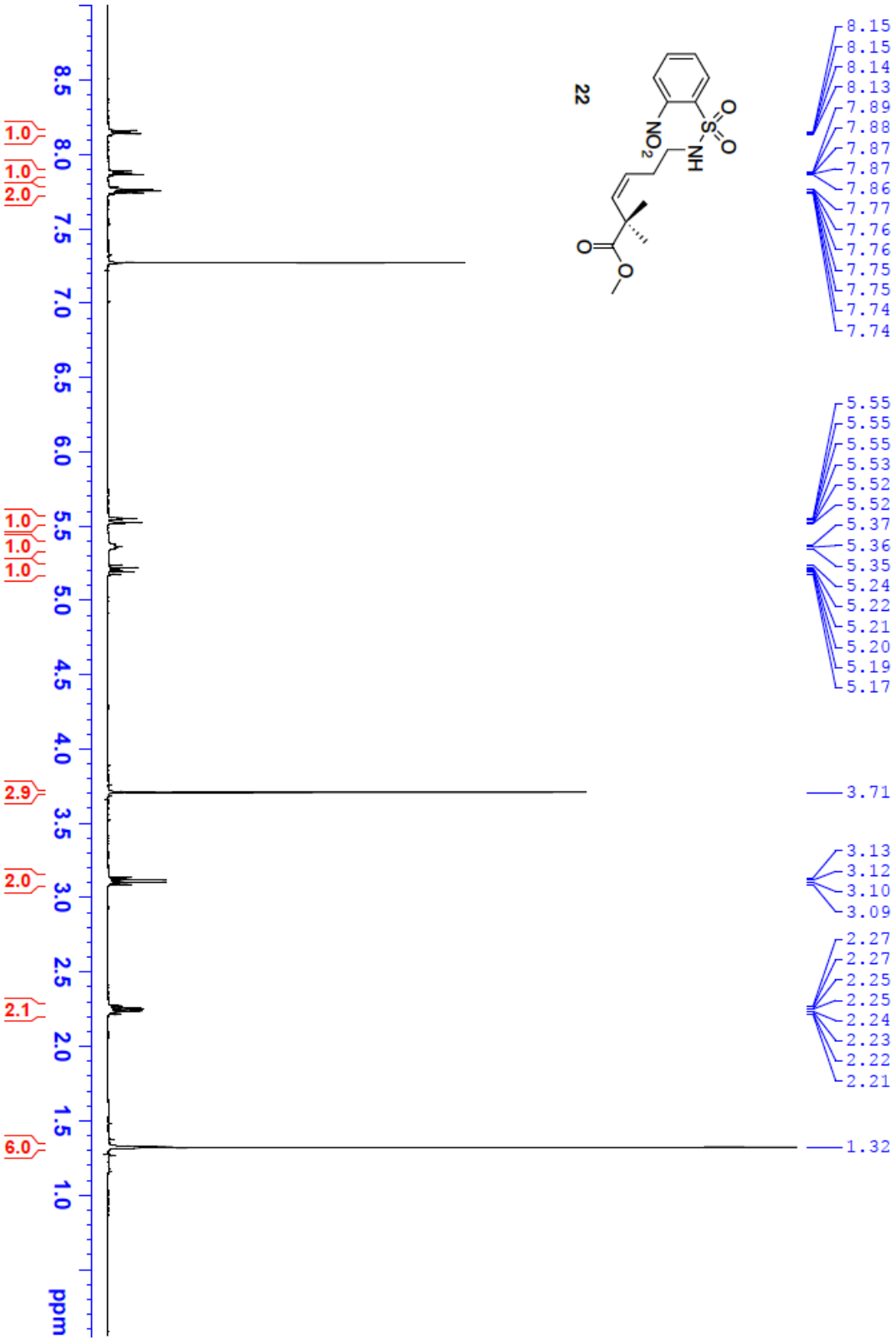
22
8.15
8.15
8.14
8.13
7.89
7.88
7.87
7.87
7.86
7.77
7.76
7.76
7.75
7.75
7.74
7.74
5.55
5.55
5.55
5.53
5.52
5.52
5.37
5.36
5.35
5.24
5.22
5.21
5.20
5.19
5.17
3.71
3.13
3.12
3.10
3.09
2.27
2.27
2.25
2.25
2.24
2.23
2.22
2.21
1.32
1.0
1.0
2.0
1.0
1.0
1.0
2.9
2.0
2.1
6.0
ppm

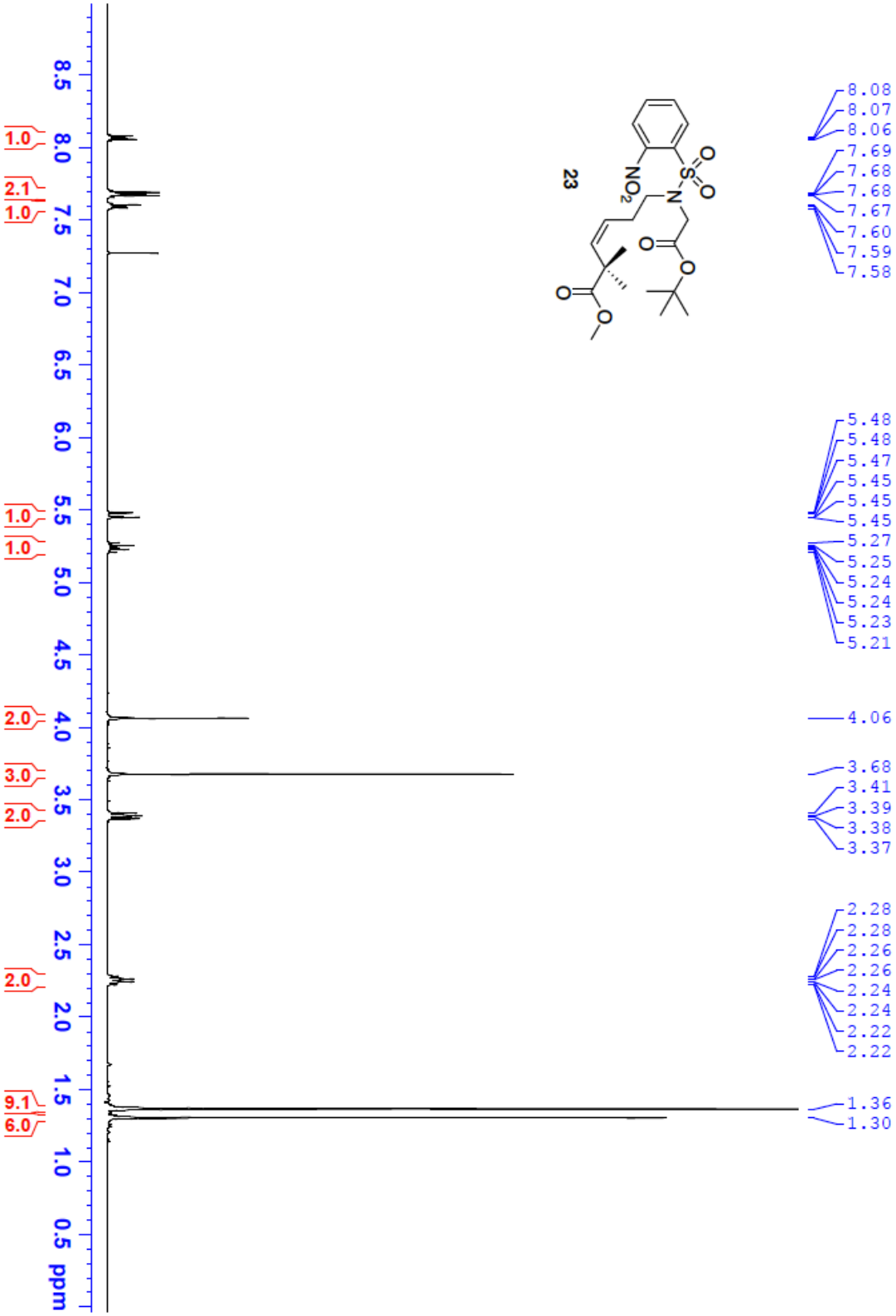
23
8.08
8.07
8.06
7.69
7.68
7.68
7.67
7.60
7.59
7.58
5.48
5.48
5.47
5.45
5.45
5.45
5.27
5.25
5.24
5.24
5.23
5.21
4.06
3.68
3.41
3.39
3.38
3.37
2.28
2.28
2.26
2.26
2.24
2.24
2.22
2.22
1.36
1.30
1.0
2.1
1.0
1.0
1.0
2.0
3.0
2.0
2.0
9.1
6.0
ppm

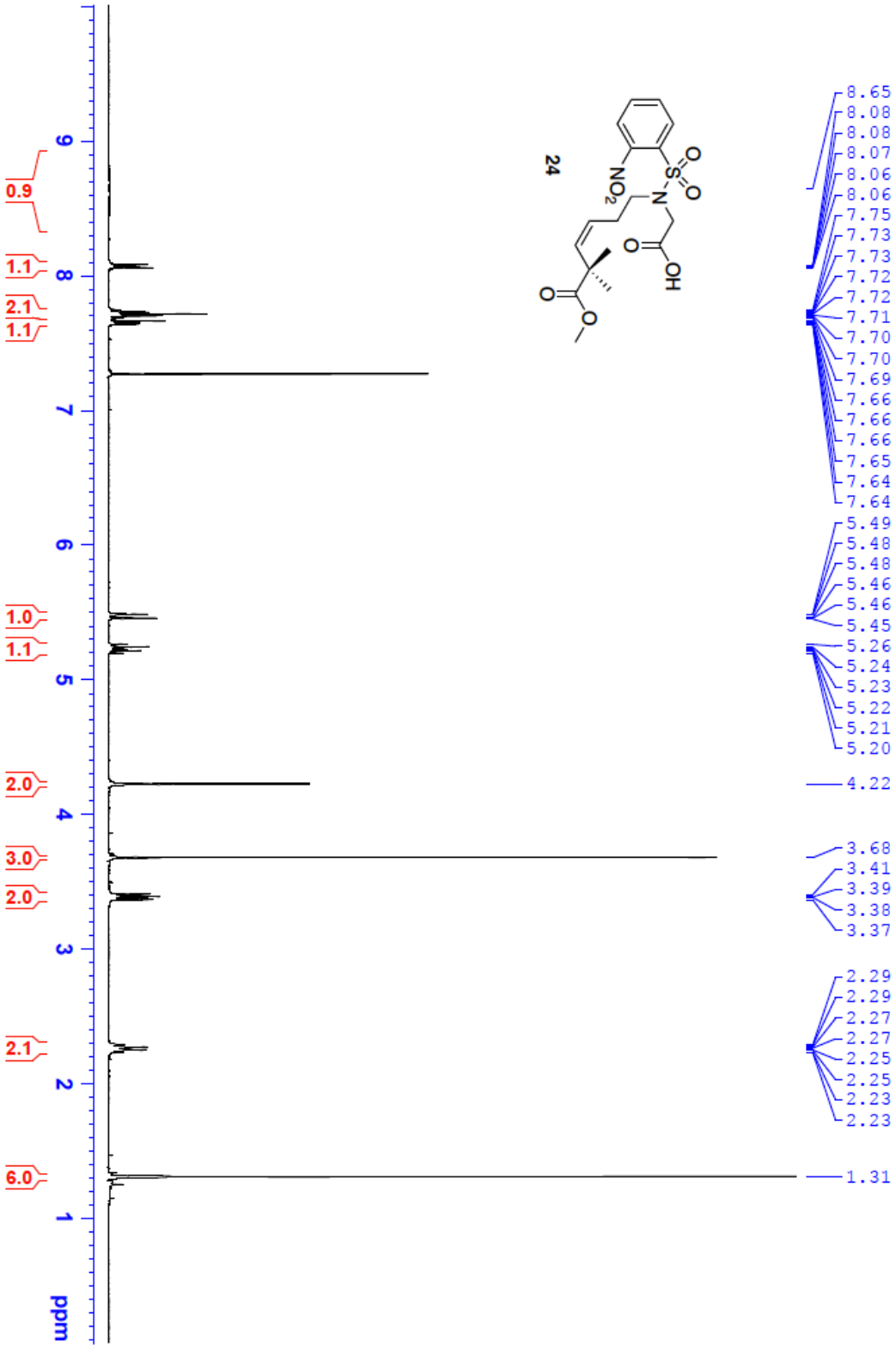
24
8.65
8.08
8.08
8.07
8.06
8.06
7.75
7.73
7.73
7.72
7.72
7.71
7.70
7.70
7.69
7.66
7.66
7.66
7.65
7.64
7.64
5.49
5.48
5.48
5.46
5.46
5.45
5.26
5.24
5.23
5.22
5.21
5.20
4.22
3.68
3.41
3.39
3.38
3.37
2.29
2.29
2.27
2.27
2.25
2.25
2.23
2.23
1.31
0.9
1.1
2.1
1.1
1.0
1.1
2.0
3.0
2.0
2.1
6.0
ppm

^{13}C NMR Spectra.

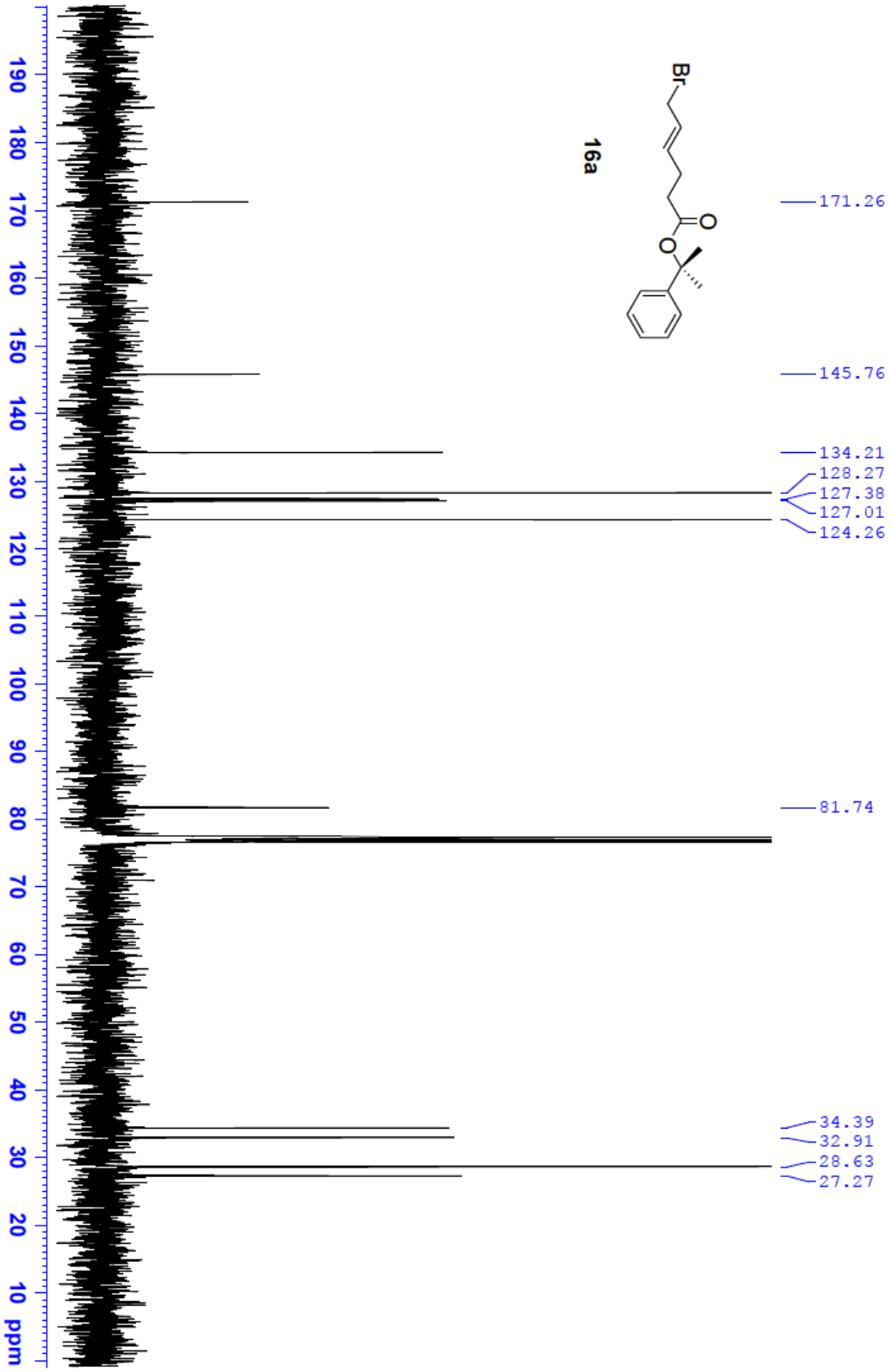

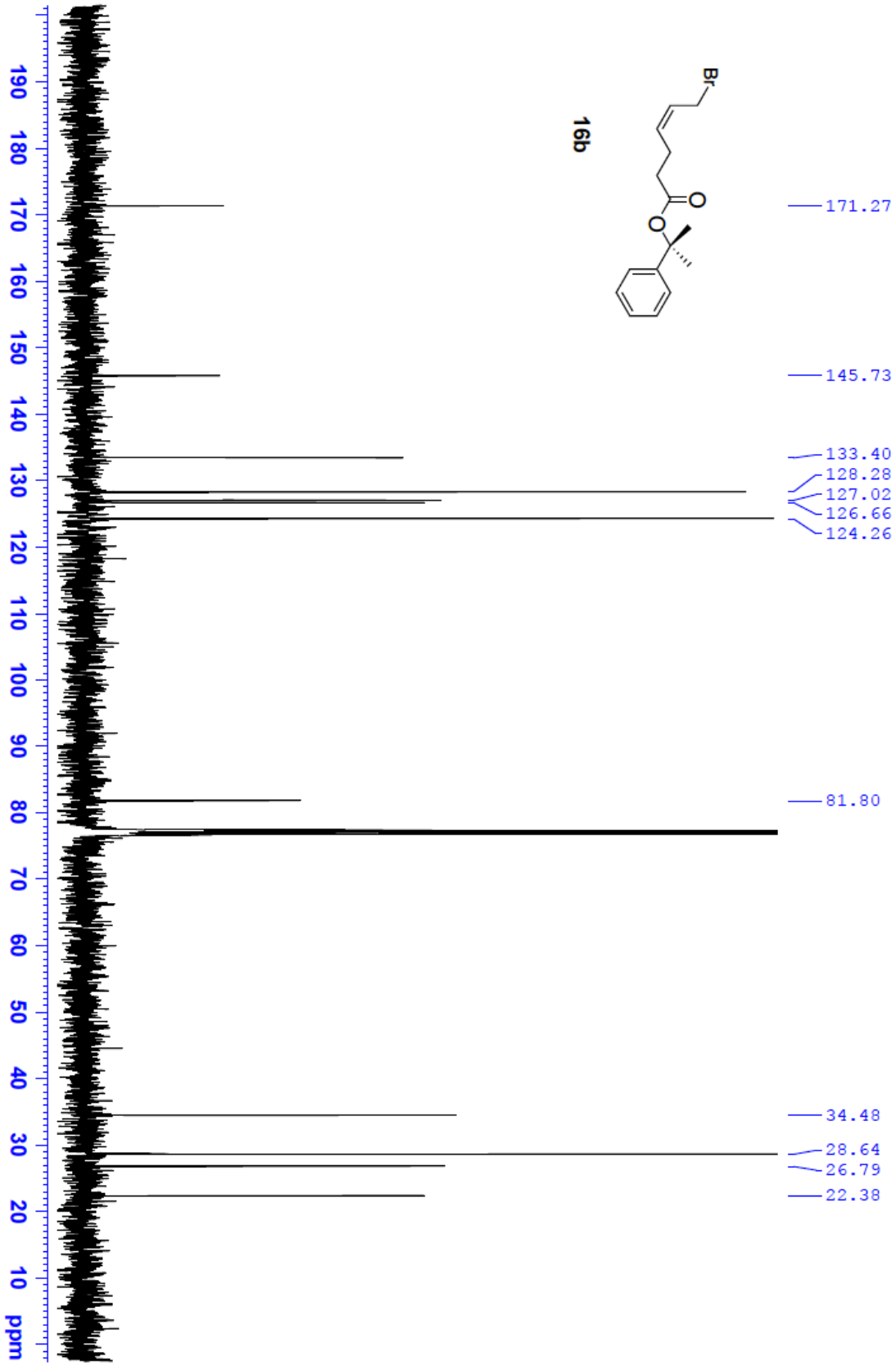
16b
Br
O
O
171.27
145.73
133.40
128.28
127.02
126.66
124.26
81.80
34.48
28.64
26.79
22.38
190
180
170
160
150
140
130
120
110
100
90
80
70
60
50
40
30
20
10
ppm

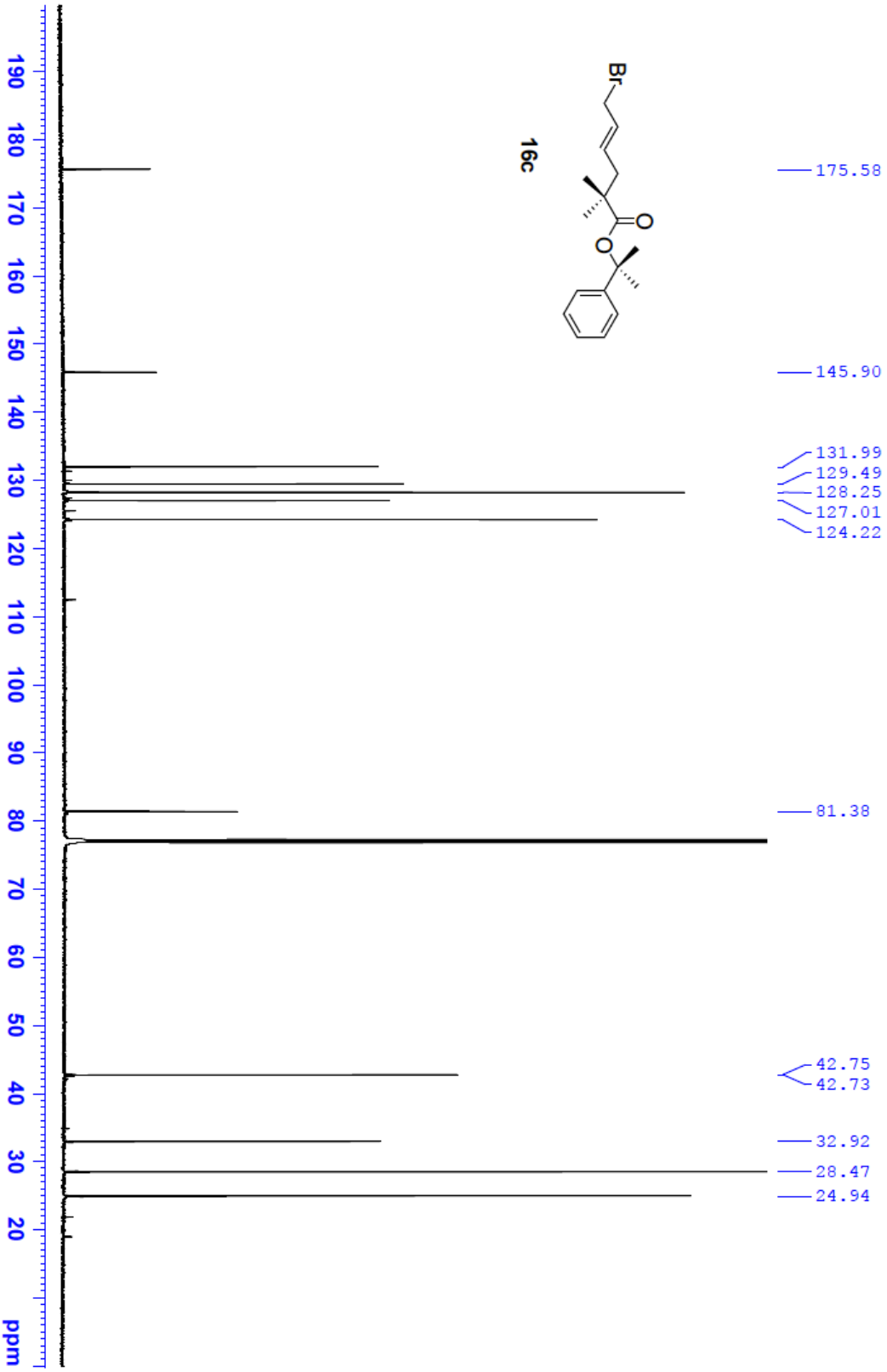
16c
Br
O
O
175.58
145.90
131.99
129.49
128.25
127.01
124.22
81.38
42.75
42.73
32.92
28.47
24.94
190
180
170
160
150
140
130
120
110
100
90
80
70
60
50
40
30
20
ppm

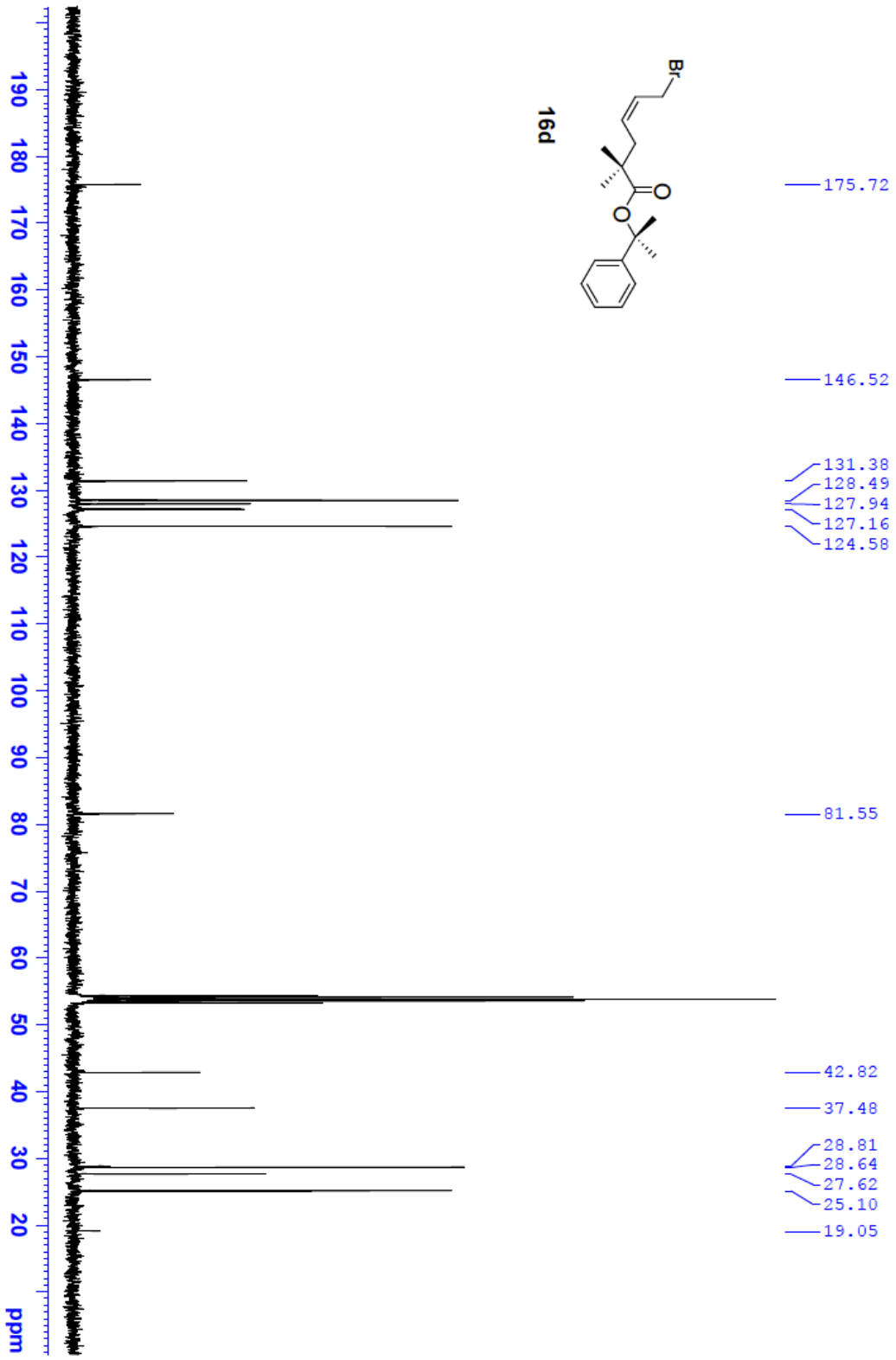
16d
Br
O
O
175.72
146.52
131.38
128.49
127.94
127.16
124.58
81.55
42.82
37.48
28.81
28.64
27.62
25.10
19.05
ppm

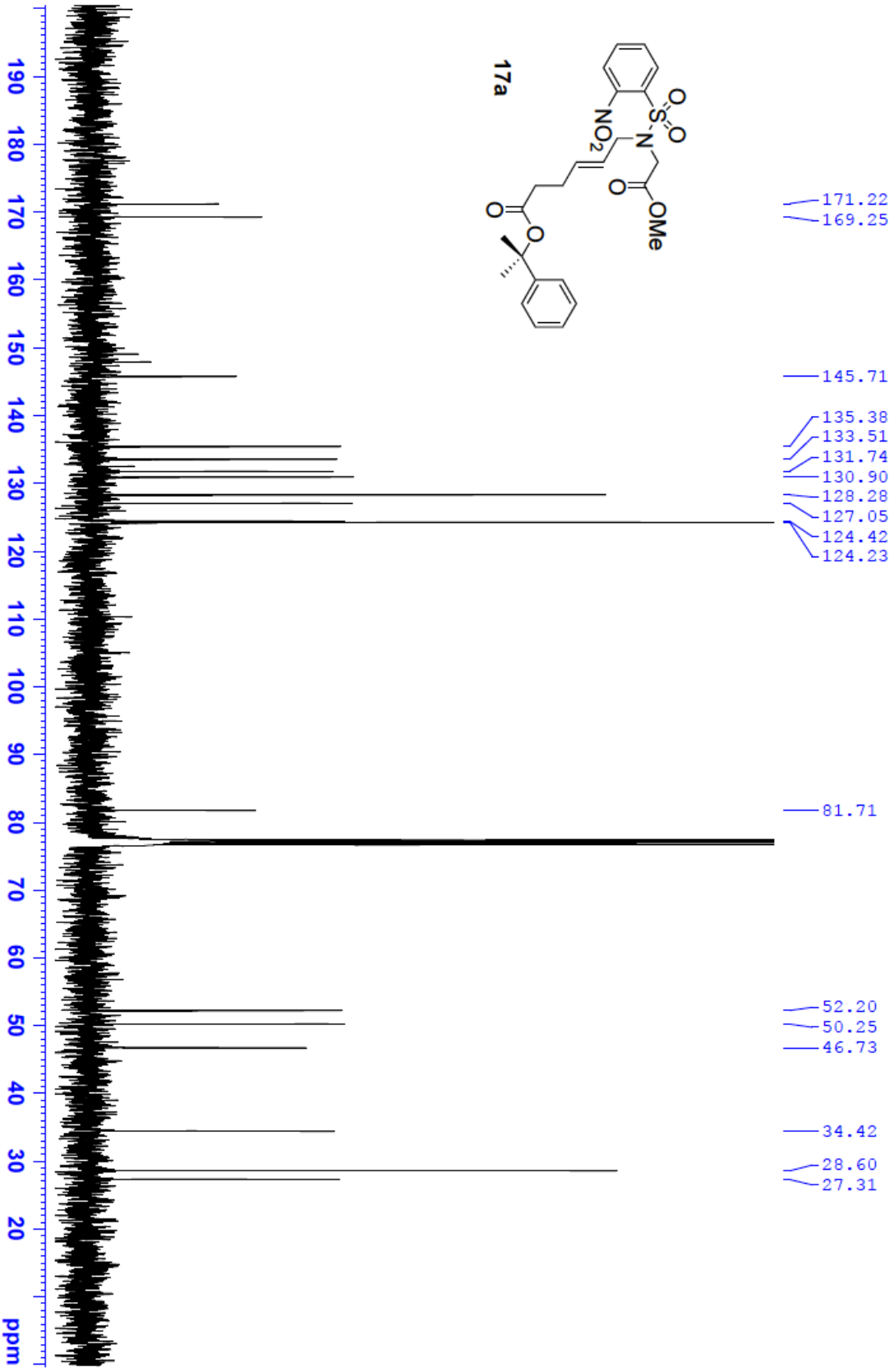
17a
171.22
169.25
145.71
135.38
133.51
131.74
130.90
128.28
127.05
124.42
124.23
81.71
52.20
50.25
46.73
34.42
28.60
27.31
ppm

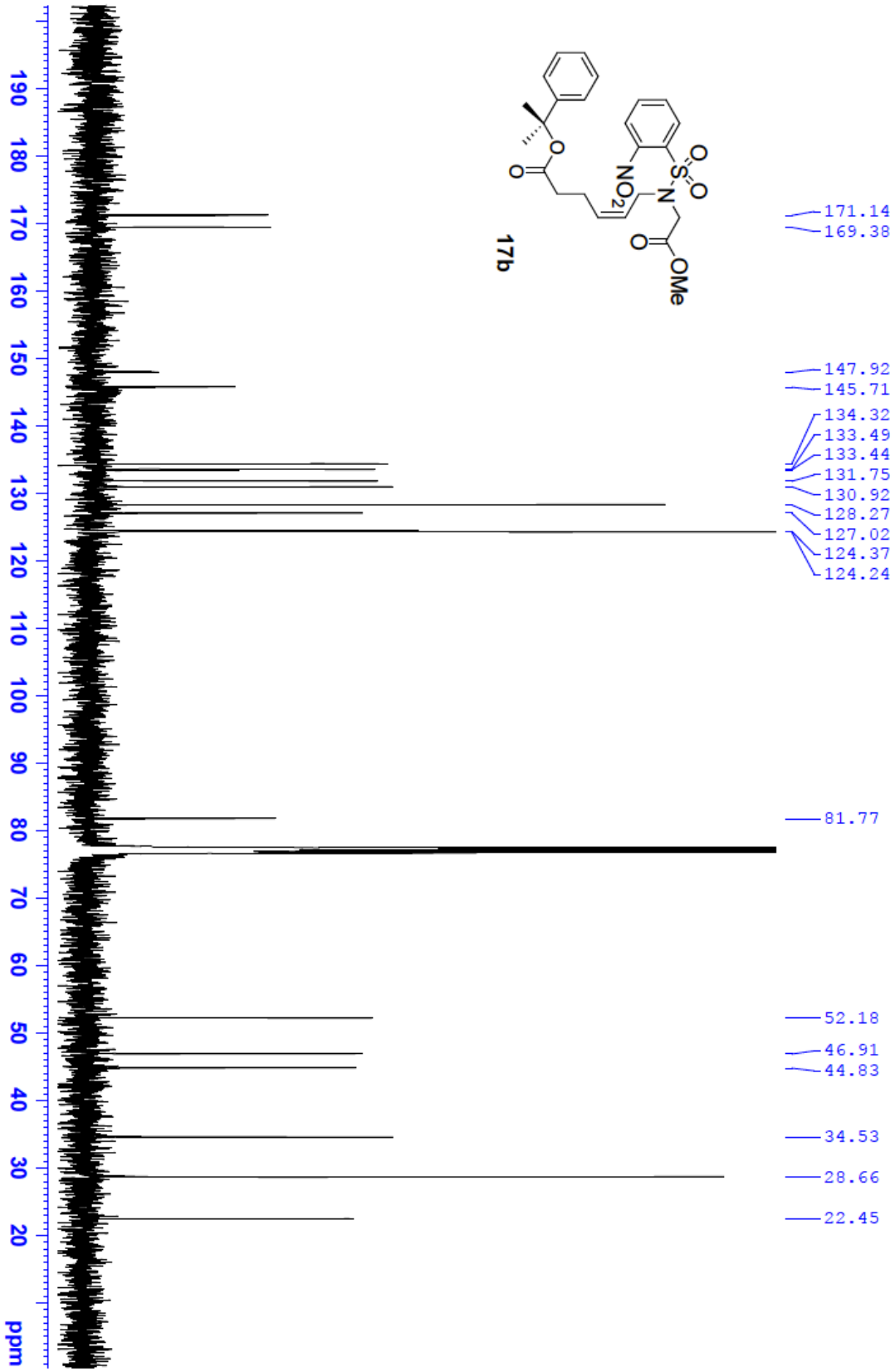
17b
171.14
169.38
147.92
145.71
134.32
133.49
133.44
131.75
130.92
128.27
127.02
124.37
124.24
81.77
52.18
46.91
44.83
34.53
28.66
22.45
ppm

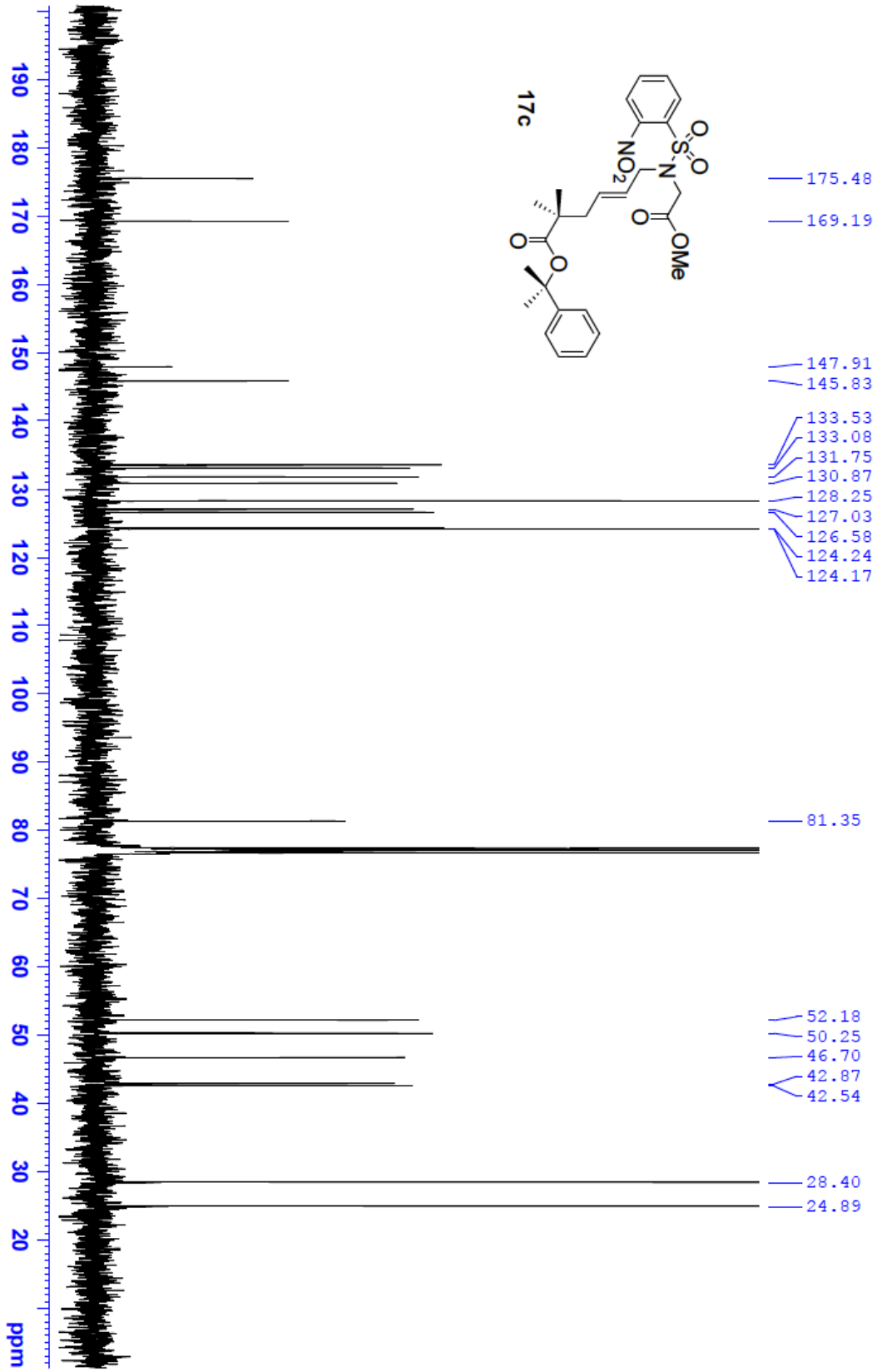
17c
175.48
169.19
147.91
145.83
133.53
133.08
131.75
130.87
128.25
127.03
126.58
124.24
124.17
81.35
52.18
50.25
46.70
42.87
42.54
28.40
24.89
ppm

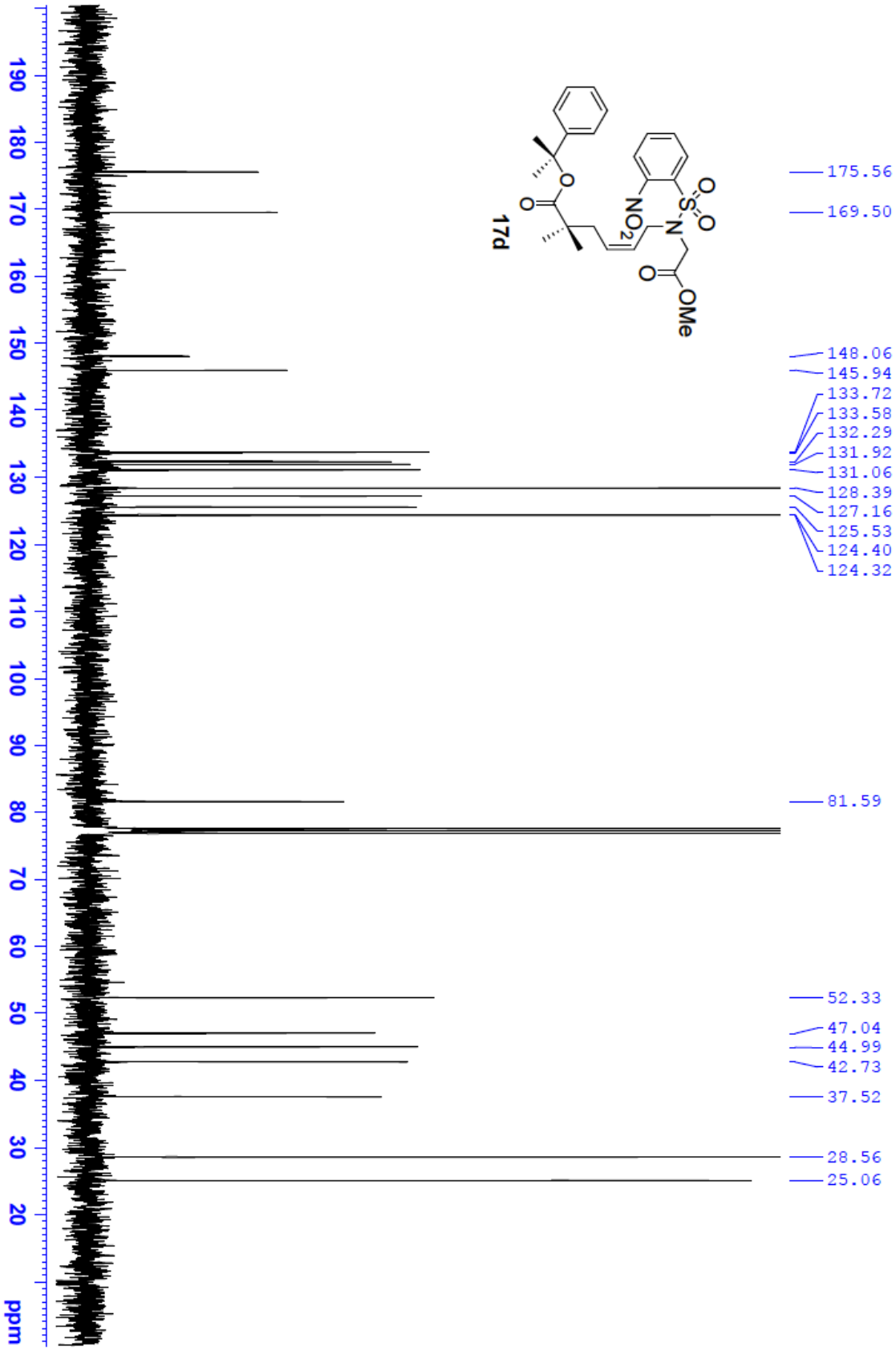
17d
175.56
169.50
148.06
145.94
133.72
133.58
132.29
131.92
131.06
128.39
127.16
125.53
124.40
124.32
81.59
52.33
47.04
44.99
42.73
37.52
28.56
25.06
ppm

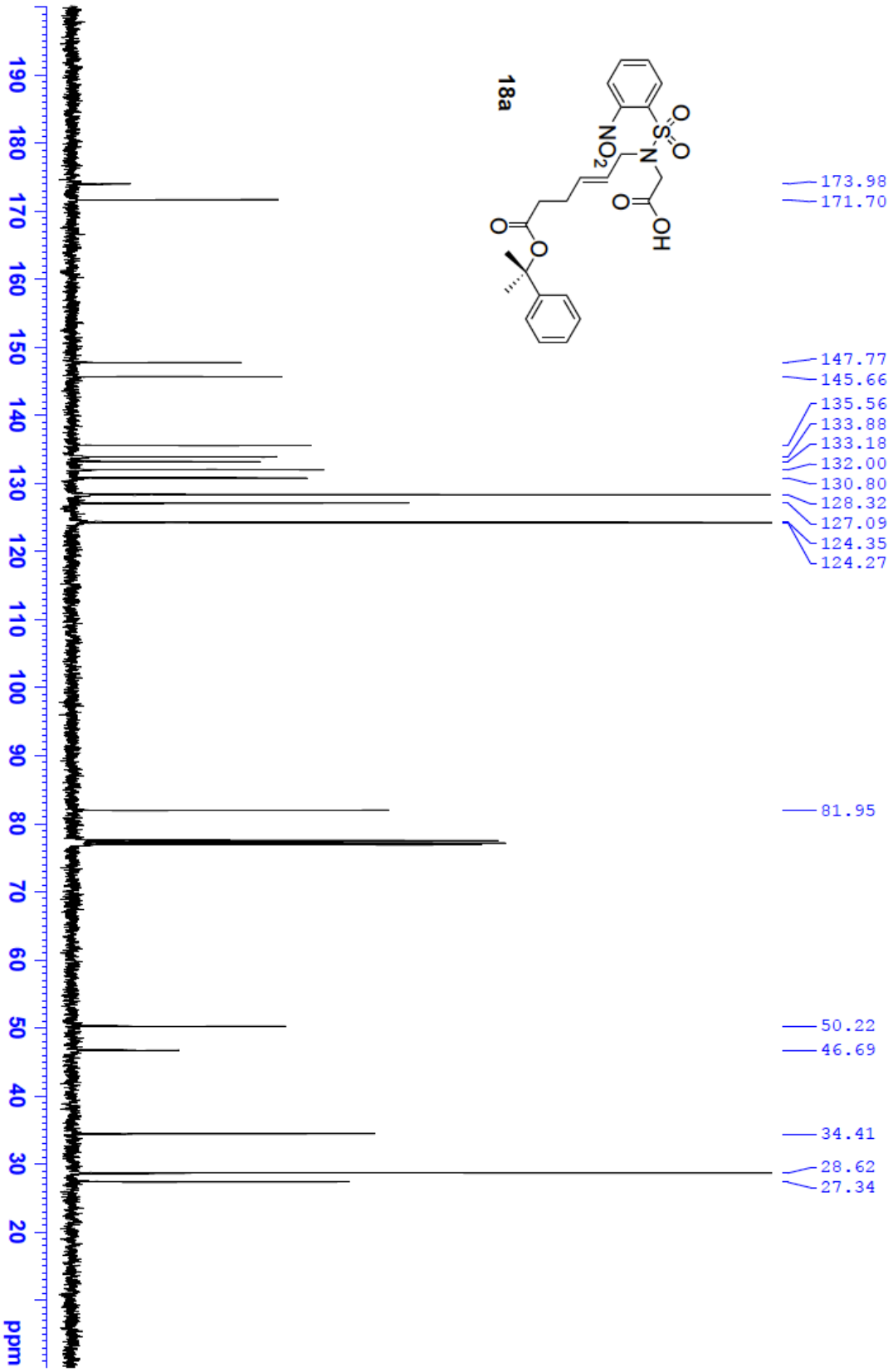
18a
173.98
171.70
147.77
145.66
135.56
133.88
133.18
132.00
130.80
128.32
127.09
124.35
124.27
81.95
50.22
46.69
34.41
28.62
27.34
ppm

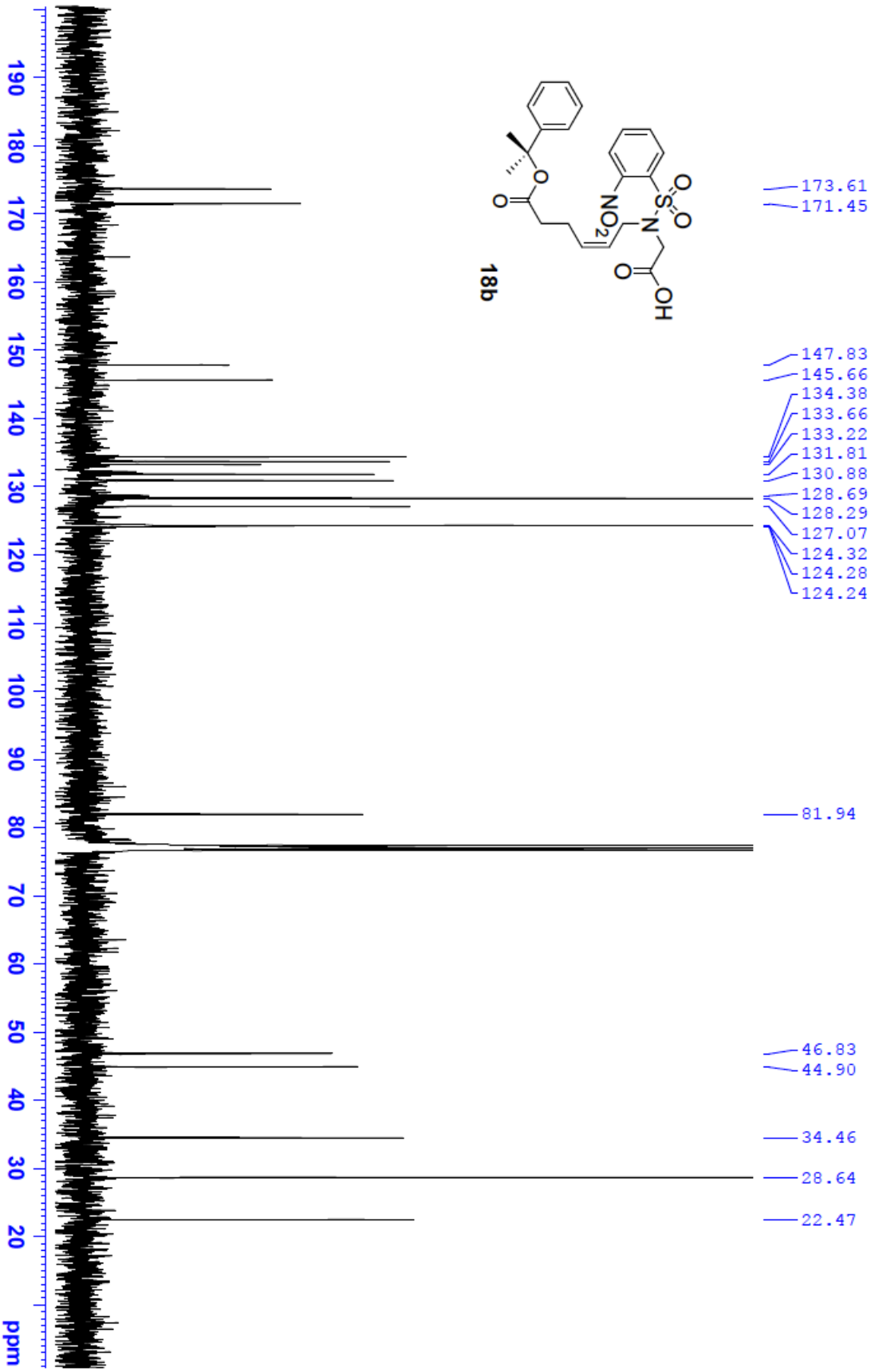
18b
173.61
171.45
147.83
145.66
134.38
133.66
133.22
131.81
130.88
128.69
128.29
127.07
124.32
124.28
124.24
81.94
46.83
44.90
34.46
28.64
22.47
ppm

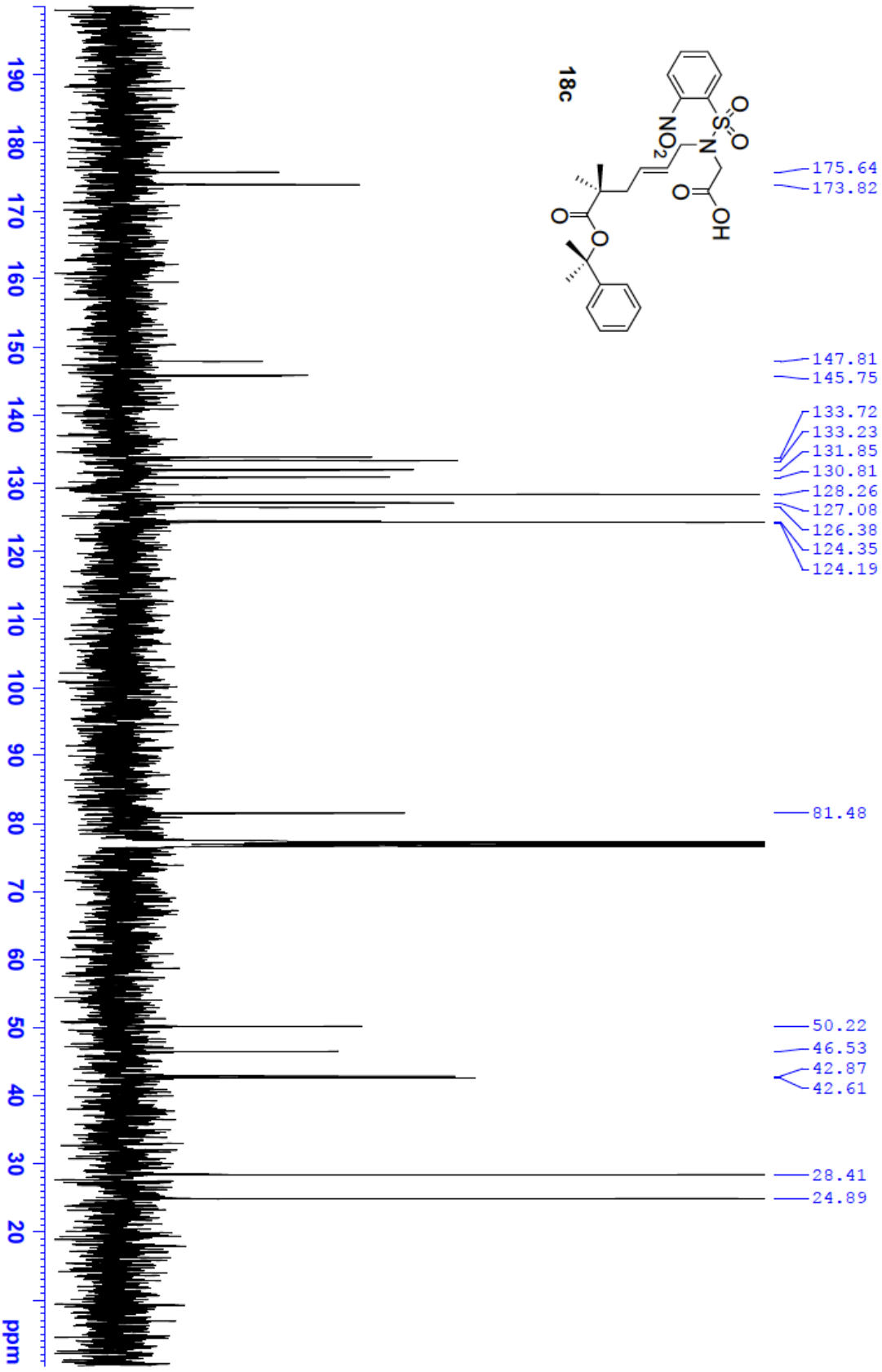
18c
175.64
173.82
147.81
145.75
133.72
133.23
131.85
130.81
128.26
127.08
126.38
124.35
124.19
81.48
50.22
46.53
42.87
42.61
28.41
24.89
ppm

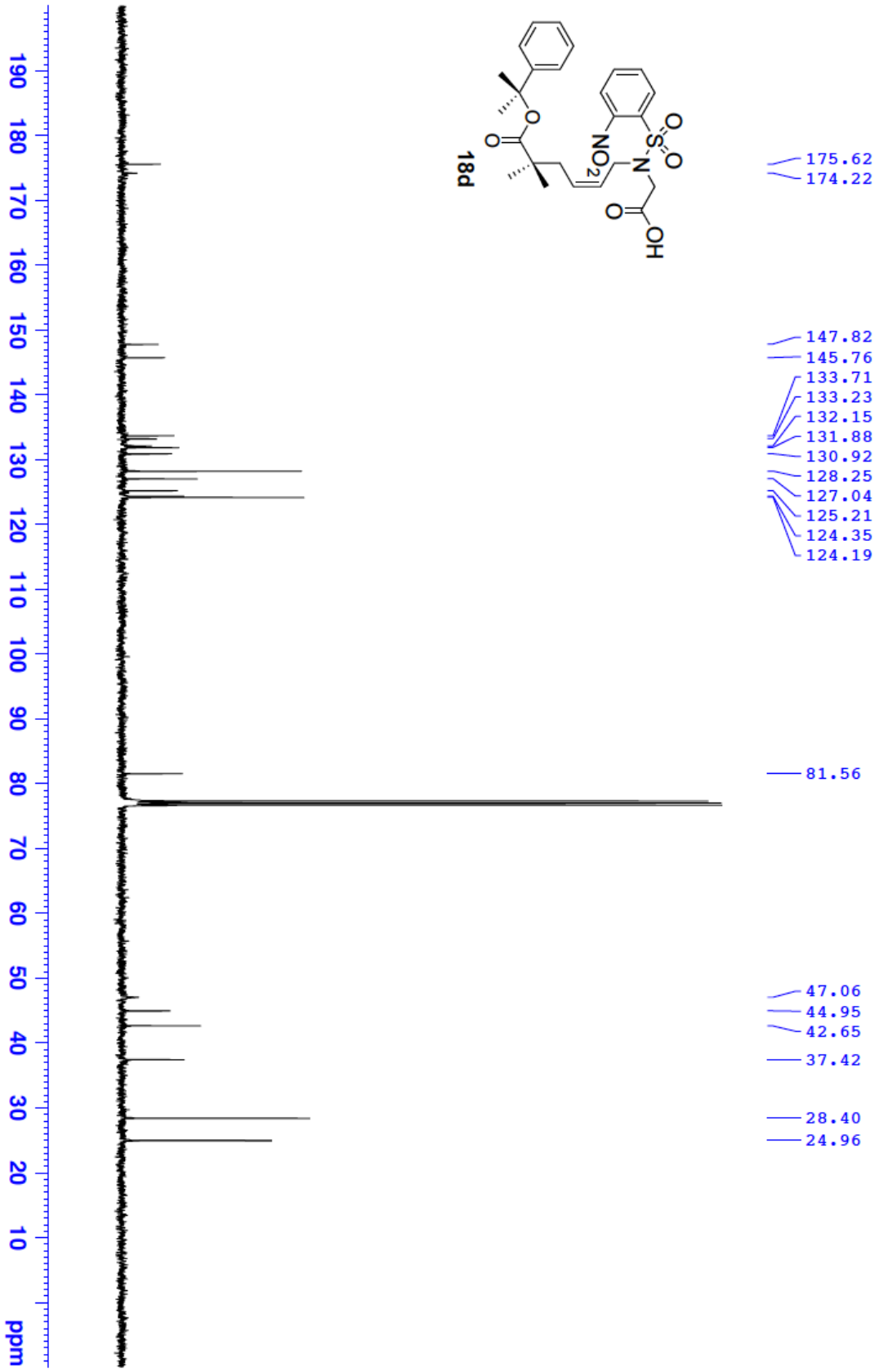
18d
175.62
174.22
147.82
145.76
133.71
133.23
132.15
131.88
130.92
128.25
127.04
125.21
124.35
124.19
81.56
47.06
44.95
42.65
37.42
28.40
24.96
190
180
170
160
150
140
130
120
110
100
90
80
70
60
50
40
30
20
10
ppm

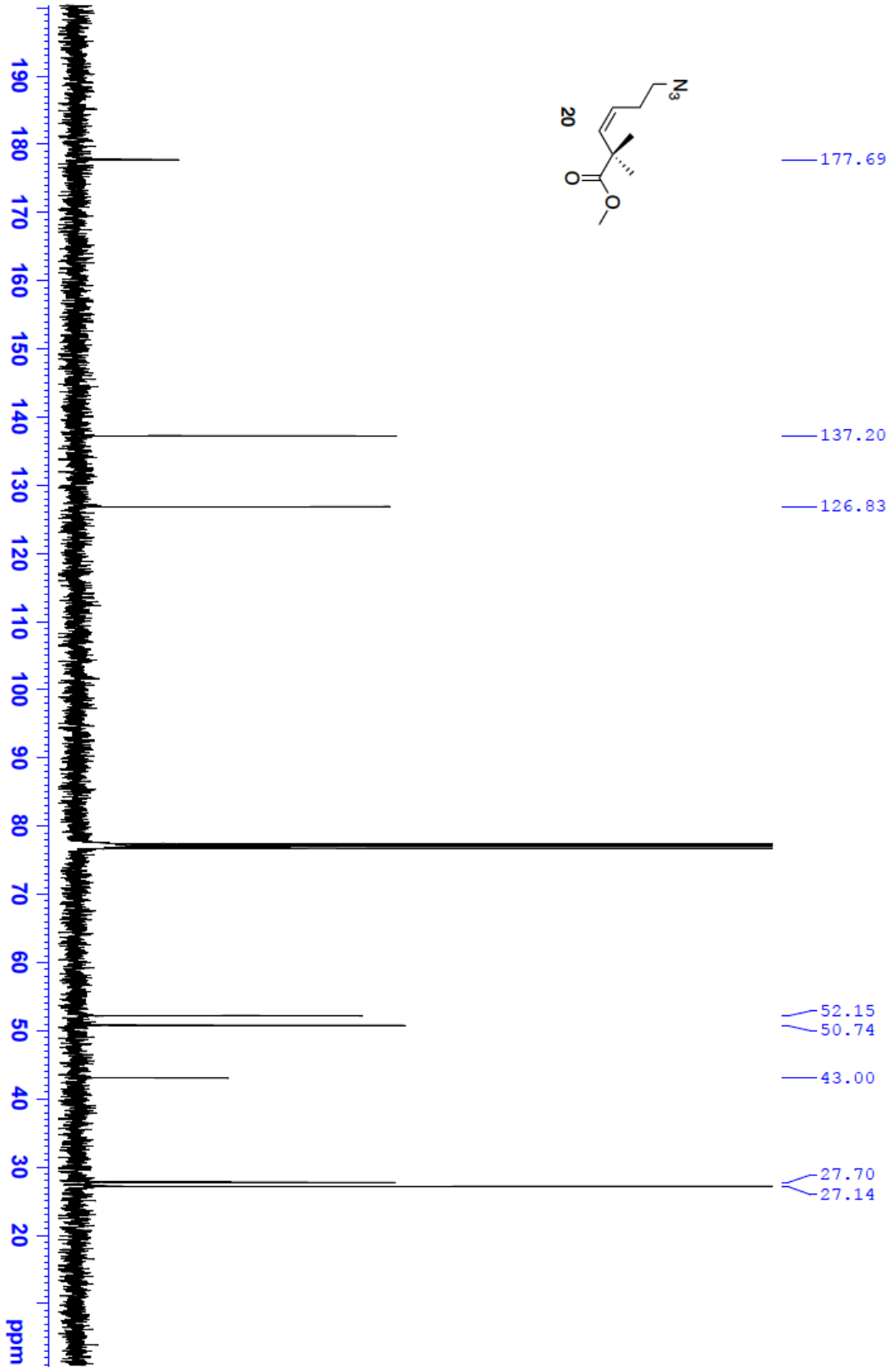
177.69
137.20
126.83
52.15
50.74
43.00
27.70
27.14
ppm

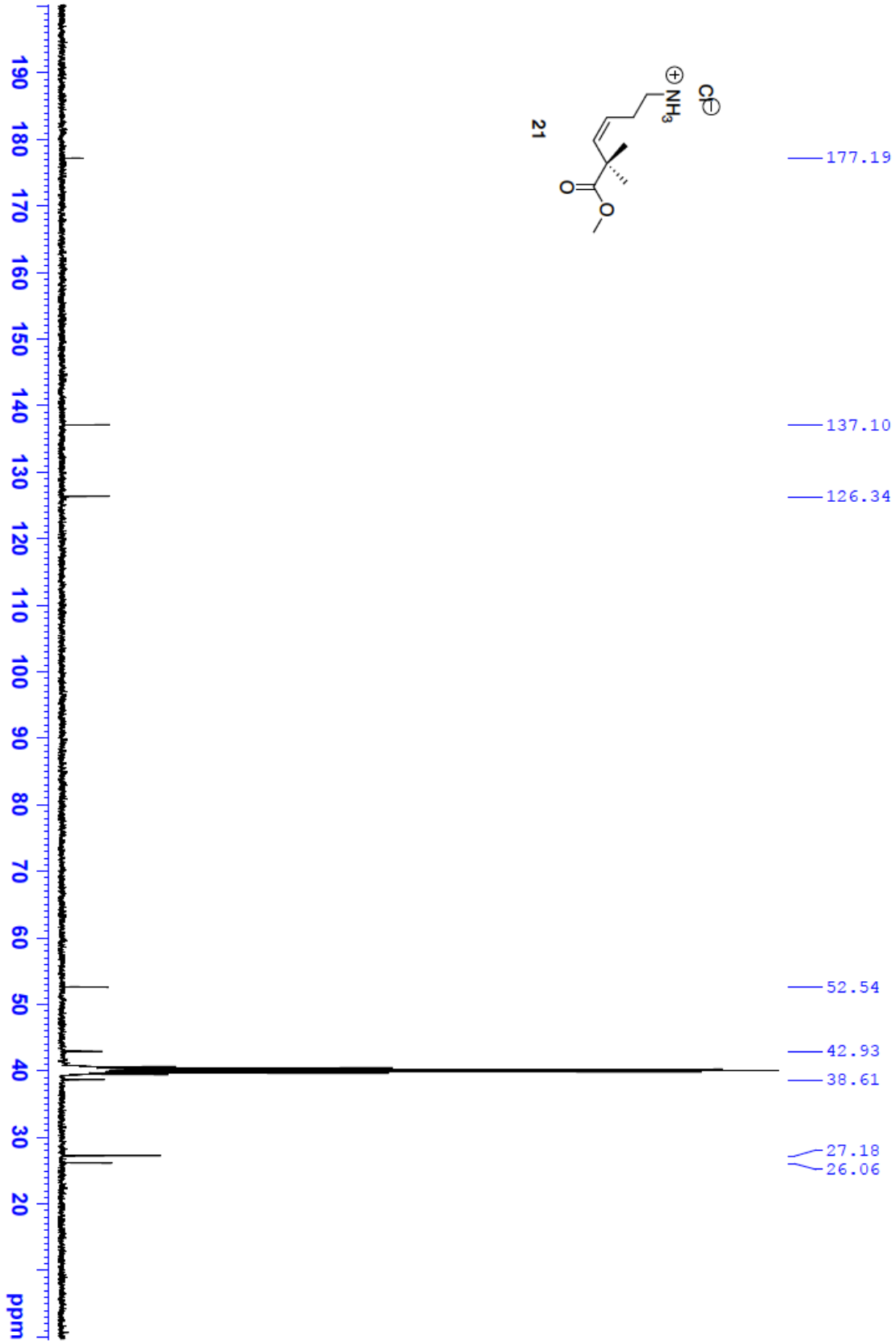
21
177.19
137.10
126.34
52.54
42.93
38.61
27.18
26.06
ppm

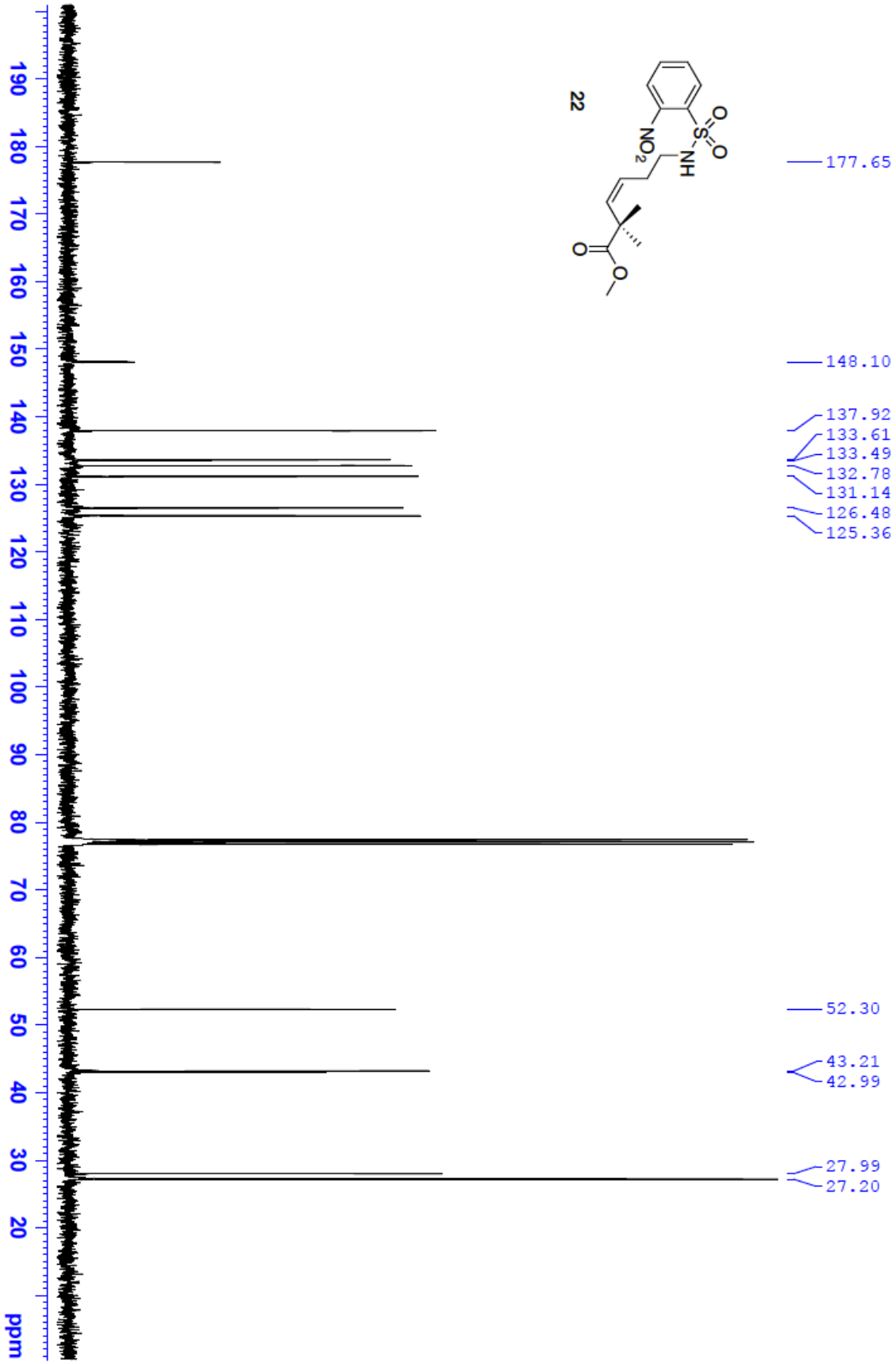
22
177.65
148.10
137.92
133.61
133.49
132.78
131.14
126.48
125.36
52.30
43.21
42.99
27.99
27.20
ppm

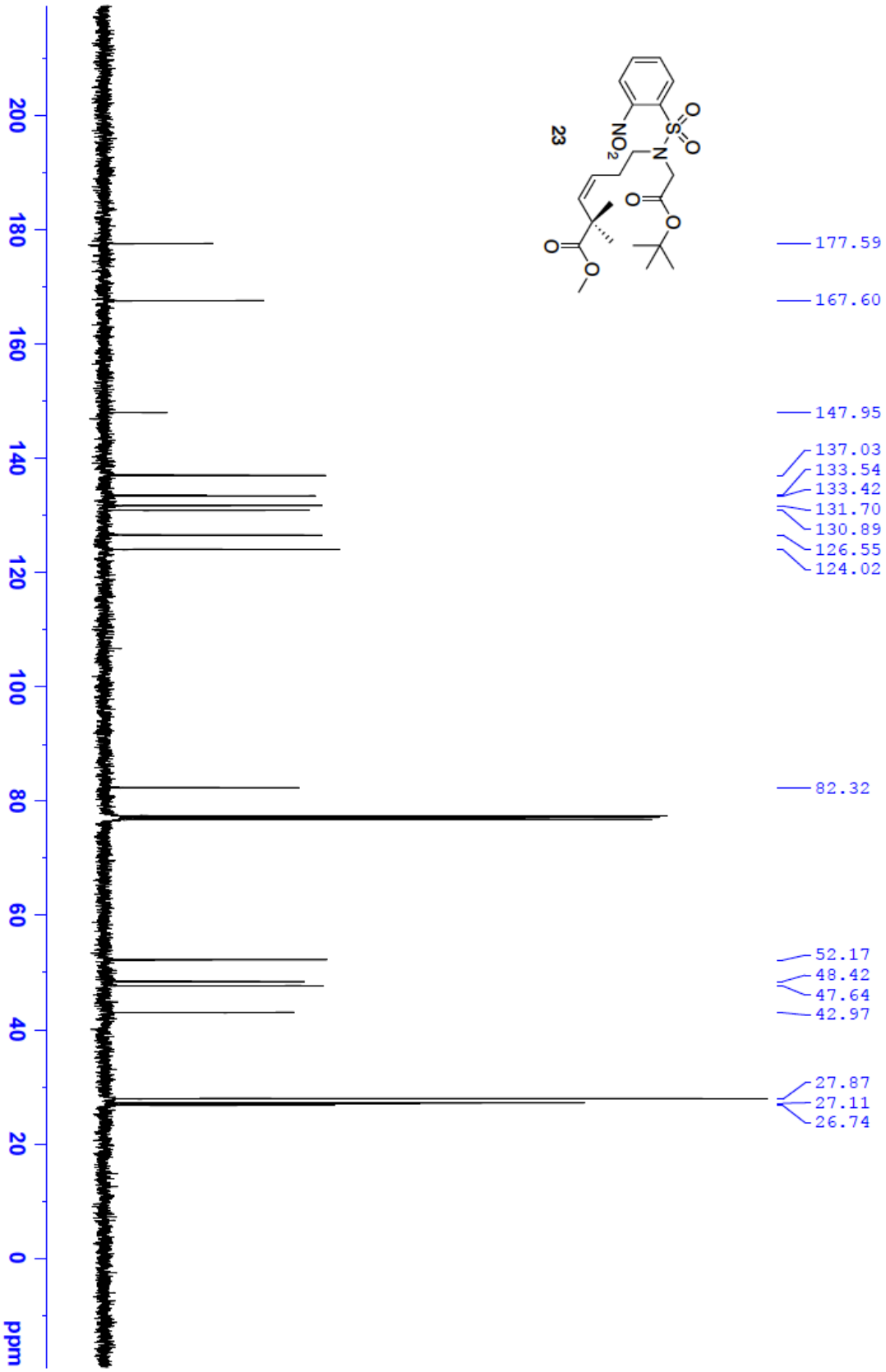
23
177.59
167.60
147.95
137.03
133.54
133.42
131.70
130.89
126.55
124.02
82.32
52.17
48.42
47.64
42.97
27.87
27.11
26.74
200
180
160
140
120
100
80
60
40
20
0
ppm

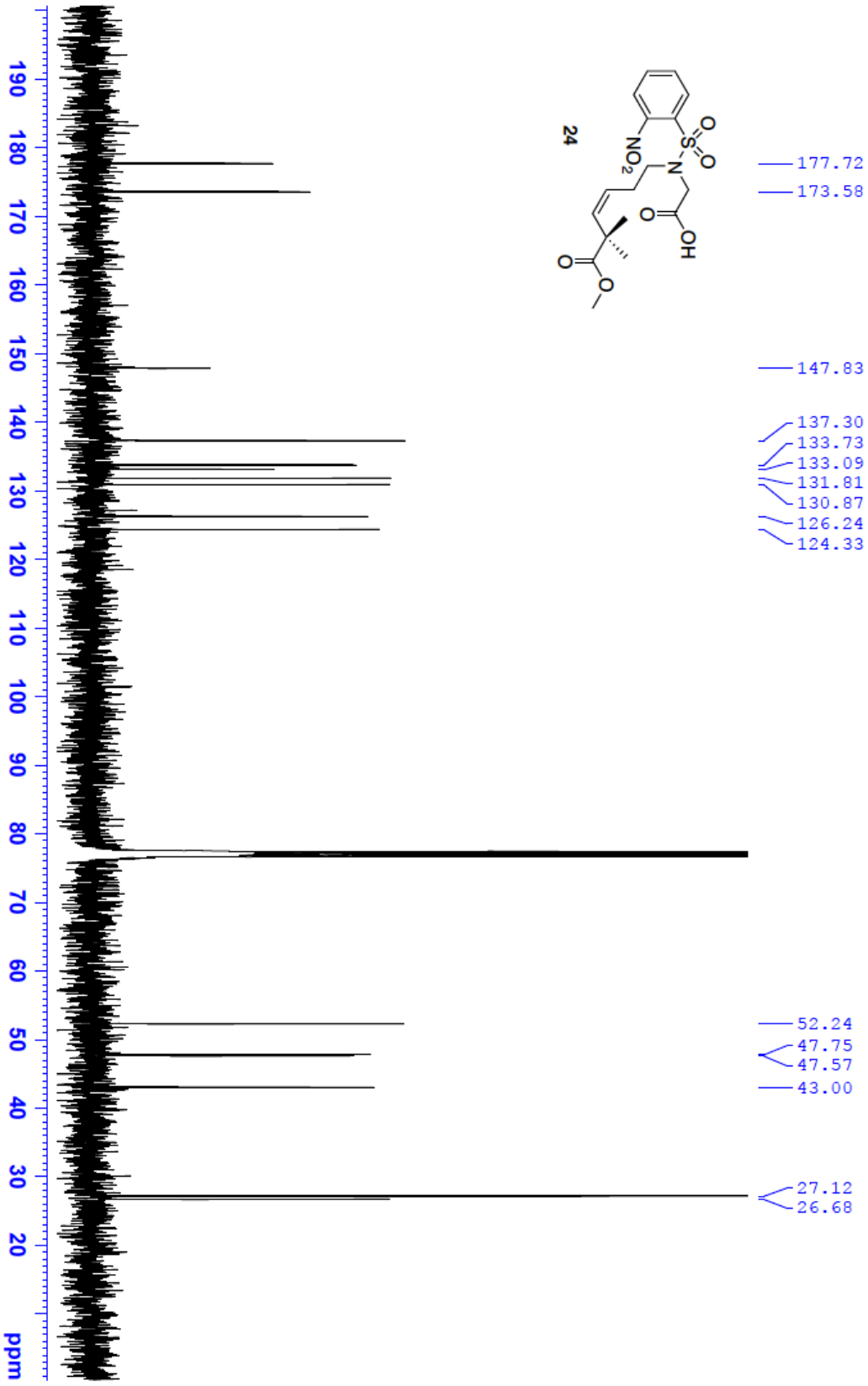
24
177.72
173.58
147.83
137.30
133.73
133.09
131.81
130.87
126.24
124.33
52.24
47.75
47.57
43.00
27.12
26.68
ppm

References

1. (a) S. E. Miller, P. F. Thomson and P. S. Arora, *Curr. Protoc. Chem. Biol.*, 2014, **6**, 101-116. (b) A. Patgiri, M. Z. Menzenski, A. B. Mahon and P. S. Arora, *Nat. Protoc.*, 2010, **5**, 1857-1865.
2. A. G.-M. Faucher, C., *Synth. Commun.*, 2006, **33**, 3503-3511.
3. (a) J. Y. Thierry, C.; Potier, P., *1998*, 1998, **39**, 1557-1560. (b) C. T. Yue, J.; Potier, P., *1993*, 1993, **34**, 323-326.
4. A. Sakakura, K. Kawajiri, T. Ohkubo, Y. Kosugi and K. Ishihara, *J. Am. Chem. Soc.*, 2007, **129**, 14775-14779.
5. C. Visintin, A. E. Aliev, D. Riddall, D. Baker, M. Okuyama, P. M. Hoi, R. Hiley and D. L. Selwood, *Org. Lett.*, 2005, **7**, 1699-1702.
6. T. Fukuyama, C. K. Jow and M. Cheung, *Tetrahedron Lett.*, 1995, **36**, 6373-6374.
7. M. Abe, R. Niibayashi, S. Koubori, I. Moriyama and H. Miyoshi, *Biochemistry*, 2011, **50**, 8383-8391.
8. (a) A. V. Chhen, M.; Carrie, R., *Tetrahedron Lett.*, 1989, **30**, 4953-4956. (b) I. H. de Miguel, B.; Mann, E., *Adv. Synth. Catal.*, 2012, **354**, 1731-1736. (c) S. J. C. Knight J.D.; Sauer, D.M., *Org. Lett.*, 2011, **13**, 3118-3121. (d) P. H. G. P. Zarbin, J.L.; de Lima, E.R.; dos Santos, A.A.; Ambrogio, B.G.; de Oliveira, A.R.M., *2004*, 2004, **45**, 239-241.
9. D. Bandyopadhyay, D. Prashar and Y. Y. Luk, *Chem. Commun.*, 2011, **47**, 6165-6167.
10. T. Matsuo, T. Yoshida, A. Fujii, K. Kawahara and S. Hirota, *Organometallics*, 2013, **32**, 5313-5319.
11. (a) N. J. Zondlo, S. C. Zondlo and A. E. Lee, *Biochemistry*, 2006, **45**, 11945-11957. (b) L. K. Henchey, J. R. Porter, I. Ghosh and P. S. Arora, *ChemBiochem*, 2010, **11**, 2104-2107. (c) A. Patgiri, S. T. Joy and P. S. Arora, *J. Am. Chem. Soc.*, 2012, **134**, 11495-11502.